August 2018

Neutron Star Tidal Deformability and Gravitational Self-force

Eric Van Oeveren
University of Wisconsin-Milwaukee

NEUTRON STAR TIDAL DEFORMABILITY AND GRAVITATIONAL SELF-FORCE

by

Eric D. Van Oeveren

A Dissertation Submitted in
Partial Fulfillment of the
Requirements for the degree of

Doctor of Philosophy
in Physics

at

The University of Wisconsin–Milwaukee
August 2018

ABSTRACT
NEUTRON STAR TIDAL DEFORMABILITY AND GRAVITATIONAL SELF-FORCE
by
Eric D. Van Oeveren

The University of Wisconsin–Milwaukee, August 2018
Under the Supervision of Professor Alan Wiseman

The recent direct observations of gravitational waves by the LIGO-Virgo collaboration [1–6] have been important pieces of evidence in agreement with Einstein's theory of gravity, the General Theory of Relativity. In addition, they open an era of gravitational-wave astronomy that promises to give us much more information on the systems that produce gravitational radiation. Perhaps most prominent among these are binary systems composed of either two black holes, two neutron stars, or one black hole and one neutron star. This dissertation details theoretical predictions regarding such systems.

It is hoped that gravitational radiation emanating from binary systems that include at least one neutron star will allow us to determine the equation of state of matter at very high densities, and therefore information on the composition of such matter. We place a theoretical upper limit on the tidal deformability of neutron stars, which describes how easily the shape of neutron stars change in response to an external gravitational field. This upper limit exists because of causality: the sound speed inside a neutron star must be less than the speed of light. This puts a limit on the stiffness of high-density matter, and therefore on the size of neutron stars, which closely corresponds to the tidal deformability. Our upper limit is consistent with observational information from the observation of gravitational waves emanating from a neutron star-neutron star binary [6, 7].

Another system that produces gravitational waves is one made of two black holes. We study such systems, specifically ones where one black hole is much more massive than the other. The gravitational waves sourced by these systems will not be observable by LIGO, but will require a space-based gravitational wave detector. We use a scalar

point charge as a toy model for the smaller black hole and apply a method discovered by Hikida et al. [8, 9] to compute the self-force on an accelerated scalar charge in circular orbit analytically through 6th Post-Newtonian order. Our results are compatible with previous Post-Newtonian calculations [9] and with numerical work on accelerated scalar charges [10].

Finally, we extend the method of Hikida et al. to the gravitational case. In particular, we calculate a gauge-invariant quantity discovered by Detweiler [11] through 6th Post-Newtonian order. We also calculate the time derivative of that quantity, which gives the power of the radiated gravitational waves. Interestingly, we find that if the Equivalence Principle is not obeyed and freely-falling particles can follow non-geodesic paths, dipolar gravitational radiation is produced. When we do enforce the Equivalence Principle, our results are consistent with previous Post-Newtonian calculations [12, 13].

TABLE OF CONTENTS

LIST OF FIGURES

CONVENTIONS

- We use metric signature $(-+++)$.

- We use Einstein sum notation. That is, $g_{\mu\nu}u^\nu = \sum_\nu g_{\mu\nu}u^\nu$.

- We use units where $c = G = 1$.

ACKNOWLEDGMENTS

reason why our assumptions in the paper that became chapter 2 of this dissertation are so clearly stated. His patience with me as I learned to write an academic paper is also greatly appreciated.

Finally, I must thank my graduate advisor Alan Wiseman. I feel lucky to have worked exclusively on theoretical gravitational physics as a graduate student, and that opportunity was due to his presence in the CGCA. His straightforward feedback over the years has been invaluable, as was his intuition for self-force problems. I would not understand the final two chapters of this dissertation as well if it were not for him.

Chapter 1

Introduction

This dissertation will discuss my contributions to predictions regarding gravitational waves, which were originally predicted by Albert Einstein in 1916 [14] and directly detected for the first time in 2015 [1]. These predictions all involve *binary systems*, that is, systems of two objects. There are several techniques used in General Relativity to study such systems, and we start with a conceptual explanation of three of them.

1.1 Numerical Relativity, Post-Newtonian Theory, and Self-Force

The remaining chapters of this dissertation will discuss different sources of gravitational waves and make predictions regarding their motion. All of the sources discussed in this dissertation are binary systems. While the gravitational fields surrounding isolated, spherically-symmetric objects are well-understood, binary systems are notoriously tricky to study in General Relativity due to the non-linearity of Einstein's equation. In order to study binary systems theoretically, physicists have developed three different techniques that are discussed in this dissertation: numerical relativity, Post-Newtonian theory, and self-force. Each technique is useful in a different situation (see Fig. 1). Here we also briefly mention the Effective One Body (EOB) formalism pioneered by Buonanno and Damour [15]. The EOB formalism attempts to combine information from all three of the
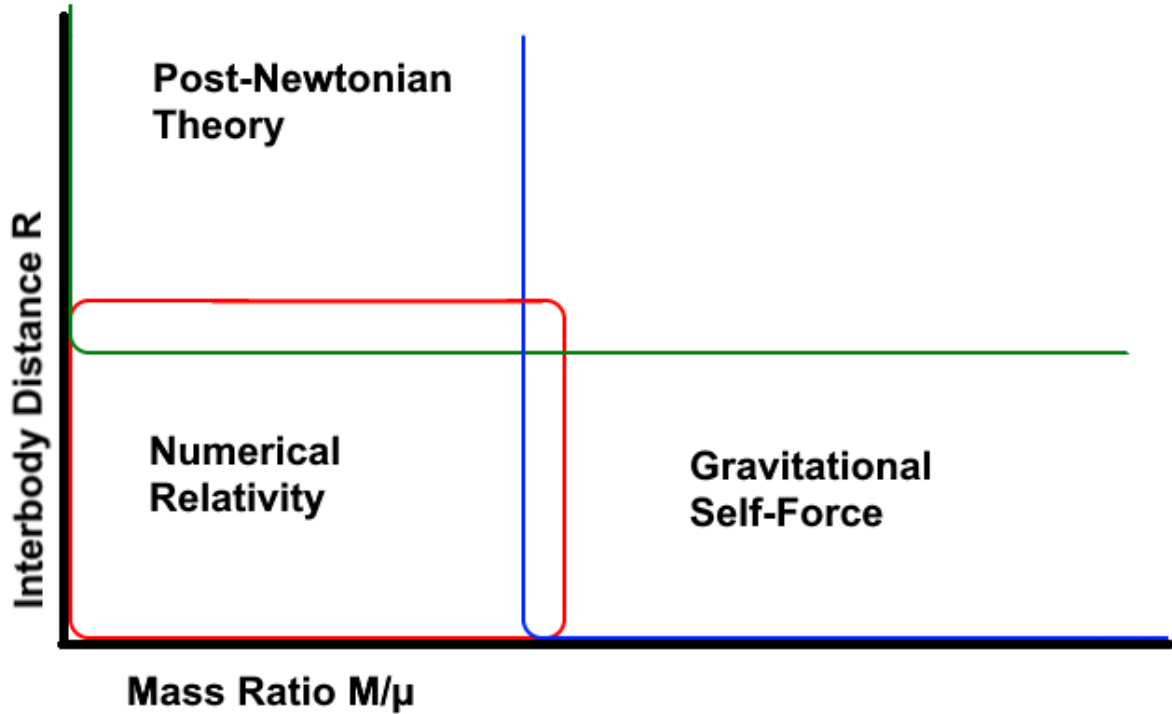
Figure 1 : Different methods for solving the binary problem. For small mass ratios and small interbody distances, numerical relativity is most useful. For large interbody distances, Post-Newtonian theory reigns supreme. For large mass ratios, gravitational self-force is used.

techniques discussed below to give analytical results applicable to all binaries, with much success. For more information on the EOB formalism, we direct the reader to the review by Damour [16].

1.1.1 Numerical Relativity

In numerical relativity, one uses computers to solve Einstein's equation. Foundational work in numerical relativity was originally done by Arnowitt, Deser, and Misner [17]; their methods were later improved upon by Shibata and Nakamura [18] and Baumgarte and Shapiro [19]. In principle, any problem in gravitational physics could be solved this way, but in practice, it is difficult in situations where the two objects involved are far from each other or have very different masses. This is where the two other formalisms come into play.

1.1.2 Post-Newtonian Theory

Post-Newtonian (PN) Theory was developed to accurately describe binary systems comprised of two objects that are slow-moving and far from each other. The two objects are considered to be far enough from each other that they can each be considered point particles. Post-Newtonian results are given in powers of the quantity M/r or v^2, where M is the total mass of the system, r is the separation distance, and v is the speed of one of the objects. Since these two quantities are small when r is large and v is small, this simplifies Einstein's equation to the point where it is solvable. In non-geometrized units, a PN expansion can be thought of as a series in $1/c^2$; since c is large compared to velocites we encounter in our solar system, a PN expansion is useful in describing a system that is not relativistic. The term "Post-Newtonian" comes from the fact that, as the separation distance increases, the predictions from General Relativity become indistinguishable from those of Newtonian gravity. Each new term in a PN expansion therefore gives a finer correction to Newtonian predictions. For a review on PN Theory, see [20].

1.1.3 Self-Force

Self-force is applicable when the mass of one object is much smaller than that of the other, but can be used for any inter-object distance r. In this situation, numerical relativity is insufficient because the gravitational field due to the smaller mass is quite small and difficult to compute. Self-force gives results in a series of the ratio of the masses. This ratio, again, is small in situations where self-force is used, and writing answers in terms of this quantity simplifies Einstein's equation. For more details on how self-force calculations are performed, see the third and fourth chapters of this dissertation. For a review on self-force, see [21].

1.2 The Format of this Dissertation

The rest of this dissertation is split into three chapters. Chapter 2 will describe work I did with John Friedman that placed a theoretical upper limit on the tidal deformability

of a neutron star and its effects on gravitational waves sourced by binaries including neutron stars. This work was originally published in *Physical Review D* [22]. Since then, gravitional waves from a neutron star-neutron star binary have been observed [6], and the 90% confidence interval based on that data [7] is consistent with our results.

Chapter 3 will detail work I did with Tom Linz under the supervision of Alan Wiseman, with help from John Friedman. This work used a method pioneered by Hikida et al. [8, 9] to generate a PN expansion for the self-force on a scalar charge in an accelerated circular orbit around a non-spinning black hole. Our results are consistent with Hikida et al. and numerical self-force data reported in [10] on accelerated scalar charges.

Chapter 4 will report work I did under the supervision of Alan Wiseman that extended the method of Hikida et al. to the gravitational case. Once again, we study a particle in circular orbit around a non-spinning black hole, and we treat the particle's orbital angular velocity as independent from its radial coordinate. However, we do not calculate the radial self-force—which is gauge-dependent—and instead find a related gauge-invariant quantity discovered by Detweiler [11] and its time-derivative, which gives the temporal component of the force. Furthermore, we cannot claim that the results accurately portray the gravitational perturbation from an accelerated particle, since we have not included the stress-energy of the accelerating force as a source for the gravitational field. Nevertheless, treating the particle's angular velocity as independent of its radial coordinate leads to an interesting result: if such a freely-falling particle were to follow a non-geodesic path, it would result in dipolar gravitational radiation. When we enforce geodesic motion on the particle, our results are consistent with previous PN gravitational self-force results, including those from Bini and Damour [12], Kavanagh et al. [13], and Fujita [111].

Chapter 2

Neutron Star Tidal Deformability

In this chapter, we discuss work I did with John Friedman constraining the tidal deformability of a neutron. In particular, we set an upper limit on the tidal deformability and its effect on the gravitational waveform of a black hole-neutron star binary. This upper limit is based on causality, which prevents anything from traveling faster than light. Applying this speed limit to the sound speed through neutron stars constrains the stiffness of high-density matter, which in turn constrains the size of neutron stars. This size constraint corresponds to a constraint on the tidal deformability, as we show in this chapter. This work was originally published in *Physical Review D* [22], and I reproduce it here with minimal changes. I also compare our results to the 90% confidence interval [7] on the dimensionless tidal deformability that arose from the observation of GW170817 [6].

2.1   Introduction

Recently, Advanced LIGO [6] detected gravitational waves sourced by a coalescing neutron star binary, and in the future we are likely to detect each year the inspiral and coalescence of several compact binary systems that include neutron stars, both black hole-neutron star (BHNS) and binary neutron-star (BNS) systems. These observations can constrain the neutron-star equation of state (EOS), which gives the pressure p in terms of the energy density ϵ. A stiffer EOS, where the pressure increases rapidly with density, yields stars with larger radii and larger tidal effects on the waveform, governed

by the star's *tidal deformablity*. In particular, tidal distortion during inspiral increases with the stiffness of the EOSs. Because energy is lost both to gravitational waves and to the work needed to distort the stars, the inspiral proceeds more rapidly for stars with greater tidal deformability. The result is a waveform in which the increase in frequency is more rapid and in which coalescence occurs sooner – at lower frequency.

Beginning with work by Kochanek [23] and Lai and Wiseman [24], a number of authors have studied the effect of tides on inspiral waveforms. Simulations [25–43] of BHNS and BNS systems and analytic approximations in the context of post-Newtonian theory [44] and the Effective-One-Body (EOB) formalism [45–47] are nearing the precision needed to extract neutron-star deformability from observations with the projected sensitivity of Advanced LIGO. Recent estimates of the measurability of tidal effects and the ability of these observatories to constrain the EOS with signals from BHNS and BNS systems are given in [48–52] and references therein.

In this work, we obtain the upper limit imposed by causality on the tidal deformability of neutron stars and estimate the resulting constraint on the maximum departure of the waveform of a BHNS inspiral from a corresponding spinless binary black hole (BBH) inspiral.[1] The limit is analogous to the upper limits on neutron-star mass M_{NS} [55, 56] and radius R [57]. In each case, one assumes an EOS of the form $p = p(\epsilon)$ that is known below an energy density $\epsilon_{\mathrm{match}}$, and one obtains a limit on M and R by requiring that the EOS be causal for $\epsilon > \epsilon_{\mathrm{match}}$ in the sense that the sound speed, given by $\sqrt{dp/d\epsilon}$, must be less than the speed of light. Because the sound speed is a measure of the stiffness of the EOS, this is a constraint on the stiffness. An upper limit on tidal deformability then implies an upper limit on the departure of gravitational wave phase shifts from corresponding waveforms of BBH inspiral.

---

[1]After this paper was posted to arXiv, Moustakidis [53] pointed out a preprint by him and his coauthors that also obtains upper limits on neutron star mass and tidal deformability imposed by bounds on the speed of sound, including $v_{\mathrm{sound}} \leq c$. However, they use a matching density (described in the next section) 50% higher than ours, giving less conservative results. Furthermore, they do not consider tidal effects during late inspiral, whereas we apply the results of [54] to do so.

2.2 Method

2.2.1 Causal EOS

For a perfect fluid with a one-parameter EOS $p = p(\epsilon)$, where p is the pressure and ϵ the density of the fluid in its own rest frame, causality implies that the speed of sound, $\sqrt{dp/d\epsilon}$, is less than the speed of light. That is, the dynamical equations describing the evolution of fluid and metric are hyperbolic, with characteristics associated with fluid degrees of freedom lying outside the light cone unless

$$\frac{dp}{d\epsilon} \leq 1. \tag{2.2.1}$$

There is some inaccuracy in using the one-parameter EOS that governs the equilibrium star to define the characteristic velocities of the fluid, because fluid oscillations with the highest velocities have frequencies too high for the temperature of a fluid element and the relative density Y_i of each species of particle to reach their values for the background fluid star. Nevertheless, using a result of Geroch and Lindblom [58], we show in Appendix A that causality implies the equilibrium inequality (2.2.1) for locally stable relativistic fluids satisfying a two-parameter EOS $p = p(\epsilon, s)$, where s is the entropy per baryon. For the multi-parameter equation of state $p = p(\epsilon, s, Y_i)$, with Y_i the relative density of each species of particle, one must assume without proof that causality implies $v_{\mathrm{sound}} < 1$; the equilibrium inequality (2.2.1) again follows from local stability.

The speed of sound is a measure of the stiffness of the EOS. The well-known upper limit on the mass of a neutron star and a corresponding upper limit on its radius are obtained by using the stiffest EOS consistent with causality and with an assumed known form at low density. That is, above a density $\epsilon_{\mathrm{match}}$, the EOS is given by

$$p - p_{\mathrm{match}} = \epsilon - \epsilon_{\mathrm{match}}, \tag{2.2.2}$$

where p_{match} is fixed by continuity to be the value of p at $\epsilon_{\mathrm{match}}$ for the assumed low-density EOS. The upper limits on mass and radius are then found as functions of the matching density $\epsilon_{\mathrm{match}}$.

In this work, we again use an EOS of this form to find an upper limit on neutron-star deformability. To be conservative, as our low-density EOS we choose the MS1 EOS [59], which is among the stiffest candidate equations of state. Our *matched causal EOS* is then given by

$$p(\epsilon) = \begin{cases} p_{\mathrm{MS1}}(\epsilon), & \epsilon \leq \epsilon_{\mathrm{match}} \\ \epsilon - \epsilon_{\mathrm{match}} + p_{\mathrm{MS1}}(\epsilon_{\mathrm{match}}), & \epsilon \geq \epsilon_{\mathrm{match}}. \end{cases} \quad (2.2.3)$$

In computing the deformability, we consider only irrotational neutron stars; and in estimating the effect of tides on the inspiral phase, we neglect resonant coupling of tides to neutron-star modes. Tidal deformation of slowly rotating relativistic stars is treated by Pani *et al.* [60]; and Essick *et al.* [61] argue that tidal excitation of coupled modes may alter the waveform in BNS systems.

2.2.2 Static, Spherical Stars

We next construct the sequence of static spherical stars based on the causal EOS (2.2.3). We numerically integrate the Tolman-Oppenheimer-Volkoff (TOV) equation [62],

$$\left(1 - \frac{2m}{r}\right)\frac{dp}{dr} = -\frac{1}{r^2}(\epsilon + p)(m + 4\pi r^3 p), \quad (2.2.4)$$

where $m(r)$ is the total mass-energy inside radius r, related to ϵ by

$$\frac{dm}{dr} = 4\pi r^2 \epsilon. \quad (2.2.5)$$

A member of the sequence is specified by its central density ϵ_c. Its circumferential radius R is the value of the Schwarzschild coordinate r at which $p(r) = 0$, and its gravitational mass is $M = m(R)$.

2.2.3 Calculating the Tidal Deformability

The departure of the inspiral of a BHNS binary from point-particle (or spinless BBH) inspiral depends on the tidal deformation of the neutron star due to the tidal field of its companion. For large binary separation, the metric near the neutron star can be written as a linear perturbation of the Schwarzschild metric of the unperturbed star that has two

parts: The tidal field of the companion, expressed in Schwarzschild coordinates about the center of mass of the neutron star, has the form of an external quadrupole field; and the induced quadrupole distortion of the neutron star gives a second quadrupole contribution to the perturbed metric. That is, outside the support of the star, the quadrupole perturbation is a sum,

$$\delta g_{\alpha\beta} = \delta_{\text{external}}\, g_{\alpha\beta} + \delta_{\text{induced}}\, g_{\alpha\beta}, \tag{2.2.6}$$

of two time-independent solutions to the field equations linearized about a vacuum Schwarzschild geometry. In a gauge associated with asymptotically Cartesian and mass centered coordinates, the contributions to the perturbed metric have the form

$$\delta_{\text{external}}\, g_{tt} = -r^2 \mathcal{E}_{ij} n^i n^j + \mathcal{O}(r), \tag{2.2.7}$$

with no r^{-3} contribution, and

$$\delta_{\text{induced}}\, g_{tt} = \frac{3}{r^3} Q_{ij} \left(n^i n^j - \frac{1}{3} \delta^{ij} \right) + \mathcal{O}(r^{-4}). \tag{2.2.8}$$

Here $n^i = x^i/r$ is an outward-pointing unit vector, $\mathcal{E}_{ij}$ is the tracefree tidal field from the black hole, and Q_{ij} is the neutron star's induced quadrupole moment. The quadrupole moment tensor Q_{ij} is proportional to $\mathcal{E}_{ij}$,

$$Q_{ij} = -\lambda \mathcal{E}_{ij}, \tag{2.2.9}$$

and the constant of proportionality λ is the *tidal deformability* of the neutron star. It measures the magnitude of the quadrupole moment induced by an external tidal field and is proportional to the (dimensionless) $\ell = 2$ tidal Love number [63]

$$k_2 = \frac{3\lambda}{2R^5}. \tag{2.2.10}$$

After constructing the one-parameter family of spherical stars satisfying Eqs. (2.2.3), (2.2.4), and (2.2.5), we tidally perturb them, compute k_2 and the radius R of each star, and then find the tidal deformability λ from Eq. (2.2.10). To calculate k_2, we use the method described by Hinderer [64]: A perturbation of the spherically symmetric background metric

$$\mathbf{g} = -e^{2\nu} dt^2 + \frac{1}{1 - 2m/r} dr^2 + r^2 (d\theta^2 + \sin^2\theta d\phi^2), \tag{2.2.11}$$

with $\nu(r)$ determined by

$$\left(1 - \frac{2m}{r}\right)\frac{d\nu}{dr} = \frac{1}{r^2}(m + 4\pi r^3 p),$$

is found in the Regge-Wheeler gauge [65], with $\delta\mathbf{g}$ a linear, quadrupolar, static, polar-parity perturbation given by [64] [2]

$$\delta\mathbf{g} = (-e^{2\nu}dt^2 + \frac{1}{1 - 2m/r}dr^2)H\,Y_{2,m}(\theta,\phi)$$
$$+ r^2(d\theta^2 + \sin^2\theta d\phi^2)K\,Y_{2,m}(\theta,\phi), \tag{2.2.12}$$

where H and K are both functions of r. The perturbed Einstein equation gives a differential equation for H [64]:

$$0 = \frac{d^2H}{dr^2}\left(1 - \frac{2m}{r}\right) + \frac{dH}{dr}\left[\frac{2}{r} - \frac{2m}{r^2} + 4\pi r(p - \epsilon)\right]$$
$$- H\left[\frac{6}{r^2} - 4\pi\left(5\epsilon + 9p + \frac{\epsilon + p}{dp/d\epsilon}\right)\right.$$
$$\left. + 4\left(1 - \frac{2m}{r}\right)\left(\frac{d\nu}{dr}\right)^2\right].$$

In vacuum, H can be written as a linear combination of $P_2^2(r/M - 1)$ and $Q_2^2(r/M - 1)$, where P_2^2 and Q_2^2 are the $\ell = m = 2$ associated Legendre functions. When expanded in powers of M/r at infinity, $P_2^2(r/M - 1) = \mathcal{O}(M/r)^3$ and $Q_2^2(r/M - 1) = \mathcal{O}(r/M)^2$. The coefficient of P_2^2 is therefore related to the quadrupole moment of the star, and the coefficient of Q_2^2 is related to the tidal field applied by the black hole. By matching $H(r)$ and its derivative across the surface of the star, one can show [64]

$$k_2 = \frac{8}{5}C^5(1 - 2C)^2[2 + 2C(Y - 1) - Y]$$
$$\times \left\{2C[6 - 3Y + 3C(5Y - 8) + 2C^2(13 - 11Y)\right.$$
$$+ 2C^3(3Y - 2) + 4C^4(Y + 1)]$$
$$\left. + 3(1 - 2C)^2[2 - Y + 2C(Y - 1)]\log(1 - 2C)\right\}^{-1}, \tag{2.2.13}$$

[2]Note that, because this gauge does not conform to the constraints of an asymptotically Cartesian and mass-centered chart, there are additional terms in the expansion of the asymptotic metric.

where $C = M_{NS}/R$ is the compactness of the star, $Y = RH'(R)/H(R)$, and R is the radius of the star. Since k_2 depends on Y and not H or H' individually, Postinkov, Prakash, and Lattimer [66] and Lindblom and Indik [67] define

$$y(r) = r\frac{H'(r)}{H(r)},$$

which gives rise to the first-order differential equation

$$\frac{dy}{dr} = -\frac{y^2}{r} - \frac{r + 4\pi r^3(p - \epsilon)}{r(r - 2m)}y + \frac{4(m + 4\pi r^3 p)^2}{r(r - 2m)^2}$$
$$+ \frac{6}{r - 2m} - \frac{4\pi r^2}{r - 2m}\left[5\epsilon + 9p + \frac{(\epsilon + p)^2}{\epsilon dp/d\epsilon}\right]. \tag{2.2.14}$$

To find $Y = y(R)$, we numerically integrate Eq. (2.2.14) and evaluate y at the surface of the star.

Despite appearances, the expression in curly braces in Eq. (2.2.13) is $\mathcal{O}(C^5)$ due to cancellations of terms in curly brackets that are polynomial in C with terms from the expansion of $\log(1 - 2C)$. For stars of small compactness, calculating k_2 directly from Eq. (2.2.13) is difficult because it requires that both the numerator and denominator of the right side are accurately calculated to a large number of decimal places. A calculation this accurate is challenging due to errors introduced while finding the surface of the star, where $p \to 0$, and therefore the radius R. As a result, we expand k_2 to 20 orders in C. Since k_2 is $\mathcal{O}(C^0)$, this allows for much more accurate results for small C. The compactness has a maximum value of $1/2$, so this expansion converges for all stars.

2.2.4 Estimating the Gravitational Wave Phase Shift due to Tidal Deformability

The tidal deformability λ defined in the last section accurately describes the actual deformation of a neutron star in a binary system only when the neutron star is far from the other compact object. This is for several reasons: As the neutron star approaches the other object, linear perturbation theory and the assumption of a static spacetime used to define λ break down; higher-order multipoles in the metric become important; as the star spirals in, its orbital angular velocity increases and becomes comparable to the frequencies

11

of the star's normal modes, and this enhances the star's response to the tidal perturbation [45]; and, finally, the neutron star may be tidally disrupted before merger. Nevertheless, the tidal deformability turns out essentially to determine the departure of gravitational waveforms from those spinless BBH inspiral in numerical simulations [54, 68, 69].

A post-Newtonian expansion [44] describes the effect of tidal deformability on the phase of the gravitational waveform to linear order in λ:

$$\Delta\Phi_{\text{PN}} = -\frac{3\Lambda}{128\eta}(\pi M f)^{5/3}\left[a_0 + a_1(\pi M f)^{2/3}\right],\qquad(2.2.15)$$

where $\Delta\Phi$ is the difference in gravitational wave phase between a spinless BBH and a BHNS binary, $\Lambda = \lambda/M_{\text{NS}}^5$ is the dimensionless tidal deformability, $M = M_{\text{BH}} + M_{\text{NS}}$ is the total mass of the binary system, $\eta = M_{\text{BH}}M_{\text{NS}}/M^2$ is the symmetric mass ratio, f is the linear frequency of the gravitational radiation, and a_0 and a_1 are functions of η:

$$a_0 = 12[1 + 7\eta - 31\eta^2 - \sqrt{1-4\eta}(1 + 9\eta - 11\eta^2)],$$
$$a_1 = \frac{585}{28}\left[1 + \frac{3775}{234}\eta - \frac{389}{6}\eta^2 + \frac{1376}{117}\eta^3\right.$$
$$\left. - \sqrt{1-4\eta}\left(1 + \frac{4243}{234}\eta - \frac{6217}{234}\eta^2 - \frac{10}{9}\eta^3\right)\right].$$

Where Eq. (2.2.15) is valid, in the early inspiral when the frequency f is low, it allows us to easily compute the phase change (the amplitude of the waveform is also affected by tidal deformability, but in this regime the difference in amplitude is small). However, tidal effects are largest during late inspiral when the frequency is high.

To extend the analytic computation to late inspiral, Lackey *et al.* [54] fit the amplitude and phase of the gravitational waveforms of neutron star-black hole inspirals to the results of numerical simulations, for black hole spins χ_{BH} between -.5 and .75, and mass ratio $M_{\text{BH}}/M_{\text{NS}}$ in the range 2 to 5. In these simulations, the neutron stars are modeled as piecewise polytropes. The resulting expressions (below) depend on post-Newtonian theory for low frequencies, when the neutron star is still far from the black hole. At high frequencies, the fits to numerical results take over:

$$A = \begin{cases} A_{\text{PN}}, & Mf \leq .01 \\ A_{\text{PN}}e^{-\eta\Lambda B(\Lambda,\eta,\chi_{\text{BH}})(Mf-.01)^3}, & Mf > .01 \end{cases}\qquad(2.2.16)$$

$$\Delta\Phi = \begin{cases} \Delta\Phi_{\mathrm{PN}}(Mf), & Mf \leq .02 \\ -\eta\Lambda E(\eta, \chi_{\mathrm{BH}})(Mf - .02)^{5/3} + \Delta\Phi_{\mathrm{PN}}(.02) + (Mf - .02)\Delta\Phi'_{\mathrm{PN}}(.02), & Mf > .02. \end{cases}$$

$$(2.2.17)$$

Here the subscript PN indicates the corresponding result from post-Newtonian theory; B is a function of Λ, η, and χ_{BH}; and E is a function of η and χ_{BH}. The parameters of B and E were determined by the numerical fit. In particular,

$$B = e^{b_0 + b_1\eta + b_2\chi_{\mathrm{BH}}} + \Lambda e^{c_0 + c_1\eta + c_2\chi_{\mathrm{BH}}},$$

with

$$\{b_0, \ b_1, \ b_2\} = \{-64.985, \ -2521.8, \ 555.17\},$$

$$\{c_0, \ c_1, \ c_2\} = \{-8.8093, \ 30.533, \ 0.6496\}$$

as the fitting parameters. Similarly,

$$E = e^{g_0 + g_1\eta + g_2\chi_{\mathrm{BH}} + g_3\eta\chi_{\mathrm{BH}}},$$

with

$$\{g_0, \ g_1, \ g_2, \ g_3\} = \{-1.9051, \ 15.564, \ -0.41109, \ 5.7044\}.$$

The part of B that is independent of Λ is sensitive to the binary parameters due to the large fitting parameters b_0, b_1, and b_2; it can be as large as ~ 3 for large mass ratio and positive black hole spin and essentially zero for small mass ratio and negative black hole spin. The coefficient of Λ in B varies between $\sim .002$ and $\sim .2$, depending on the same binary parameters. As we will see, Λ itself is very sensitive to the mass of the neutron star. Meanwhile, E varies between $\sim .6$ and ~ 9, with typical values of ~ 2.

While high tidal deformabilities increase $|\Delta\Phi|$ relative to a point-particle waveform at a given frequency f, they also cause stars to be tidally disrupted earlier in the inspiral, damping the resulting gravitational waves. We define the cutoff frequency f_{cutoff} to be the frequency at which effects from tidal deformation dampen the amplitude by a factor of e relative to the post-Newtonian waveforms. To estimate the total effect of tidal

deformability on the phase of the waveform throughout the inspiral, we chose to evaluate $\Delta\Phi$ at f_{cutoff}.

The errors in the fitting parameters reported in [54] correspond to errors in $\Delta\Phi(Mf_{\text{cutoff}})$ of $\sim 15\%$ for typical binary parameters. The $\Delta\Phi$-values reported below should therefore not be taken as accurate predictions of the tidally-induced phase shift. Still, we expect that applying this fit to the matched causal EOS yields an upper limit on $|\Delta\Phi|$ with roughly the same error, especially considering the emphasis in [54] on avoiding over-fitting and the lower errors reported for larger Λ-values. A more accurate calculation of the phase shift from BHNS or BNS systems with our causal EOS requires numerical simulations (now in progress for BNS systems [70]) or use of the EOB formalism.

2.3 Results

Most neutron stars observed by gravitational waves in binary inspiral are likely to have masses in or near the 1.25 $M_\odot$ to 1.45 $M_\odot$ range seen in binary neutron star systems, a range consistent with formation from an initial binary of two high-mass stars. We will see that the causal limit on the dimensionless deformability Λ is a monotonically decreasing function of M and is therefore more stringent for higher mass stars. On the other hand, the fraction of matter above nuclear density is smaller in a low-mass neutron star, and that fact limits the effect of a causal EOS above nuclear density. The net result is that the limit on Λ set by causality is close to the values of Λ associated with candidate neutron-star EOSs for matching densities near nuclear density.

2.3.1 Effect of Matching Density on Constraints

To understand the results we present in this section, it is helpful first to consider models for which the causal form (2.2.2) extends to the surface of the star, where $p = 0$. (Here we follow Brecher and Caporaso [56] and Lattimer [57].) That is, we consider models based on the EOS

$$p = \epsilon - \epsilon_{\text{S}}, \tag{2.3.1}$$

and having finite energy density ϵ_S at the surface of the star. Because the only dimensionful constant is ϵ_S, having (in gravitational units) dimension $length^{-2}$, and the mass M and radius R each have dimension $length$, we have the exact relations

$$M_{\mathrm{max}} \propto \epsilon_{\mathrm{S}}^{-1/2}, \qquad R_{\mathrm{max}} \propto \epsilon_{\mathrm{S}}^{-1/2}, \tag{2.3.2}$$

where R_{max} is the maximum radius among models with central density greater than ϵ_{nuc} (low-density models have larger radii). Because the deformability λ has dimension $length^5$, we similarly have

$$\lambda_{\mathrm{max}} \propto \epsilon_{\mathrm{S}}^{-5/2}. \tag{2.3.3}$$

Using this truncated causal EOS is equivalent to taking $\epsilon_{\mathrm{S}} = \epsilon_{\mathrm{match}}$ in the matched causal EOS and discarding the envelope of the star below $\epsilon_{\mathrm{match}}$.

We emphasize that the truncated EOS (2.3.1) is used only heuristically, to explain the near power-law dependence on $\epsilon_{\mathrm{match}}$ of the maximum mass, radius, and deformability. (The exact dependence of the maximum mass, radius, and deformability on $\epsilon_{\mathrm{match}}$ is reported below.) Because the truncated EOS sets the pressure to zero below $\epsilon_{\mathrm{match}}$, it underestimates the maximum radius and deformability. As noted earlier, to obtain a conservatively large upper limit on maximum deformability, we use the matched causal EOS (2.2.3), which has a stiff candidate EOS for $\epsilon < \epsilon_{\mathrm{match}}$.[3]

---

[3] There is something paradoxical in using the truncated EOS (2.3.1) as an approximation to the EOS that gives the largest possible neutron stars: As Lattimer [57] points out (following Koranda *et al.* [71]), this same EOS gives maximally compact neutron stars, stars with the *smallest* possible radius for a given mass, among all EOSs consistent with a maximum mass at or above a largest observed value, M_{observed}. In these and other papers [72, 73], Eq. (2.3.1) is chosen so that the softest possible EOS (namely $p = 0$) is used up to high density; the stiff causal EOS above that density then allows $M_{\mathrm{max}} \geq M_{\mathrm{observed}}$. The resolution is this: For a *fixed maximum mass*, Eq. (2.3.1) yields neutron stars with the smallest possible radii. On the other hand, *for a fixed $\epsilon_{\mathrm{match}}$* (i.e. for a given density up to which we assume a known EOS), Eq. (2.2.3) gives neutron stars with the largest possible radii; and, for low matching and surface densities, the difference between the matched causal EOS (2.2.3) and the truncated EOS (2.3.1) becomes negligible. Equivalently, $\epsilon_{\mathrm{match}} \to 0$ corresponds to $M_{\mathrm{max}} \to \infty$, and the difference between the softest and the stiffest possible EOSs vanishes as $M_{\mathrm{max}} \to \infty$. Physically, this happens because a stiff EOS is required to support large masses.
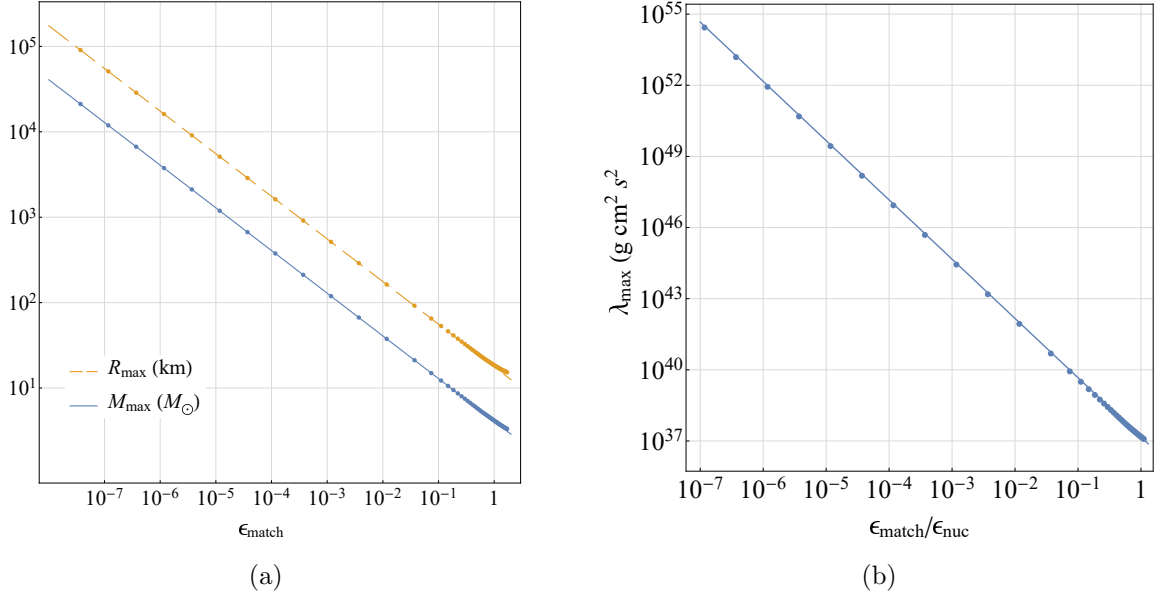
Figure 2 : The (a) maximum radius, mass, and (b) tidal deformability are plotted against the matching density. The behavior of all three quantities follow a power law except at high ϵ_{match}, with the best-fit lines given by Eq. (2.3.5).

For $\epsilon_{\text{match}} \lesssim \epsilon_{\text{nuc}}$, where

$$\epsilon_{\text{nuc}} = 2.7 \times 10^{14} \text{ g/cm}^3 \qquad (2.3.4)$$

is nuclear saturation density (the central density of large nuclei), the contribution of the envelope to mass and radius is small enough that the dependence on ϵ_{match} is very nearly the dependence on ϵ_{S} in the truncated star: M_{max} and R_{max} are each nearly proportional to $\epsilon_{\text{match}}^{-1/2}$, and λ_{max} is nearly proportional to $\epsilon_{\text{match}}^{-5/2}$, where M_{max} is the maximum neutron-star mass consistent with causality and with a low density EOS below ϵ_{match}; and R_{max} and λ_{max} are again the corresponding maximum radius and deformability among models with central density greater than ϵ_{nuc}. This behavior can be seen in Figs. 2(a) and 2(b), where linear least-squares fits to the leftmost 10 data points in each plot satisfy

$$M_{\text{max}} = (4.1 \ M_{\odot})(\epsilon_{\text{match}}/\epsilon_{\text{nuc}})^{-.4999}, \qquad (2.3.5a)$$

$$R_{\text{max}} = (17 \text{ km})(\epsilon_{\text{match}}/\epsilon_{\text{nuc}})^{-.4990}, \qquad (2.3.5b)$$

$$\lambda_{\text{max}} = (1.3 \times 10^{37} \text{g cm}^2 \text{ s}^2)(\epsilon_{\text{match}}/\epsilon_{\text{nuc}})^{-2.4996}. \qquad (2.3.5c)$$

The rightmost data points in each plot diverge from the line because, at higher matching densities, a larger envelope obeys the low-density (MS1) EOS.

16
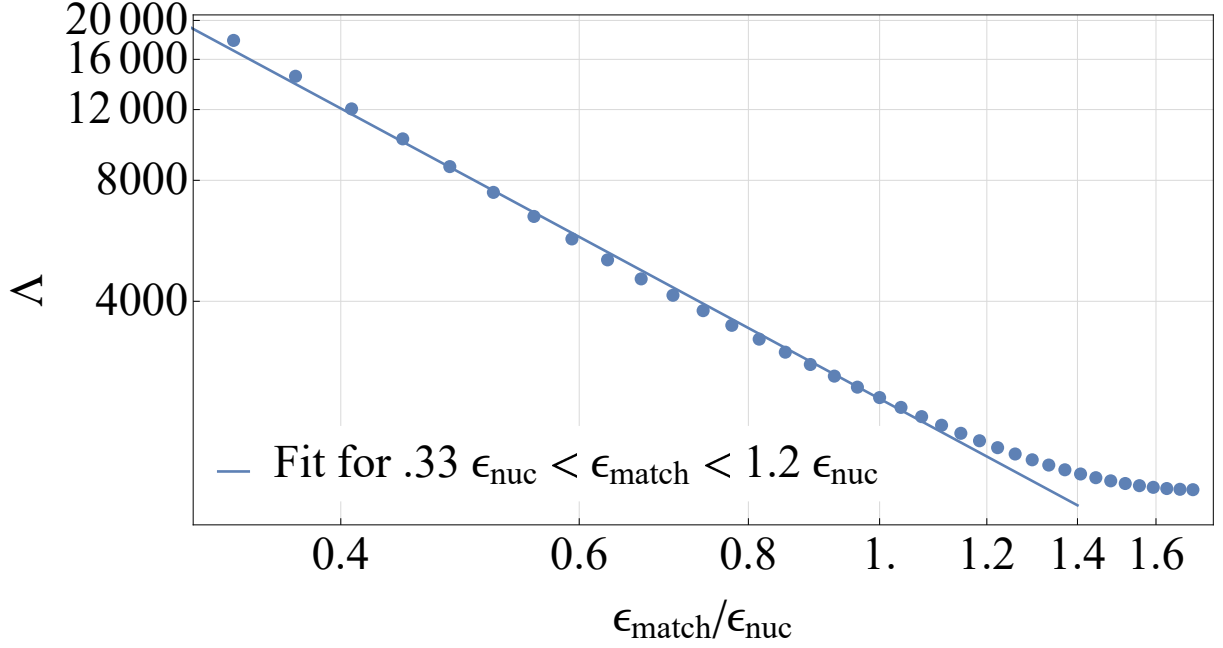
Figure 3 : The dependence of the dimensionless tidal deformability $\Lambda_{1.4}$ of $1.4 M_\odot$ stars on matching density is shown on a log-log plot. The behavior approximates a power law for $\epsilon \lesssim \epsilon_{\mathrm{nuc}}$, with the best fit given by Eq. (2.3.6).

Of greater astrophysical relevance than the upper limit on λ, however, is the constraint on the dimensionless tidal deformability, $\Lambda = \lambda/M_{\mathrm{NS}}^5 = \frac{2}{3}k_2 R^5/M^5$, that governs the waveform of a binary inspiral. As we will see below, because of the factor M_{NS}^{-5}, Λ is monotonically decreasing with increasing mass for central density above $\epsilon_{\mathrm{match}}$. The physically interesting constraint on Λ is then a constraint at known mass: Inspiral waveforms detected with a high enough signal-to-noise ratio to measure their tidal departure from point-particle inspiral will also have the most accurately measured neutron-star masses. The dependence of Λ on $\epsilon_{\mathrm{match}}$ for fixed mass cannot be found from the previous dimensional analysis, but it is easy to see that $\Lambda(M, \epsilon_{\mathrm{match}})$ is a monotonically decreasing function of $\epsilon_{\mathrm{match}}$: As $\epsilon_{\mathrm{match}}$ increases and less of the star is governed by the stiffer causal EOS, the star becomes more compact: R decreases at fixed M. In addition, as the density profile becomes more centrally condensed, the tidal Love number k_2 decreases, because, for a given radius, the external tidal force has less effect on a more centrally condensed star. Decreasing R and k_2 gives a sharp decrease in Λ, as shown in Fig. 3 for a $1.4 M_\odot$

17

star. For $.33\epsilon_{\mathrm{nuc}} < \epsilon_{\mathrm{match}} < 1.2\epsilon_{\mathrm{nuc}}$ we find a near power-law dependence,

$$\Lambda_{1.4} = 2400(\epsilon_{\mathrm{match}}/\epsilon_{\mathrm{nuc}})^{-1.8}. \tag{2.3.6}$$

2.3.2 Comparison between Constraint and Results from Candidate EOSs
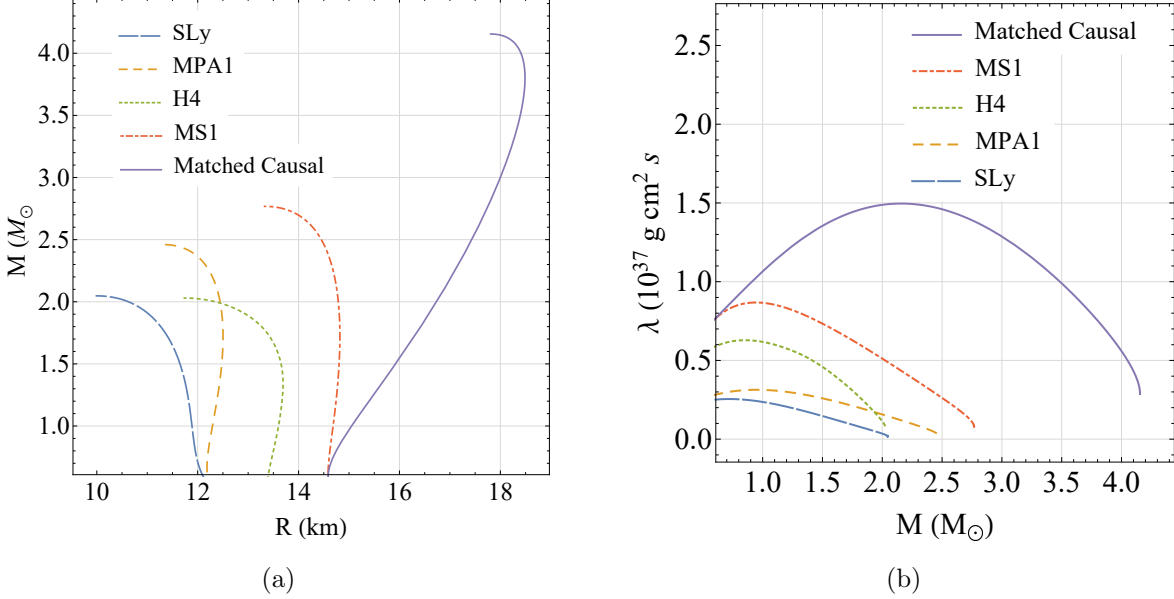
Figure 4 : (a) The mass-radius relation for the matched causal EOS with $\epsilon_{\mathrm{match}} = \epsilon_{\mathrm{nuc}}$ and for candidate neutron-star equations of state that display the range of uncertainty in stiffness.
(b) Tidal deformability versus mass for stars based on the same EOSs. The top solid curve, displaying the tidal deformability of stars based on the matched causal EOS, is an upper limit set by causality on tidal deformability. Stars based on softer EOSs have smaller tidal deformabilities.

We begin by displaying the limit set by causality on the dimensionful tidal deformability λ as a function of mass, with $\epsilon_{\mathrm{match}}$ taken to be ϵ_{nuc}. There is remaining uncertainty in the equation of state at ϵ_{nuc}, and we obtain a conservative upper limit by matching to the MS1 EOS [59], which is particularly stiff for $\epsilon \lesssim \epsilon_{\mathrm{nuc}}$.

The mass-radius relation for the family of neutron stars obeying the matched causal EOS is indicated by "Matched Causal" in Fig. 4(a). As we saw in Eqs. (2.3.5), matching to MS1 below ϵ_{nuc} is a weak constraint, giving $M_{\mathrm{max}} = 4.1 M_{\odot}$ and $R_{\mathrm{max}} > 18$ km, both significantly larger than their values for any of the candidate EOSs shown. These candidate EOSs include SLy [74], which is one of the softest EOSs that allow for $2M_{\odot}$ neutron stars, MPA1 [75], which is slightly stiffer, H4 [76], which is stiff at low densities
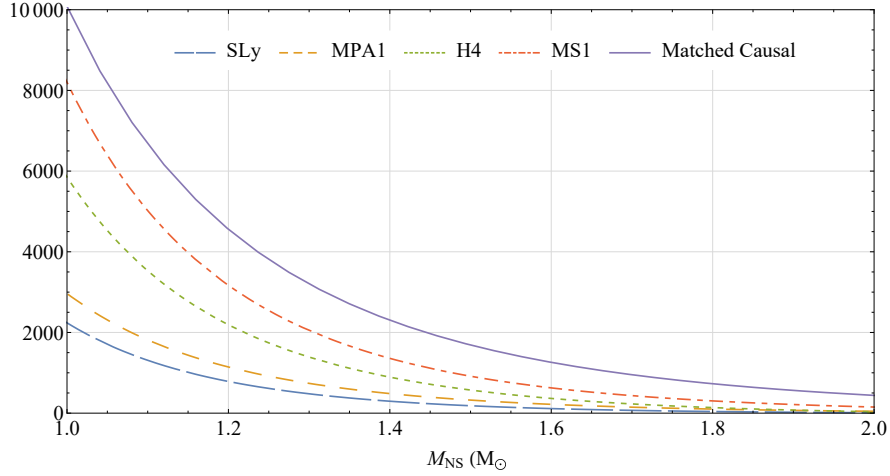
Figure 5 : The dimensionless tidal deformability Λ is plotted against mass for several EOSs. For any given mass, the Matched Causal EOS places an upper limit on the value of Λ.

and soft at high densities, and MS1 [59], which is particularly stiff at all densities. The maximum masses allowed by these EOSs are all between 2 and 2.8 $M_\odot$, and the radii are all between 10 and 15 km.

In Figure 4(b), the top curve displays an upper limit on λ as a function of neutron-star mass obtained from the matched causal EOS. The comparison $\lambda(M)$ curves for the same candidate EOSs of Fig. 4(a) show the decreasing deformability associated with stars of decreasing stiffness and radius. Note, however, that the maximum value of λ for each EOS occurs at a smaller mass than that of the model with maximum radius. This is due to the increase in central condensation as the mass increases, resulting in an decrease in k_2. The maximum of the $\lambda(M)$ curve for the matched causal EOS gives the mass-independent upper limit $\lambda < 1.5 \times 10^{37}$ g cm^2 s^2, for $\epsilon_{\rm match} = \epsilon_{\rm nuc}$, with dependence on $\epsilon_{\rm match}$ given by Eq. (2.3.5c) for smaller matching density.

The corresponding upper limit $\Lambda_{\rm max}(M)$ on the dimensionless deformability is given by the top curve in Fig. 5, for $\epsilon_{\rm match} = \epsilon_{\rm nuc}$. (The dependence on $\epsilon_{\rm match}$ was shown in Fig. 3 for a representative $1.4 M_\odot$ star.) Since $\Lambda \propto C^{-5}$, Λ is large for small masses and relatively small for larger masses. As a result, it is not meaningful to speak of a mass-independent maximum of Λ, but it is meaningful to compare Λ-values at constant mass. The most striking feature of Fig. 5 is how close the curve $\Lambda_{\rm max}(M)$ is to the range of Λ
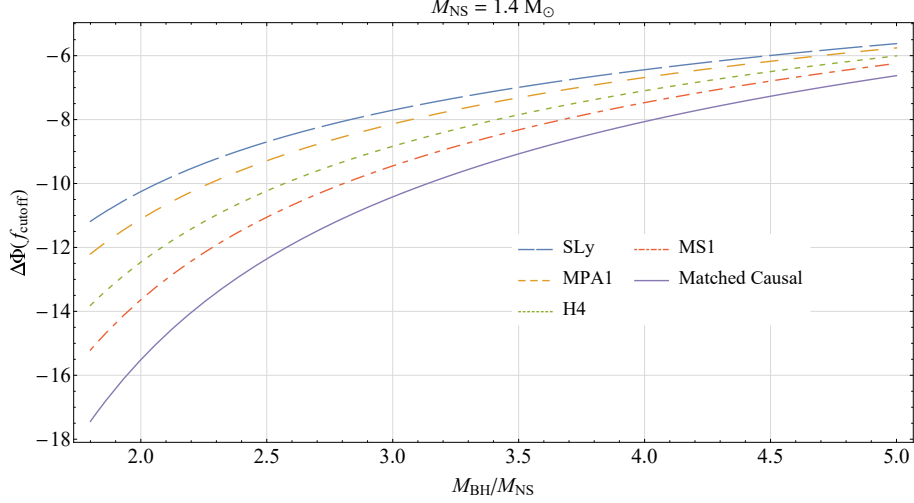
Figure 6 : The estimated total gravitational wave phase shift $\Delta\Phi(f_{\text{cutoff}})$ corresponding to a BHNS binary with $M_{\text{NS}} = 1.4\ M_\odot$ and $\chi_{\text{BH}} = 0$ is plotted against the mass ratio for several EOSs. For a given mass ratio, $|\Delta\Phi(f_{\text{cutoff}})|$ is larger for stiffer EOSs, and the Matched Causal EOS provides a constraint on it. In general, $|\Delta\Phi(f_{\text{cutoff}})|$ decreases with the mass ratio.

allowed by current candidate EOSs. This stringent constraint on Λ is in sharp contrast to the larger departures of the curves giving $R_{\max}(M)$ and $\lambda_{\max}(M)$ in Fig. 4 from the corresponding curves for candidate EOSs. For 1.4 $M_\odot$ stars, for example, it places the constraint that $\Lambda \leq 2300$. For comparison, 1.4 $M_\odot$ stars resulting from the SLy, MPA1, H4, and MS1 EOSs have Λ-values of 300, 490, 900, and 1400, respectively. Furthermore, gravitational-wave data from the one BNS coalescence detected so far [6] has constrained Λ observationally. In particular, with 90% confidence we now know [7] that $70 < \Lambda < 580$ for 1.4 $M_\odot$ neutron stars. These values are low enough to not only be consistent with our upper limit $\Lambda_{\max}(M)$ but also to strongly disfavor MS1 as a candidate EOS.

One might naively expect $|\Delta\Phi(f_{\text{cutoff}})|$ to increase monotonically with Λ and therefore to decrease monotonically with the mass M_{NS} of the neutron star (note that, although $\Delta\Phi$ is positive when evaluated at a given time, it is negative when evaluated at a given frequency). This is not the case, because while $|\Delta\Phi|$ increases with Λ (and decreases with M_{NS}) when evaluated at a fixed frequency, f_{cutoff} decreases monotonically with Λ (and increases monotonically with M_{NS}). That is, stars with high dimensionless tidal deformability are tidally disrupted at a larger distance from the black hole, corresponding to a smaller orbital (and gravitational wave) frequency. A neutron star with high tidal

20
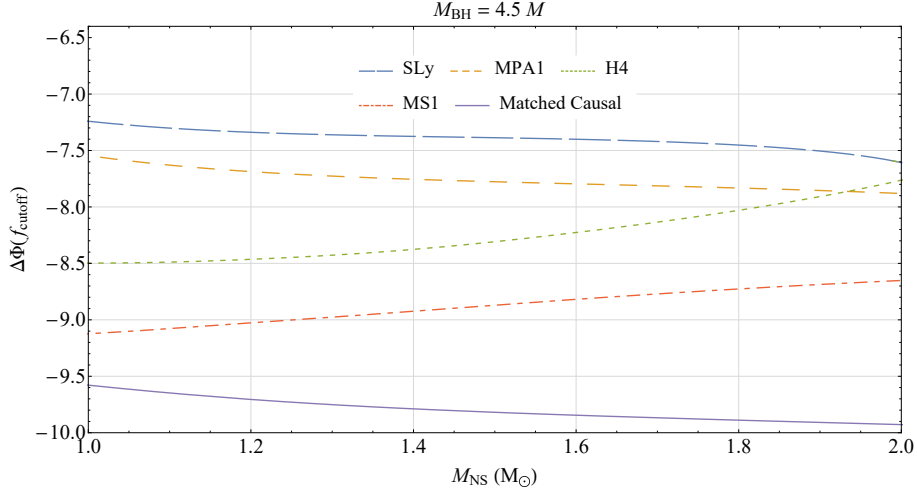
Figure 7 : The estimated total gravitational wave phase shift $\Delta\Phi(f_{\text{cutoff}})$ corresponding to a BHNS binary with $M_{BH} = 4.5\ M_\odot$ and $\chi_{\text{BH}} = 0$ is plotted against neutron star mass for several EOSs. For a given mass, $|\Delta\Phi(f_{\text{cutoff}})|$ is larger for stiffer EOSs, and the Matched Causal EOS provides a constraint on it. The dependence of $|\Delta\Phi(f_{\text{cutoff}})|$ on neutron star mass is complicated and changes with the EOS used.

deformability therefore has fewer cylces during which to accumulate phase relative to a point-particle. As a result, the effect of M_{NS} on $|\Delta\Phi(f_{\text{cutoff}})|$ is complicated, and depends on EOS and the parameters of the binary.

Nevertheless, stiffer EOSs result in larger values of $|\Delta\Phi|$ for given neutron star masses or mass ratios. As can be seen in Fig. 6, $|\Delta\Phi(f_{\text{cutoff}})|$ decreases with mass ratio for all EOSs. On the other hand, $|\Delta\Phi(f_{\text{cutoff}})|$ has complicated behavior with respect to neutron star mass for all EOSs when the spin of the companion black hole is zero (Fig. 7). In addition, one can see in Fig. 6 and Fig. 7 that $|\Delta\Phi(f_{\text{cutoff}})|$ increases with the stiffness of the EOS, and is largest for our EOS, but only by a few radians at most. Here, based on our estimate of $\Delta\Phi$, the constraint set by causality is remarkably strong, stronger than the already stringent constraint on Λ: $\Delta\Phi_{\text{max}}(M)$ differs from its value for the stiffest candidate equation of state by less than 14%. The strength of the causal constraint is due to (a) the fact that Λ is largest at small mass, where the causal EOS governs the smallest fraction of the star, and (b) a smaller cutoff frequency for the stiffest EOSs that reduces the time over which the phase can accumulate.

As shown in Fig. 8, for a given black hole mass M_{BH} and zero black hole spin χ_{BH},
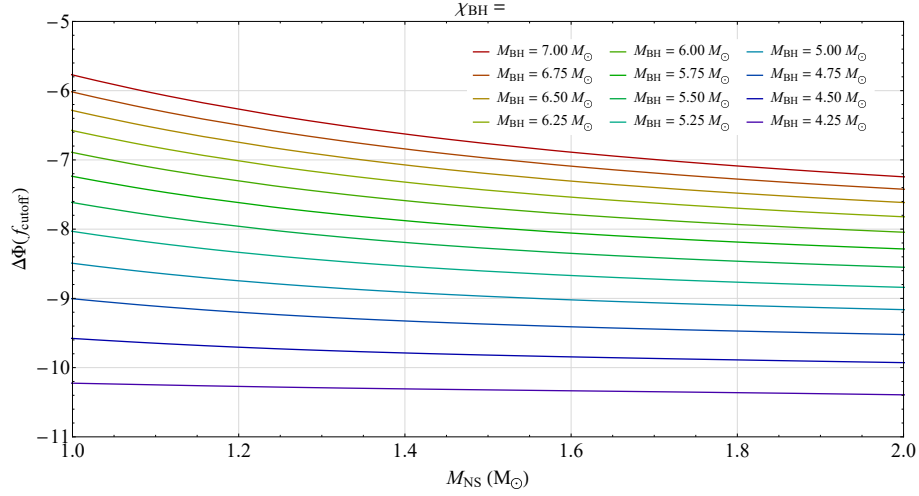
Figure 8 : The estimated constraint on $\Delta\Phi(f_{\text{cutoff}})$ is plotted against the mass of a neutron star for several different black hole masses and a black hole spin of 0. We expect that the absolute value of $\Delta\Phi$ would be lower for any real BHNS binary. The constraint on $|\Delta\Phi|$ decreases with both neutron star mass and black hole mass.

$|\Delta\Phi(f_{\text{cutoff}})|$ increases with M_{NS} for the Matched Causal EOS. In addition, for a given M_{NS}, $|\Delta\Phi(f_{\text{cutoff}})|$ decreases with M_{BH}. Changing χ_{BH} can change the qualitative behavior of $|\Delta\Phi(f_{\text{cutoff}})|$, as can be seen in Fig. 9. In particular, a corotating companion black hole tends to make $|\Delta\Phi(f_{\text{cutoff}})|$ increase with mass, while antirotating companions tend to make $|\Delta\Phi(f_{\text{cutoff}})|$ decrease with mass. For a given M_{NS}, higher (corotating) spins result in smaller $|\Delta\Phi(f_{\text{cutoff}})|$, but the effect decreases with increasing M_{NS}.

Figure 10 shows how $|\Delta\Phi(f_{\text{cutoff}})|$ varies with mass ratio for several neutron star masses and 0 black hole spin. For a given M_{NS}, $|\Delta\Phi(f_{\text{cutoff}})|$ decreases with increasing mass ratio. For a given mass ratio, $|\Delta\Phi(f_{\text{cutoff}})|$ decreases with neutron star mass. The effect decreases in magnitude as the mass ratio increases.

Finally, Fig. 11 shows $|\Delta\Phi(f_{\text{cutoff}})|$ varying with mass ratio for several black hole spins and $M_{\text{NS}} = 1.4\,M_{\odot}$. $|\Delta\Phi(f_{\text{cutoff}})|$ decreases with mass ratio regardless of the value of χ_{BH}, but for a given mass ratio, $|\Delta\Phi(f_{\text{cutoff}})|$ decreases with χ_{BH}; it is smallest for corotating black holes, and largest for antirotating black holes.
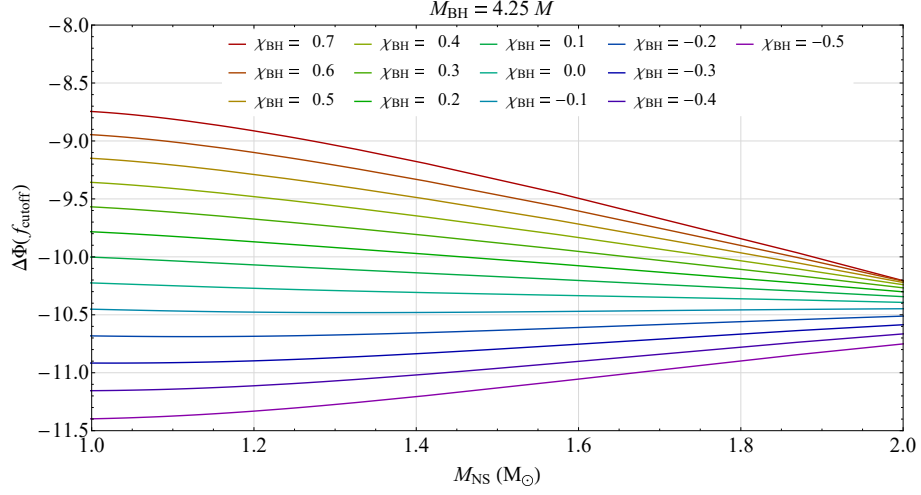
Figure 9 : The estimated constraint on $\Delta\Phi(f_{\text{cutoff}})$ is plotted against the mass of a neutron star for several different black hole spins and a black hole mass of $4M_\odot$. Different black hole spins can change how $\Delta\Phi$ qualitatively changes with neutron star mass, and $\Delta\Phi$ depends more strongly on χ_{BH} for smaller neutron star masses than for larger neutron star masses.
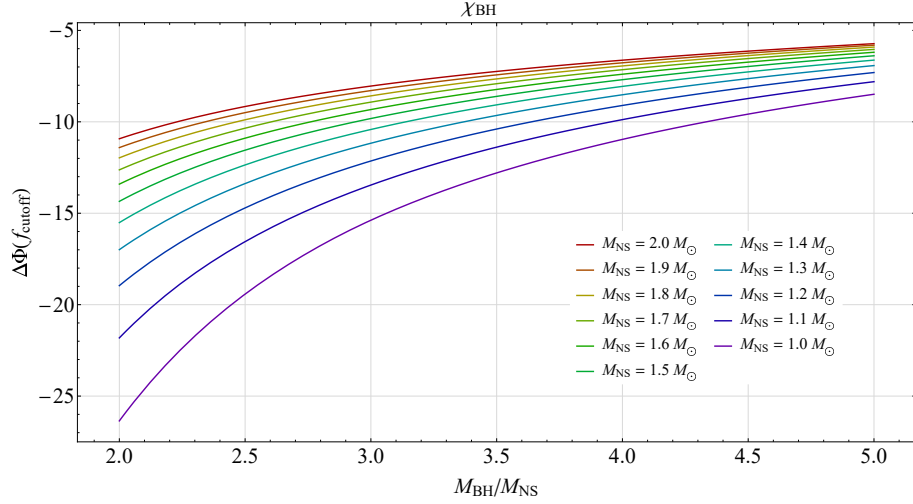
Figure 10 : The estimated constraint on $|\Delta\Phi(f_{\text{cutoff}})|$ for BHNS binaries with $\chi_{BH} = 0$ is plotted against the mass ratio for several neutron star masses. $|\Delta\Phi(f_{\text{cutoff}})|$ decreases both with mass ratio and with neutron star mass.
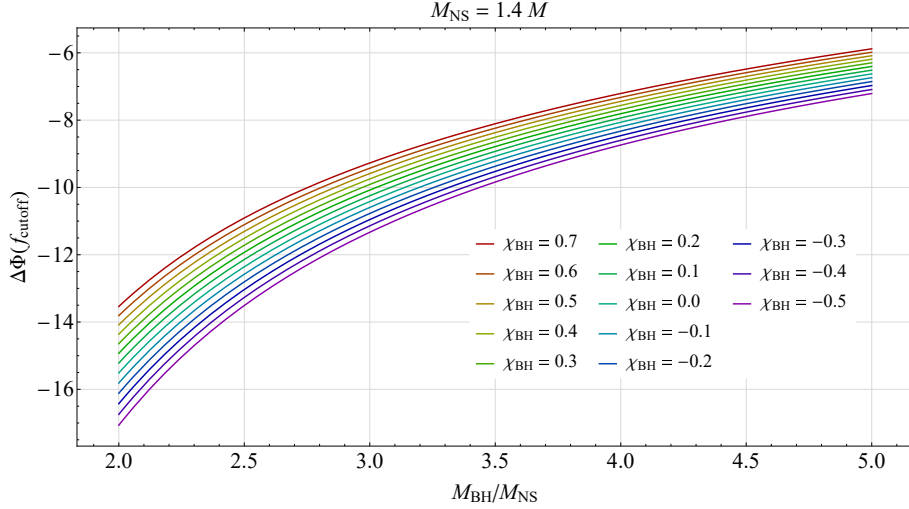
Figure 11 : The estimated constraint on $|\Delta\Phi(f_{\text{cutoff}})|$ for BHNS binaries with $M_{NS} = 1.4 \ M_\odot$ is plotted against the mass ratio for several black hole spins. The value of $|\Delta\Phi(f_{\text{cutoff}})|$ decreases with mass ratio and with spin.

2.4   Conclusion

By using a stiffest causal EOS consistent with causality at high density, matched to the MS1 [59] EOS below a density ϵ_{match}, we have set upper limits on the quadrupole tidal deformability λ and on the dimensionless tidal deformability Λ as a function of neutron star mass. The limit on Λ, given by Eq. (2.3.6) for a 1.4 $M_\odot$ neutron star, is conservative, because we have matched to an EOS (MS1) that is stiff below nuclear density: With this low-density EOS and a match at ϵ_{nuc}, the corresponding upper mass limit is $4.1 M_\odot$. We now also have observational reasons to believe that Λ cannot exceed our upper limit: the gravitational-wave event reported in reference [6] constrains Λ for a 1.4 $M_\odot$ neutron star to be between 70 and 580 with 90% confidence. This disfavors even MS1 as a candidate EOS, indicating that even our low-density EOS is stiffer than actual neutron star matter. Using the constraint on dimensionless tidal deformability and the Lackey *et al.* analytic fit to numerical data [54], we then estimated the induced phase shift of a BHNS inspiral and merger waveform.

The implied upper limit on the accumulated phase shift $|\Delta\Phi|$ at merger depends on the parameters of the binary, but it is surprisingly close to the range of phase shifts seen in candidate EOSs. Assuming one can neglect resonant interactions of the tidal field with

24

neutron-star modes, we think this conclusion is secure. We emphasize, however, that our upper limits on $|\Delta\Phi|$ rely on an analytic expression based on full numerical simulations for models with a set of EOSs significantly less stiff than the matched causal EOS. Work *has* begun on numerical simulations to obtain an upper limit on the departure of double neutron star inspiral waveforms from the point-particle (or spinless BBH) case.

2.5   Appendix: Comments on causality and sound speed

With the assumption that the equilibrium equation of state of the neutron star and its perturbations are governed by the same one-parameter equation of state, causality implies $dp/d\epsilon < 1$. That is, as mentioned in Section 2.2.1, the time-evolution of a barotropic fluid is described by a hyperbolic system whose characteristics lie within the light cone precisely when $dp/d\epsilon < 1$ [77]. The frequencies of stellar perturbations, however, are too high for the temperature of a fluid element and the relative density Y_i of each species of particle to reach their values for the background fluid at the same pressure: Heat flow and nuclear reactions are incomplete.

Because of this, one cannot precisely identify the maximum speed of signal propagation in the fluid with the equilibrium value

$$\sqrt{\left.\frac{dp}{d\epsilon}\right|_{\text{equilibrium}}} := \sqrt{\frac{dp/dr}{d\epsilon/dr}}.$$

If short wavelength, high frequency perturbations are too rapid for heat flow and for nuclear reactions to proceed, their speed of propagation is

$$v_{\text{sound}} = \sqrt{(\partial p/\partial\epsilon)|_{s,Y_i}}. \tag{2.5.1}$$

One therefore expects causality to imply

$$\left.\frac{\partial p}{\partial\epsilon}\right|_{s,Y_i} < 1. \tag{2.5.2}$$

This is known to be true for a relativistic fluid with a two-parameter EOS of the form $p = p(\epsilon, s)$: Its dynamical evolution then involves heat flow and is governed by the equations of a dissipative relativistic fluid. Causal theories of this kind were first introduced by

Israel and Stewart [78, 79] and by Liu *et al.* [80]. The general class of such theories was analyzed by Geroch and Lindblom [58], who pointed out that, for dissipative fluids obeying $p = p(\epsilon, s)$, causality implies the inequality (2.5.2),

$$\left.\frac{\partial p}{\partial \epsilon}\right|_s < 1. \tag{2.5.3}$$

Now a star is unstable to convection if

$$\left.\frac{dp}{d\epsilon}\right|_{\text{equilibrium}} > \left.\frac{\partial p}{\partial \epsilon}\right|_{s,Y_i}. \tag{2.5.4}$$

Thus, *for a locally stable spherical star (a self-gravitating equilibrium configuration of a relativistic dissipative fluid) based on a two-parameter EOS $p = p(\epsilon, s)$, causality implies*

$$\sqrt{\left.\frac{dp}{d\epsilon}\right|_{\text{equilibrium}}} < 1. \tag{2.5.5}$$

Thus, at least for two-parameter dissipative fluids, one can rule out the possibility that dispersion in a dissipative fluid could lead to a group velocity smaller than the phase velocity (see, for example Bludman and Ruderman [81]) v_{sound} and thereby allow $v_{\text{sound}} > 1$ without superluminal signal propagation.

For a dissipative fluid obeying a multi-parameter EOS of the form $p = p(\epsilon, s, Y_i)$, we are not aware of a general proof that causality implies the inequality (2.5.2). One has only the weaker statement, *for a locally stable spherical star based on an EOS equation of state $p = p(\epsilon, s)$, $v_{\text{sound}} < 1$ implies the equilibrium inequality (2.5.5).* There is one additional caveat: The core of a neutron star is likely to be a superfluid, and taking that into account could lead to small corrections in the speed of sound.

Finally, we note that for candidate EOSs, although the inequality $v_{\text{sound}} < 1$ is stronger than the the equilibrium inequality (2.5.5) used to place upper limits on mass, radius and, in the present paper, on deformability, the difference is small. The fractional difference

$$\frac{\sqrt{dp/d\epsilon|_{\text{equilibrium}}} - \sqrt{(\partial p)/(\partial \epsilon)|_{s,Y_i}}}{\sqrt{(\partial p)/(\partial \epsilon)|_{s,Y_i}}} \tag{2.5.6}$$

is primarily due to composition (to the constant values of Y_i), and it is less than 5%. (It is approximately half the fractional difference between the adiabatic index $\gamma = \Gamma_1$

and the index Γ governing the equilibrium configuration; the difference determines the Brunt-Vaïsälä frequency, a characteristic frequency of g-modes, and an estimate can be found, for example, in Ref. [82].)

Chapter 3

Scalar Self-Force and the Method of Hikida

3.1 Introduction

This chapter will center on work I did with Thomas Linz and my advisor Alan Wiseman, with help from John Friedman. The results and methods of this chapter were previously reported in Linz's dissertation [83].

The end result of this work was an analytical Post-Newtonian expression for the self-force on an accelerated scalar charge moving on a Schwarzschild background. Before we can understand that result, we must discuss black hole perturbation theory in general, and specifically the method pioneered by Mano, Suzuki, and Takasugi [84] to solve for homogeneous solutions to the Teukolsky equation [85]. We will then briefly introduce the concept of self-force—where a particle feels a force due to its own field—and how self-force calculations are carried out. Finally, we will introduce the algorithm developed by Hikida *et al.* [8, 9] which allows us to solve for the self-force analytically to high Post-Newtonian order.

3.2 Black Hole Perturbation Theory

As mentioned in section 1.1, it is difficult to study systems of more than one object in General Relativity. One way to do so is to consider small perturbations to known solutions of Einstein's equation. The next two chapters will consider perturbations to the Schwarzschild spacetime, which describes a non-rotating black hole. The Schwarzschild spacetime is a special case among black hole spacetimes. The Kerr solution to Einstein's equation describes spinning black holes, and the Kerr-Newman solution describes electrically charged black holes. In reality, we do not expect black holes to be electrically charged, so the Kerr solution describes the most general astrophysical black holes. In Boyer-Lindquist coordinates the Schwarzschild solution's spacetime interval is given by

$$ds^2 = -f(r)dt^2 + \frac{1}{f(r)}dr^2 + r^2 d\theta^2 + r^2 \sin^2\theta d\phi^2, \qquad (3.2.1)$$

with

$$f(r) = 1 - \frac{2M}{r}.$$

3.2.1 The Bardeen-Press Equation

The Bardeen-Press equation [86] describes scalar perturbations to the Schwarzschild spactime:

$$\left\{ \partial_r[(r^2 f)^{s+1}\partial_r] + (r^2 f)^s \left[\frac{-r^2}{f}\partial_t^2 + \frac{1}{\sin\theta}\partial_\theta(\sin\theta\partial_\theta) + \frac{1}{\sin^2\theta}\partial_\phi^2 \right.\right.$$
$$\left.\left. +2is\frac{\cos\theta}{\sin^2\theta}\partial_\phi - 2s\frac{r-3M}{f}\partial_t - \frac{s^2}{\sin^2\theta} + s(s+1) \right] \right\} \psi_s = 4\pi r^2 (r^2 f)^s T_s, \qquad (3.2.2)$$

where s is the spin-weight of the scalar field and T_s is a source term. The Bardeen-Press equation is a specialization of the Teukolsky equation [85], which gives solutions to perturbations to the Kerr spacetime. This chapter studies a scalar ($s = 0$) field, but we keep s general for now, because in the next chapter we will study gravitational perturbations, which involve scalars of spin-weight ± 2.

3.2.2 The MST Method to solve the homogeneous Teukolsky Equation

Mano, Suzuki, and Takasugi [84], hereafter referred to as MST, developed a method to solve the homogeneous Teukolsky equation in the frequency domain. MST begin by writing

$$\psi_s = e^{-i\omega t} {}_sY_{\ell m}(\theta, \phi) R_{\ell m \omega}(r),$$

where ${}_sY_{\ell m}(\theta, \phi)$ is a spin-weighted spherical harmonic,[1] satisfying

$$\left[\frac{1}{\sin\theta}\partial_\theta(\sin\theta\partial_\theta) + \frac{1}{\sin^2\theta}\partial_\phi^2 + 2is\frac{\cos\theta}{\sin^2\theta}\partial_\phi - \frac{s^2}{\sin^2\theta} \right] {}_sY_{\ell m}(\theta, \phi) = \ell(\ell+1){}_sY_{\ell m}(\theta, \phi).$$
(3.2.3)

The spin-weighted spherical harmonics are generalizations of the spherical harmonics ${}_0Y_{\ell,m}$; their properties will be discussed more in the next chapter. After separating the variables in this way, the equation for $R_{\ell m \omega}$ becomes

$$\frac{d}{dr}\left[(r^2f)^{s+1}\frac{dR_{\ell m \omega}}{dr} \right]$$
$$+ (r^2f)^s \left\{ \frac{r\omega}{f}\left[r\omega + 2is\left(1 - \frac{3M}{r}\right) \right] + \ell(\ell+1) + s(s+1) \right\} R_{\ell m \omega} = 0. \quad (3.2.4)$$

Note that the above equation is independent of m, so that subscript is superfluous. From here on, we drop it, and refer to $R_{\ell m \omega}$ as $R_{\ell \omega}$ instead[2]. MST find two forms of analytical solutions to Eq. (3.2.4): one as an infinite series of hypergeometric functions, and one as a series of Coulomb wave functions. We will primarily use the latter, but the former is necessary to mention because only they are regular on the horizon of the black hole, corresponding to $r = 2M$. Therefore, we must use them to set correct boundary conditions on the horizon.

To get the solution as a series of Coulomb wave functions, MST define $\epsilon \equiv 2M\omega$,

---

[1]The more general Teukolsky equation separates when the angular harmonic is a spin-weighted spheroidal harmonic. Also, since the Teukolsky and Bardeen-Press equations are linear, one can write ψ_s as a sum over an infinite number of Fourier and spherical harmonic modes. For now, this is unnecessary.

[2]Note that this is not true in Kerr; the index m appears explicitly in the radial Teukolsky equation in that case.

$z \equiv \omega r$, and $\zeta \equiv z - \epsilon$. Then, they write[3]

$$R_{\ell\omega} = \phi_c^\nu = \mathrm{Sign}(\omega)^{-\nu} \zeta^{-1-s} f_\nu(\zeta);$$

the relevance and value of ν will soon become apparent. Note that our normalization here differs from that of MST, Hikida *et al.*, and Linz [8, 83, 84]. In particular, we put a factor of $\mathrm{Sign}(\omega)^{-\nu}$ out front. This is to ensure that ω is never raised to the power of ν; instead, $|\omega|$ is. We will see the advantage of this normalization when we write our final expression for ϕ_c^ν. Inserting this expression for $R_{\ell\omega}$ in Eq. (3.2.2) gives the following equation for f_ν:

$$\zeta^2 f_\nu'' + [\zeta^2 + 2(\epsilon + is)\zeta] f_\nu = -\epsilon\zeta(f_\nu'' + f_\nu) + \epsilon(s+1)f_\nu' - \frac{\epsilon(s+1+i\epsilon)(1-i\epsilon)}{\zeta}f_\nu$$
$$+ [\ell(\ell+1) - 3\epsilon^2 - is\epsilon]f_\nu.$$

While this equation—particularly the right-hand side—appears intractable, MST employ a trick: they subtract $\nu(\nu+1)f_\nu$ from each side of the equation, where ν is a heretofore undetermined constant. The equation for f_ν then reads

$$\zeta^2 f_\nu'' + [\zeta^2 + 2(\epsilon + is)\zeta - \nu(\nu+1)]f_\nu$$
$$= -\epsilon\zeta(f_\nu'' + f_\nu) + \epsilon(s+1)f_\nu' - \frac{\epsilon(s+1+i\epsilon)(1-i\epsilon)}{\zeta}f_\nu$$
$$+ [\ell(\ell+1) - \nu(\nu+1) - 3\epsilon^2 - is\epsilon]f_\nu. \tag{3.2.5}$$

MST then let $\nu = \ell + \mathcal{O}(\epsilon)$, which makes Eq. (3.2.5) match the differential equation for Coulomb wave functions in the limit $\epsilon \to 0$. This suggests a representation for f_ν as a series of Coulomb wave functions:

$$f_\nu = \sum_{n=-\infty}^{\infty} i^n \left|\frac{(\nu+1+s+i\epsilon)_n}{(\nu+1-s+i\epsilon)_n}\right|^2 a_n^\nu F_{n+\nu}, \tag{3.2.6}$$

with

$$F_{n+\nu} = e^{-i\zeta}(2\zeta)^{n+\nu}\zeta\frac{(\nu+1-s+i\epsilon)_n}{(2\nu+2)_{2n}}{}_1F_1(n+\nu+1-s+i\epsilon; 2n+2\nu+2; 2i\zeta). \tag{3.2.7}$$

---

[3]This notation differs from that of [84], in which ζ is denoted by z and the Coulomb-type radial function is denoted by R_c^ν. We choose our notation to match that of Hikida *et al.* [8]

31

Here, we use the Pochhammer symbol $(a)_n \equiv \Gamma(a+n)/\Gamma(a)$, and denote by ${}_1F_1$ the regular confluent hypergeometric function:

$$
{}_1F_1(a;b;x) = \sum_{k=0}^{\infty} \frac{(a)_k}{(b)_k} \frac{x^k}{k!}.
$$

We expect that the series (3.2.6) will correspond to a power series in ϵ.

What remains is to solve for ν, which MST call the renormalized angular momentum, and the coefficients a_n^ν. First, MST use the recurrence relations of the Coulomb wave functions to show that a_n^ν satisfies a three-term recurrence relation:

$$
\alpha_n^\nu a_{n+1}^\nu + \beta_n^\nu a_n^\nu + \gamma_n^\nu a_{n-1}^\nu = 0, \tag{3.2.8}
$$

where

$$
\alpha_n^\nu = \frac{i\epsilon|n + \nu + 1 + s + i\epsilon|^2(n + \nu + 1 + i\epsilon)}{(n + \nu + 1)(2n + 2\nu + 3)},
$$

$$
\beta_n^\nu = -\ell(\ell + 1) + (n + \nu)(n + \nu + 1) + 2\epsilon^2 + \frac{\epsilon^2(s^2 + \epsilon^2)}{(n + \nu)(n + \nu + 1)},
$$

and

$$
\gamma_n^\nu = -\frac{i\epsilon|n + \nu - s + i\epsilon|^2(n + \nu - i\epsilon)}{(n + \nu)(2n + 2\nu - 1)}.
$$

We can then introduce ratios of consecutive coefficients:

$$
R_n^\nu = \frac{a_n^\nu}{a_{n-1}^\nu}, \quad L_n^\nu = \frac{a_n^\nu}{a_{n+1}^\nu}. \tag{3.2.9}
$$

The ratios R_n^ν and L_n^ν can be thought of as continued fractions in the parameters appearing in the recurrence relation for a_n^ν:

$$
R_n^\nu = -\frac{\gamma_n^\nu}{\beta_n^\nu + \alpha_n^\nu R_{n+1}^\nu}, \quad L_n^\nu = -\frac{\alpha_n^\nu}{\beta_n^\nu + \gamma_n^\nu L_{n-1}^\nu} \tag{3.2.10}
$$

We are free to choose $a_0^\nu = 1$, as this is essentially a choice of normalization for f_ν. Then, we can solve for a_n^ν with $n \neq 0$ by repeatedly multiplying by the R_n^ν to get the positive-n coefficients, and multiplying by the L_n^ν to get the negative-n coefficients. At first, this seems futile, since to know R_1^ν exactly, one must also know R_2^ν, and so on. However, to find the positive-n coefficients to finite order in ϵ, it is sufficient to know that $R_n^\nu = \mathcal{O}(\epsilon)$ for all $n > 0$. This follows from that fact that, for all $n > 0$, $\alpha_n^\nu = \mathcal{O}(\epsilon)$, $\gamma_n^\nu = \mathcal{O}(\epsilon)$, and

$\beta_n^\nu = \mathcal{O}(1)$. The negative-$n$ coefficients are a bit more complicated; we will discuss them shortly.

In the meantime, it will be useful to see that we can simultaneously solve for ν by requiring that repeatedly applying R_n^ν or L_n^ν gives a consistent set of coefficients; in particular, it must be true that

$$R_{n+1}^\nu L_n^\nu = 1. \tag{3.2.11}$$

If we apply the above equation to the $n = 0$ case and write

$$\nu = \ell + \sum_{k=1}^\infty \nu_k \epsilon^k, \tag{3.2.12}$$

we can solve for ν_1. First, we see immediately from 3.2.11 that $L_0^\nu = \mathcal{O}(\epsilon^{-1})$, since $R_1^\nu = \mathcal{O}(\epsilon)$. This in turn requires that $\beta_0^\nu + \gamma_0^\nu L_{-1}^\nu = \mathcal{O}(\epsilon^2)$. By looking at the expressions for α_n^ν, β_n^ν, and γ_n^ν, one can easily see that, as long as $\ell > 0$, $L_{-1}^\nu = \mathcal{O}(\epsilon)$.[4] Since $\gamma_0^\nu = \mathcal{O}(\epsilon)$, it must be true that $\beta_0^\nu = \mathcal{O}(\epsilon^2)$. This requirement, coupled with the expression for β_0^ν, leads to the knowledge that

$$\nu_1 = 0.$$

Now that we know that $\nu = \ell + \mathcal{O}(\epsilon^2)$, we can study the behavior of a_n^ν for negative n. For most negative values of n, $L_n^\nu = \mathcal{O}(\epsilon)$, but there are two exceptions. Since $\alpha_n^\nu = \mathcal{O}(1)$ when $n = -\ell - 1$[5] and $\beta_n^\nu = \mathcal{O}(\epsilon^2)$ when $n = -2\ell - 1$,

$$L_{-\ell-1}^\nu = \mathcal{O}(1), \quad L_{-2\ell-1}^\nu = \mathcal{O}(\epsilon^{-1}). \tag{3.2.13}$$

The coefficients therefore behave in the following ways, depending on how n compares to

---

[4]With a bit more effort, it is also possible to show that $L_{-1}^\nu = \mathcal{O}(1)$ in the $\ell = s = 0$ case. Even then, the value of ν_1 ends up being the same as it is in the nonzero-ℓ situation.

[5]Again, there is an exception in the $s = 0$ case, where $\alpha_n^\nu = \mathcal{O}(\epsilon^2)$ when $n = -\ell - 1$.

ℓ:

$$a_n^\nu = \begin{cases} \mathcal{O}(\epsilon^n), & n > 0, \\[6pt] 1, & n = 0, \\[6pt] \mathcal{O}(\epsilon^{|n|}), & -1 \geq n \geq -\ell, \\[6pt] \mathcal{O}(\epsilon^\ell), & n = -\ell - 1, \\[6pt] \mathcal{O}(\epsilon^{|n|-1}), & -\ell - 2 \geq n \geq -2\ell, \\[6pt] \mathcal{O}(\epsilon^{2\ell-2}), & n = -2\ell - 1, \\[6pt] \mathcal{O}(\epsilon^{|n|-3}), & -2\ell - 2 \geq n. \end{cases} \tag{3.2.14}$$

To get f_ν to finite order in ϵ, then, one only needs to solve for a finite number of coefficients. We will see later that expanding f_ν in ϵ and z results in a Post-Newtonian expansion for the self-force. Thus, we have exactly what we need to find the self-force analytically to finite Post-Newtonian order.

It is instructive to solve for ν and a_n^ν explicitly to $\mathcal{O}(\epsilon^2)$, so we will do so here. We start with ν, and for now we assume $\ell > 1$ to avoid the special values of n mentioned above. To solve Eq. 3.2.11 to zeroth order in ϵ, we need α_{-1}^ν, β_{-1}^ν, α_0^ν, β_0^ν, γ_0^ν, α_1^ν, β_1^ν, γ_1^ν, β_2^ν, and γ_2^ν all to leading order in ϵ. Remember that $\beta_0^\nu = \mathcal{O}(\epsilon^2)$ and contains ν_2 at leading order. Eq. (3.2.11), after setting $n = 0$ and $\nu = \ell + \nu_2 \epsilon^2 + \mathcal{O}(\epsilon^3)$, then gives

$$\frac{(\ell + 1 + s)^2 (\ell + 1 - s)^2}{(2\ell + 1)(2\ell + 2)(2\ell + 3)\left[(2\ell + 1)\nu_2 + 2 + \frac{s^2}{\ell(\ell+1)} + \frac{(\ell+s)^2(\ell-s)^2}{(2\ell+1)(2\ell)(2\ell-1)}\right]} + \mathcal{O}(\epsilon^2) = 1,$$

so that

$$\nu_2 = \frac{1}{2\ell + 1}\left[-2 - \frac{s^2}{\ell(\ell+1)} - \frac{(\ell + s)^2(\ell - s)^2}{(2\ell+1)(2\ell)(2\ell-1)} + \frac{(\ell + 1 + s)^2(\ell + 1 - s)^2}{(2\ell+1)(2\ell+2)(2\ell+3)}\right]. \tag{3.2.15}$$

Now for the a_n^ν's. Again, for now we assume $\ell > 1$. Since the numerators of R_n^ν and L_n^ν are $\mathcal{O}(\epsilon)$ and the denominators are equal to $-\ell(\ell+1) + (n+\ell)(n+\ell+1) + \mathcal{O}(\epsilon^2)$, we only need to know the denominators to leading order to get a_n^ν to second order in ϵ. To get $a_1^\nu = R_1^\nu$, we need γ_1^ν to second order in ϵ. To get $a_2^\nu = R_2^\nu R_1^\nu$, we only need R_2^ν–and therefore γ_2^ν to first order in ϵ. Similar arguments apply to α_{-1}^ν and α_{-2}^ν for the purpose

of calculating a^ν_{-1} and a^ν_{-2}. The results are

$$a^\nu_2 = -\frac{(\ell+1-s)^2(\ell+2-s)^2}{2(2\ell+1)(2\ell+2)(2\ell+3)^2}\epsilon^2 + \mathcal{O}(\epsilon^3)$$

$$a^\nu_1 = \frac{(\ell+1-s)^2}{(2\ell+1)(2\ell+2)}i\epsilon + \frac{(\ell+1-s)^2}{(\ell+1)(2\ell+1)(2\ell+2)}\epsilon^2 + \mathcal{O}(\epsilon^3)$$

$$a^\nu_0 = 1$$

$$a^\nu_{-1} = \frac{(\ell+s)^2}{2\ell(2\ell+1)}i\epsilon - \frac{(\ell+s)^2}{2\ell^2(2\ell+1)}\epsilon^2 + \mathcal{O}(\epsilon^3)$$

$$a^\nu_{-2} = -\frac{(\ell+s-1)^2(\ell+s)^2}{4\ell(2\ell-1)^2(2\ell+1)}\epsilon^2 + \mathcal{O}(\epsilon^3) \tag{3.2.16}$$

For completeness, we will solve for ν_2 and the a^ν_n's for $\ell = 0, 1$ as well. Since the spin-weighted spherical harmonics vanish when $\ell < |s|$, the $\ell = 0$ case is only relevant for $s = 0$. In this case, $\beta^\nu_{-1} = \mathcal{O}(\epsilon^2)$. As a result, we not only have to calculate L^ν_{-1}, but also L^ν_{-2}, in order to find L^ν_0 to leading order in ϵ. After doing the necessary calculations, we find

$$R^\nu_1 L^\nu_0 = \frac{1}{6}\left[\nu_2 + 2 + \frac{1}{\nu_2} + \frac{1}{\nu_2^2(-\nu_2 + \frac{11}{6} - \frac{1}{\nu_2})}\right]^{-1} + \mathcal{O}(\epsilon).$$

Setting the above equal to one, we find an equation for ν_2:

$$0 = \nu_2^2\left(\nu_2 + \frac{7}{6}\right)\left(\nu_2 - \frac{7}{6}\right)$$

The appearance of $1/\nu_2$ in β^ν_0 and β^ν_{-1} precludes the apparent solution $\nu_2 = 0$. However, we are free to choose $\nu_2 = \pm 7/6$. Following Hikida $et\ al.$ [8] and noting that $\nu_2 < 0$ for every other value of ℓ, we choose $\nu_2 = -7/6$. Because of the particularities of the $\ell = 0$ case, solving for the coefficients to second order in ϵ requires knowledge of ν_3 and ν_4. These are solved for by setting the $\mathcal{O}(\epsilon)$ and $\mathcal{O}(\epsilon^2)$ contributions to $R^\nu_1 L^\nu_0$ equal to zero. This is quite cumbersome to do by hand, so here we simply report the results, obtained with the aid of $Mathematica$:

$$\nu_3 = 0$$

$$\nu_4 = -\frac{9449}{7560}.$$

One can find the nonnegative-n coefficients using the general-ℓ expressions above. The

negative-n coefficients, to second order in ϵ, are as follows:

$$a^\nu_{-1} = -\frac{2}{9} - \frac{7}{27}i\epsilon - \frac{1591}{2835}\epsilon^2 + \mathcal{O}(\epsilon^3)$$

$$a^\nu_{-2} = -\frac{1}{9}i\epsilon + \frac{1}{54}\epsilon^2 + \mathcal{O}(\epsilon^3)$$

$$a^\nu_{-3} = \frac{2}{81}\epsilon^2 + \mathcal{O}(\epsilon^3).$$

Now for the $\ell = 1$ case, which is relevant when s is 0 or ± 1. These calculations are much easier when we treat the $s = 0$ case separately from the $s = \pm 1$ case. We will treat the $\ell = 1$, $s = 0$ case first. In this case,

$$L^\nu_0 = -\frac{4i}{5\epsilon(3\nu_2 + \frac{13}{6})} + \mathcal{O}(\epsilon^0),$$

and Eq. 3.2.11 leads to

$$\frac{4}{15(3\nu_2 + \frac{13}{6})} = 1,$$

so that

$$\nu_2 = -\frac{19}{30}.$$

This leads directly to

$$a^\nu_{-1} = \frac{1}{6}i\epsilon - \frac{1}{6}\epsilon^2 + \mathcal{O}(\epsilon^3)$$

$$a^\nu_{-2} = \mathcal{O}(\epsilon^3).$$

When $\ell = 1$ and $s = \pm 1$, $\gamma^\nu_0 L^\nu_{-1} = \mathcal{O}(\epsilon^4)$, so knowledge of that term is unnecessary for calculating L_0. We are therefore free to use the general-ℓ expression for ν_2, giving

$$\nu_2 = -\frac{47}{60}.$$

For the $s = 1$ case, finding the coefficients to second order in ϵ again requires knowledge of ν_3 and ν_4. Again, this is not very feasible by hand, and we simply cite the results below:

$$\nu_3 = 0$$

$$\nu_4 = -\frac{43908007}{71064000}$$

36

For $s = 1$, then,

$$a_{-1}^{\nu} = \frac{34}{141}i\epsilon - \frac{34}{141}\epsilon^2 + \mathcal{O}(\epsilon^3)$$

$$a_{-2}^{\nu} = \frac{20}{47}i\epsilon - \frac{107}{141}\epsilon^2 + \mathcal{O}(\epsilon^3)$$

$$a_{-3}^{\nu} = -\frac{200}{2209}\epsilon^2 + \mathcal{O}(\epsilon^3).$$

While ν remains the same after the replacement $s \to -s$, the coefficients for $s = -1$ can be found using the symmetry property reported in [87]:

$$a_n^{\nu}(-s) = \left| \frac{(\nu + 1 + s + i\epsilon)_n}{(\nu + 1 - s + i\epsilon)_n} \right|^2 a_n^{\nu}(s).$$

Now that we know how to solve for ν and the coefficients, we are ready to write ϕ_c^{ν} explicitly:

$$\phi_c^{\nu} = e^{-i\zeta}|2\zeta|^{\nu}\zeta^{-s} \sum_{n=-\infty}^{\infty} a_n^{\nu} \left| \frac{(\nu + 1 + s + i\epsilon)_n}{(\nu + 1 - s + i\epsilon)_n} \right|^2 \frac{(\nu + 1 - s + i\epsilon)_n}{(2\nu + 2)_{2n}}$$

$$\times (2i\zeta)^n {}_1F_1(n + \nu + 1 - s + i\epsilon; 2n + 2\nu + 2, 2i\zeta). \quad (3.2.17)$$

Here, we can see the advantage of our normalization of ϕ_c^{ν}, which results in a factor of $|2\zeta|^{\nu}$ in front of the sum instead of $(2\zeta)^{\nu}$. First, note that the expressions for α_n^{ν}, β_n^{ν}, γ_n^{ν}, and therefore R_n^{ν}, L_n^{ν}, ν, and a_n^{ν}, all satisfy the property

$$X = \overline{X}|_{\epsilon \to -\epsilon},$$

where X stands for any of the afore-mentioned quantities. Also note that both ϵ and ζ are both equal to positive quantities multiplied by ω. Then it is clear from Eq. (3.2.17) that

$$\phi_c^{\nu} = (-1)^s \overline{\phi_c^{\nu}}|_{\omega \to -\omega}. \quad (3.2.18)$$

This symmetry property is not satisfied if the normalization of Hikida and Linz [8, 9, 83] is used. In particular, the quantity $(2\zeta)^{\nu}$ goes from real to complex when ω goes from positive to negative because ν is not an integer. We will see later that our normalization also makes it easier to construct Green functions that satisfy the proper boundary conditions.

The homogeneous Bardeen-Press equation is second-order and linear, so there are two linearly independent solutions to it. Since Eq. (3.2.5) remains the same after the replacement $\nu \to -\nu - 1$, we can create another solution, $\phi_c^{-\nu-1}$, by replacing ν in Eq. (3.2.17) with $-\nu - 1$. MST [84] show that ϕ_c^ν and $\phi_c^{-\nu-1}$ are linearly independent.

Finally, we need to mention here that the sum in Eq. (3.2.17) only converges if $\zeta \neq 0$—that is, when $r > 2M$, outside the event horizon [84]. In order to construct a Green's function that satisfies proper boundary conditions on the horizon, then, we need another linearly independent pair of solutions that are regular on the horizon. MST finds such a pair, called R_0^ν and $R_0^{-\nu-1}$ and written as series of hypergeometric functions. Remarkably, they use the same coefficients $\{a_n^\nu\}$ and renormalized angular momentum ν. With the definition $x \equiv -\zeta/\epsilon$, R_0^ν is given by

$$R_0^\nu = e^{i\epsilon x}(-x)^{\nu-s} \sum_{n=-\infty}^{\infty} a_n^\nu \frac{\Gamma(1-s-2i\epsilon)\Gamma(2n+2\nu+1)}{\Gamma(n+\nu+1-i\epsilon)\Gamma(n+\nu+1-s-i\epsilon)}$$
$$\times (-x)^n {}_2F_1\left(-n-\nu-i\epsilon, -n-\nu+s+i\epsilon; -2n-2\nu; \frac{1}{x}\right),$$

(3.2.19)

while $R_0^{-\nu-1}$ is obtained by replacing ν with $-\nu - 1$. The solutions R_0^ν and $R_0^{-\nu-1}$ are regular everywhere except in the limit $|x| \to \infty$, corresponding to $r \to \infty$. Furthermore, in the region $2M < r < \infty$ where both R_0^ν and ϕ_c^ν converge, the two types of solutions are related by a constant factor:

$$R_0^\nu = K_c^\nu \phi_c^\nu,$$

(3.2.20)

with

$$K_c^\nu = |2\epsilon|^{-\nu}\epsilon^s \frac{\Gamma(1-s-2i\epsilon)}{|\Gamma(1+\nu-s+i\epsilon)|^2}\left[\sum_{n=0}^{\infty}\frac{\Gamma(n+\nu+1+i\epsilon)\Gamma(n+2\nu+1)}{n!\Gamma(n+\nu-1-i\epsilon)}a_n^\nu\right]$$
$$\times \left[\sum_{n=-\infty}^{0}\left|\frac{(\nu+1+s-i\epsilon)_n}{(\nu+1-s+i\epsilon)_n}\right|^2 \frac{1}{(-n)!(2\nu+2)_n}a_n^\nu\right]^{-1}.$$

(3.2.21)

3.2.3 Solving the sourced Bardeen-Press equation with a Green's function

We seek to solve the sourced Bardeen-Press equation, which we plan to do with the use of a Green's function. That is, if we let $\mathcal{D}$ be the differential operator on the left side of

Eq. (3.2.2) so that

$$\mathcal{D}\psi_s = 4\pi r^2 (r^2 f)^s T_s,$$

we seek a function $G(x, x')$[6] such that

$$\mathcal{D}G(x, x') = r^2 \delta^{(4)}(x, x'), \tag{3.2.22}$$

so that a solution to Eq. (3.2.2) is

$$\psi_s = 4\pi \int d^4 x' G(x, x') \left[r'^2 f(r') \right]^s T_s(x'). \tag{3.2.23}$$

Here, x stands for the Schwarzschild coordinates (t, r, θ, ϕ), and by $\delta^{(4)}(x, x')$ we mean

$$\delta^{(4)}(x, x') = \frac{\delta(t - t')\delta(r - r')\delta(\theta - \theta')\delta(\phi - \phi')}{\sqrt{-\det(g_{\mu\nu})}},$$

while by $d^4 x'$ we mean

$$d^4 x' = \sqrt{-\det(g_{\mu'\nu'})} \ dt' dr' d\theta' d\phi',$$

and $g_{\mu'\nu'}$ is the metric in the primed coordinates. Noting that

$$\delta(t - t') = \frac{1}{2\pi} \int_{-\infty}^{\infty} d\omega\, e^{-i\omega(t-t')}$$

and

$$\frac{\delta(\theta - \theta')\delta(\phi - \phi')}{\sin\theta} = \sum_{\ell=|s|}^{\infty} \sum_{m=-\ell}^{\ell} {}_sY_{\ell m}(\theta, \phi)_s\overline{Y}_{\ell m}(\theta', \phi'),$$

we also decompose the Green's function into Fourier and angular harmonic modes:

$$G(x, x') = \frac{1}{2\pi} \int_{-\infty}^{\infty} d\omega \sum_{\ell=|s|}^{\infty} \sum_{m=-\ell}^{\ell} g_{\ell\omega}(r, r') e^{-i\omega(t-t')} {}_sY_{\ell m}(\theta, \phi)_s\overline{Y}_{\ell m}(\theta', \phi'). \tag{3.2.24}$$

Eq. (3.2.22) then leads to an equation for the radial part of the Green's function:

$$\frac{d}{dr}\left[(r^2 f)^{s+1} \frac{dg_{\ell\omega}(r, r')}{dr} \right] + (r^2 f)^s \left\{ \frac{r\omega}{f}\left[r\omega + 2is\left(1 - \frac{3M}{r} \right) \right] \right.$$

$$\left. + \ell(\ell + 1) + s(s + 1) \right\} g_{\ell\omega}(r, r')$$

$$= \delta(r - r'), \tag{3.2.25}$$

---

[6]The Green's function we define here is the additive opposite of that defined in Hikida. This is because Hikida anticipated that $T_0 < 0$.

which is Eq. (3.2.4) with a delta function source. This problem thus reduces to solving for a one-dimensional Green's function. At this point, it is important to choose retarded boundary conditions for G so that we get a causal solution for ψ_s. This means that our solution must have upgoing radiation—that is, outgoing radiation at future null infinity—and ingoing radiation—that is, ingoing radiation on the future horizon. Mathematically, $g \sim e^{i[\omega r + 2M \ln(\omega r)]}/r^{1-2s}$ as $r \to \infty$ and $g \sim (-x)^{-s} e^{i\omega(x + 2M \ln(-x))}$ as $x \equiv -\zeta/\epsilon \to 0$. Following Arfken [88], we write

$$g_{\ell\omega}(r, r') = \frac{\phi_{\text{in}}^{\nu}(r_<) \phi_{\text{up}}^{\nu}(r_>)}{W_{\ell\omega}(\phi_{\text{in}}^{\nu}, \phi_{\text{up}}^{\nu})},$$

where ϕ_{up}^{ν} is a solution to the homogeneous radial Bardeen-Press equation with upgoing boundary conditions, ϕ_{in}^{ν} is that with ingoing boundary conditions, $r_>$ is the greater of r and r', $r_<$ is the lesser of r and r', and $W_{\ell\omega}(\phi_{\text{up}}^{\nu}, \phi_{\text{in}}^{\nu})$ is constant in r and proportional to the Wronskian of ϕ_{up}^{ν} and ϕ_{in}^{ν}:

$$W_{\ell\omega}(\phi_{\text{up}}^{\nu}, \phi_{\text{in}}^{\nu}) = (r^2 f)^{s+1} \left[\phi_{\text{up}}^{\nu} \frac{d}{dr} \phi_{\text{in}}^{\nu} - \phi_{\text{in}}^{\nu} \frac{d}{dr} \phi_{\text{up}}^{\nu} \right].$$

To construct $G(x, x')$, we now need to find the linear combinations of ϕ_c^{ν} and $\phi_c^{-\nu-1}$ that give ϕ_{up}^{ν} and ϕ_{in}^{ν}. We start with ϕ_{up}^{ν}. Following the notation of Hikida *et al.* [8], we seek the constant γ_c^{ν} such that

$$\phi_{\text{up}}^{\nu} = \gamma_c^{\nu} \phi_c^{\nu} + \phi_c^{-\nu-1}$$

gives outgoing radiation at infinity. To find γ_c^{ν}, we need to derive the behavior of ϕ_c^{ν} and $\phi_c^{-\nu-1}$ in the limit $r \to \infty$. We start with an identity for the confluent hypergeometric function:

$$
\begin{aligned}
{}_1F_1(a; b; z) =& \frac{\Gamma(b)}{\Gamma(b-a)} e^{i\pi \text{Sign}(\Im(z))a} U(a; b; z) \\
& + \frac{\Gamma(b)}{\Gamma(a)} e^{-i\pi \text{Sign}(\Im(z))(b-a)} e^z U(b-a; b; e^{-i\pi \text{Sign}(\Im(z))} z),
\end{aligned}
$$

where $U(a; b; z)$ is the irregular confluent hypergeometric function. This is useful because U has a simple asymptotic form:

$$\lim_{z \to \infty} U(a; b; z) = z^{-a}.$$

Before going further, we define the following constants:

$$A_1 = \nu + 1 - s + i\epsilon$$

$$A_2 = \nu + 1 + s - i\epsilon$$

$$B = 2\nu + 2,$$

which themselves satisfy the following properties:

$$A_1 = B - A_2$$

$$A_2 = B - A_1$$

$$A_1|_{\nu \to -\nu - 1} = 1 - A_2$$

$$A_2|_{\nu \to -\nu - 1} = 1 - A_1$$

Now, when we insert the above identity for $_1F_1$ into Eq. (3.2.17), we get

$$\phi_c^\nu = \tilde{U}_1^\nu(\zeta) + \tilde{U}_2^\nu(\zeta),$$

where

$$\tilde{U}_1^\nu(\zeta) = e^{-i\zeta} |2\zeta|^\nu \zeta^{-s} \sum_{n=-\infty}^{\infty} a_n^\nu \left| \frac{(A_2)_n}{(A_1)_n} \right|^2 \frac{(A_1)_n}{(B)_{2n}} \frac{\Gamma(B + 2n)}{\Gamma(A_2 + n)} e^{i\pi\sigma_\omega(A_1 + n)}$$

$$\times (2i\zeta)^n U(A_1 + n; B + 2n; 2i\zeta),$$

$$\tilde{U}_2^\nu(\zeta) = e^{i\zeta} |2\zeta|^\nu \zeta^{-s} \sum_{n=-\infty}^{\infty} a_n^\nu \left| \frac{(A_2)_n}{(A_1)_n} \right|^2 \frac{(A_1)_n}{(B)_{2n}} \frac{\Gamma(B + 2n)}{\Gamma(A_1 + n)} e^{-i\pi\sigma_\omega(A_2 + n)}$$

$$\times (2i\zeta)^n U(A_2 + n; B + 2n; e^{-i\pi\sigma_\omega} 2i\zeta),$$

and

$$\sigma_\omega = \text{Sign}(\omega).$$

When we apply the asymptotic form of $U(a; b; z)$, we find

$$\lim_{\zeta \to \infty} \tilde{U}_1^\nu = \frac{e^{-i(\zeta + \ln(\zeta))}}{\zeta} (i\sigma_\omega)^{-\nu} (2i)^{s-1-i\epsilon} \sum_{n=-\infty}^{\infty} a_n^\nu \left| \frac{(A_2)_n}{(A_1)_n} \right|^2 \frac{(A_1)_n}{(B)_{2n}} \frac{\Gamma(B)}{\Gamma(A_2)} e^{i\pi\sigma_\omega(A_1 + n)},$$

corresponding to incoming radiation at infinity. Meanwhile,

$$\lim_{\zeta \to \infty} \tilde{U}_2^\nu = \frac{e^{i(\zeta + \ln(\zeta))}}{\zeta^{1+2s}} (i\sigma_\omega)^{-\nu} (2i)^{-s-1+i\epsilon} \sum_{n=-\infty}^{\infty} a_n^\nu \left| \frac{(A_2)_n}{(A_1)_n} \right|^2 \frac{\Gamma(B)}{\Gamma(A_1)},$$

41

corresponding to outgoing radiation at infinity. We are therefore seeking the value of γ_c^ν such that

$$\gamma_c^\nu \phi_c^\nu + \phi_c^{-\nu-1} \propto \tilde{U}_2^\nu.$$

We must now write $\phi_c^{-\nu-1}$ as a linear combination of $\tilde{U}_1^\nu$ and $\tilde{U}_2^\nu$. By replacing ν with $-\nu-1$, one finds $\tilde{U}_1^{-\nu-1}$ and $\tilde{U}_2^{-\nu-1}$ such that

$$\phi_c^{-\nu-1} = \tilde{U}_1^{-\nu-1}(\zeta) + \tilde{U}_2^{-\nu-1}(\zeta).$$

Remarkably, it turns out that $\tilde{U}_1^{-\nu-1}(\zeta) \propto \tilde{U}_1^\nu(\zeta)$ and $\tilde{U}_2^{-\nu-1}(\zeta) \propto \tilde{U}_2^\nu(\zeta)$. By using one of the properties of the coefficients [87]

$$a_n^\nu = a_{-n}^{-\nu-1},$$

another property of the irregular confluent hypergeometric functions [89]

$$U(a;b;z) = z^{1-b}U(a-b+1;2-b;z),$$

and two properties of the Gamma function [89]

$$\Gamma(z+1) = z\Gamma(z),$$
$$\Gamma(z)\Gamma(1-z) = \frac{\pi}{\sin(\pi z)},$$

and a fair amount of algebra, one finds

$$\tilde{U}_1^{-\nu-1}(\zeta) = (-1)^s e^{-i\pi\sigma_\omega\left(\nu+\frac{1}{2}\right)} \frac{\Gamma(A_2)\Gamma(A_1)}{\Gamma(B)\Gamma(B-1)} \frac{\sin\pi(\nu+i\epsilon)}{\sin(2\pi\nu)} \tilde{U}_1^\nu(\zeta),$$

and

$$\tilde{U}_2^{-\nu-1}(\zeta) = (i\sigma_\omega)^{2\nu+1} \frac{\Gamma(2-B)\Gamma(A_1)}{\Gamma(1-A_2)\Gamma(B)} \tilde{U}_2^\nu$$

Finally, we can solve for γ_c^ν such that the coefficient of $\tilde{U}_1^\nu$ vanishes. The result is

$$\gamma_c^\nu = -(-1)^s e^{-i\pi\sigma_\omega\left(\nu+\frac{1}{2}\right)} \frac{\Gamma(A_1)\Gamma(A_2)}{\Gamma(B)\Gamma(B-1)} \frac{\sin\pi(\nu+i\epsilon)}{\sin(2\pi\nu)}$$

$$= (-1)^s \frac{\Gamma(\nu+1-s+i\epsilon)\Gamma(\nu+1+s-i\epsilon)}{\Gamma(2\nu+2)\Gamma(2\nu+1)\sin(2\pi\nu)} \qquad (3.2.26)$$

$$\times \left[\sin^2(\pi\nu)e^{\pi|\epsilon|} - \sinh(\pi|\epsilon|) + \frac{i\sigma_\omega}{2}\sin(2\pi\nu)e^{\pi|\epsilon|}\right]. \qquad (3.2.27)$$

Now, we need to find ϕ_{in}^ν, equivalent to finding β_c^ν such that

$$\phi_{\text{in}}^\nu = \phi_c^\nu + \beta_c^\nu \phi_c^{-\nu-1}$$

has purely ingoing radiation on the horizon. MST actually define R_{in}^ν, which satisfies exactly that boundary condition, before they define R_0^ν:

$$R_{\text{in}}^\nu = e^{i\epsilon x}(-x)^{-s-i\epsilon} \sum_{n=-\infty}^{\infty} a_n^\nu \, {}_2F_1(n+\nu+1-i\epsilon, -n-\nu-i\epsilon; 1-s-2i\epsilon; x).$$

MST then use a property of ${}_2F_1$, [89]

$$
\begin{aligned}
{}_2F_1(a,b,;c;z) =& \frac{\Gamma(c)\Gamma(a-b)}{\Gamma(a)\Gamma(c-b)}(-z)^{-b} \, {}_2F_1\left(b, b-c+1; b-a+1; \frac{1}{z}\right) \\
&+ \frac{\Gamma(c)\Gamma(b-a)}{\Gamma(b)\Gamma(c-a)}(-z)^a \, {}_2F_1\left(a, a-c+1; a-b+1; \frac{1}{z}\right),
\end{aligned}
$$

to show that

$$R_{\text{in}}^\nu = R_0^\nu + R_0^{-\nu-1}. \tag{3.2.28}$$

MST later define R_{out}^ν, which has an outgoing radiative boundary condition on the horizon:

$$
\begin{aligned}
R_{\text{out}}^\nu = e^{i\epsilon x}(-x)^{i\epsilon}(1-x)^{-s} \sum_{n=-\infty}^{\infty} a_n^\nu & \frac{(\nu+1+s+i\epsilon)_n(\nu+1+i\epsilon)_n}{(\nu+1-s-i\epsilon)_n(\nu+1-\epsilon)_n} \\
& \times {}_2F_1(n+\nu+1+i\epsilon, -n-\nu+i\epsilon; 1+s+2i\epsilon; x).
\end{aligned}
$$

The function R_{out}^ν can also be written as a linear combination of R_0^ν and $R_0^{-\nu-1}$. To find it, we again use the identity for ${}_2F_1$ above to see that

$$
\begin{aligned}
R_{\text{out}}^\nu =& \frac{\Gamma(\nu+1-s-i\epsilon)\Gamma(\nu+1-i\epsilon)}{\Gamma(\nu+1+s+i\epsilon)\Gamma(\nu+1+i\epsilon)} e^{i\epsilon x}(-x)^\nu(1-x)^{-s} \\
& \times \sum_{n=-\infty}^{\infty} a_n^\nu \frac{\Gamma(1+s+2i\epsilon)\Gamma(2n+2\nu+1)}{\Gamma(n+\nu+1-s-i\epsilon)\Gamma(n+\nu+1-i\epsilon)}(-x)^n \\
& \times {}_2F_1\left(-n-\nu+i\epsilon, -n-\nu-s-i\epsilon; -2n-2\nu; \frac{1}{x}\right) + (\nu \to -\nu-1),
\end{aligned}
$$

where by $+(\nu \to -\nu-1)$ we mean to add the same expression with ν replaced by $-\nu-1$. Meanwhile, using another identity [89]

$${}_2F_1(a,b,;c;z) = (1-z)^{c-a-b} \, {}_2F_1(c-a, c-b; c; z),$$

we see that

$$R_0^\nu = e^{i\epsilon x}(-x)^\nu(1-x)^{-s} \sum_{n=-\infty}^{\infty} a_n^\nu \frac{\Gamma(1-s-2i\epsilon)\Gamma(2n+2\nu+1)}{\Gamma(n+\nu+1-i\epsilon)\Gamma(n+\nu+1-s-i\epsilon)}(-x)^n$$

$$\times\, {}_2F_1\left(-n-\nu+i\epsilon, -n-\nu-s-i\epsilon; -2n-2\nu; \frac{1}{x}\right).$$

By comparing the expression for R_0^ν above with that of R_{out}^ν, one can see that

$$R_{\text{out}}^\nu = A_\nu R_0^\nu + A_{-\nu-1}R_0^{-\nu-1}, \tag{3.2.29}$$

where

$$A_\nu = \frac{\Gamma(\nu+1-s-i\epsilon)\Gamma(\nu+1-i\epsilon)\Gamma(1+s+2i\epsilon)}{\Gamma(\nu+1+s+i\epsilon)\Gamma(\nu+1+i\epsilon)\Gamma(1-s-2i\epsilon)}$$

and $A_{-\nu-1}$ can be found by replacing ν in the above expression with $-\nu-1$. Remembering that $R_0^\nu = K_c^\nu \phi_c^\nu$ in the region where both R_0^ν and $R_0^{-\nu-1}$ converge, we now have an expression for $\phi_c^\nu + \beta_c^\nu \phi_c^{-\nu-1}$ in terms of R_{in}^ν and R_{out}^ν:

$$\phi_c^\nu + \beta_c^\nu \phi_c^{-\nu-1} = \left[\frac{\Gamma(2\nu+2)}{\Gamma(\nu+1-s+i\epsilon)}\frac{1}{K_c^\nu(A_\nu - A_{-\nu-1})}\right.$$

$$\left. -\beta_c^\nu \frac{\Gamma(-2\nu)}{\Gamma(-\nu-s+i\epsilon)}\frac{1}{K_c^{-\nu-1}(A_\nu - A_{-\nu-1})}\right] R_{\text{out}}^\nu$$

$$+\left[-\frac{\Gamma(2\nu+2)}{\Gamma(\nu+1-s+i\epsilon)}\frac{A_{-\nu-1}}{K_c^\nu(A_\nu - A_{-\nu-1})}\right.$$

$$\left. +\beta_c^\nu \frac{\Gamma(-2\nu)}{\Gamma(-\nu-s+i\epsilon)}\frac{A_\nu}{K_c^{-\nu-1}(A_\nu - A_{-\nu-1})}\right] R_{\text{in}}^\nu.$$

Since the coefficient of R_{out}^ν needs to vanish,

$$\beta_c^\nu = \frac{\Gamma(2\nu+2)}{\Gamma(-2\nu)}\frac{\Gamma(-\nu-s+i\epsilon)}{\Gamma(\nu+1-s+i\epsilon)}\frac{K_c^{-\nu-1}}{K_c^\nu}$$

$$= \frac{(-1)^s}{\pi}2^{2\nu}|\epsilon|^{2\nu+1}\frac{\Gamma(\nu+1+s+i\epsilon)\Gamma(\nu+1-s-i\epsilon)}{\Gamma(2\nu+2)\Gamma(2\nu+1)}|\Gamma(\nu+1+i\epsilon)|^2$$

$$\times \frac{\Xi_{-\nu-1}}{\Xi_\nu}[\csc(2\pi\nu) - \cot(2\pi\nu)\cosh(2\pi\epsilon) + i\sinh(2\pi\epsilon)], \tag{3.2.30}$$

where

$$\Xi_\nu = \left[\sum_{n=0}^{\infty}\frac{1}{n!}(2\nu+1)_n\frac{(\nu+1+i\epsilon)_n}{(\nu+1-i\epsilon)_n}a_n^\nu\right]\left[\sum_{n=0}^{\infty}\frac{(-1)^n}{n!}(2\nu+1)_n\left|\frac{(\nu+1+s-i\epsilon)_n}{(\nu+1-s+i\epsilon)_n}\right|^2 a_n^\nu\right].$$

The last quantity we need to calculate for $g_{\ell\omega}(r,r')$ is $W_{\ell\omega}$. While we are free to get $W_{\ell\omega}$ directly from ϕ_{in}^ν, ϕ_{up}^ν, and their derivatives, it is also useful to have a more explicit

44

expression. To do this, we again follow Arfken [88] and note that

$$W[\phi_c^\nu, \phi_c^{-\nu-1}] = W[\phi_c^\nu, \phi_c^{-\nu-1}]|_{r=b} \exp\left[-\int_b^r dr' \frac{2(s+1)(r'-M)}{r'^2 - 2Mr'}\right]$$

$$= W[\phi_c^\nu, \phi_c^{-\nu-1}]|_{r=b} \left(\frac{r^2 - 2Mr}{b^2 - 2Mb}\right)^{-s-1},$$

where $W[f_1, f_2]$ is the Wronskian of f_1 and f_2 and b is any constant. Since we understand the behavior of ϕ_c^ν and $\phi_c^{-\nu-1}$ at infinity, we will take the limit as $b \to \infty$. The result is

$$\lim_{b\to\infty} W[\phi_c^\nu, \phi_c^{-\nu-1}]|_{r=b} = -\frac{2\nu+1}{2}|\omega|^{-2s-1}b^{-2s-2}\left[\sum_{n=-\infty}^{\infty}\left|\frac{(\nu+1+s-i\epsilon)_n}{(\nu+1-s+i\epsilon)_n}\right|^2 a_n^\nu\right]$$

$$\times \left[\sum_{n=-\infty}^{\infty}(-1)^n\frac{(\nu+1+s+i\epsilon)_n}{(\nu+1-s-i\epsilon)_n}a_n^\nu\right].$$

This means that the Wronskian at any r-value is

$$W[\phi_c^\nu, \phi_c^{-\nu-1}] = -(r^2 - 2Mr)^{-s-1}\frac{2\nu+1}{2}|\omega|^{-2s-1}\left[\sum_{n=-\infty}^{\infty}\left|\frac{(\nu+1+s-i\epsilon)_n}{(\nu+1-s+i\epsilon)_n}\right|^2 a_n^\nu\right]$$

$$\times \left[\sum_{n=-\infty}^{\infty}(-1)^n\frac{(\nu+1+s+i\epsilon)_n}{(\nu+1-s-i\epsilon)_n}a_n^\nu\right],$$

and $W_{\ell\omega}(\phi_c^\nu, \phi_c^{-\nu-1}) \equiv (r^2 - 2Mr)^{s+1}W[\phi_c^\nu, \phi_c^{-\nu-1}]$ is given by

$$W_{\ell\omega}(\phi_c^\nu, \phi_c^{-\nu-1}) = -\frac{2\nu+1}{2}|\omega|^{-2s-1}\left[\sum_{n=-\infty}^{\infty}\left|\frac{(\nu+1+s-i\epsilon)_n}{(\nu+1-s+i\epsilon)_n}\right|^2 a_n^\nu\right]$$

$$\times \left[\sum_{n=-\infty}^{\infty}(-1)^n\frac{(\nu+1+s+i\epsilon)_n}{(\nu+1-s-i\epsilon)_n}a_n^\nu\right]. \tag{3.2.31}$$

It is easy to show that

$$W_{\ell\omega}(\phi_{\text{in}}^\nu, \phi_{\text{up}}^\nu) = (1 - \beta_c^\nu\gamma_c^\nu)\,W_{\ell\omega}(\phi_c^\nu, \phi_c^{-\nu-1}).$$

We now know how to construct $g_{\ell\omega}(r, r')$ and therefore $G(x, x')$, which will be indispensable in finding the self-force on a point particle orbiting a Schwarzschild black hole.

3.3 Scalar Self-Force

For the rest of this chapter, we specialize to the scalar ($s = 0$) case. The source term is $T_0 = -\rho$ in this case[7], and the Bardeen-Press equation reduces to[8]

$$\nabla_\alpha \nabla^\alpha \psi = -4\pi\rho, \tag{3.3.1}$$

where ρ is the scalar charge density, and we now refer to ψ_0 from the last section as ψ.

We now wish to consider a scalar charge in circular orbit around a Schwarzschild black hole. In particular, we take the charged particle to be small—both in the sense that its volume is small compared to the black hole and in the sense that its charge q is small. The latter condition means that ψ's influence on the gravitational field can be neglected, and we can consider ψ to be a scalar field on the background Schwarzschild spacetime. The former condition leads us to treat the scalar charge as a point particle, so that ρ is given by a delta function. This allows us to easily integrate the Green's function we derived in the last section against ρ to find the retarded scalar field ψ.

However, there is a problem with this: namely, the retarded field diverges at the particle's position. Our goal is to derive the self-force F^α of the particle; that is, the force that the particle feels due to its own field. Naively, we would try to take a derivative of the field and multiply by the charge of the particle. The divergent field blows a hole in this prescription. We therefore need a way to *renormalize* the field, so that

$$F^{\mathrm{R},\alpha} = \lim_{x \to x_0} P^\alpha_\beta \nabla^\beta \psi^{\mathrm{R}} \tag{3.3.2}$$

exists, where ψ^{R} is continuous and differentiable at the particle. Meanwhile, $P^\alpha_\beta = \delta^\alpha_\beta + u^\alpha u_\beta$ projects the force onto a direction perpendicular to u^α; this keeps the scalar charge constant and is conventionally used in scalar self-force work. We explain how to do this in the following subsection.

---

[7]Hikida *et al.* [8, 9] implicitly choose $T_0 = -\rho/4\pi$. This is not materially different and their expression can be thought of as the result of defining the unit of scalar charge differently. Nevertheless, our results will appear to differ with theirs by a factor of 4π.

[8]Sometimes, the scalar field is defined to couple to the background spacetime via a term proportional to $R\psi$, where R is the Ricci scalar. A scalar field defined as it is here is referred to as *minimally coupled*.

3.3.1 Mode-Sum Renormalization

Quinn's axiomatic approach to renormalizing the field[90] is consistent with that of Quinn and Wald [91] in the electromagnetic and gravitational cases. Furthermore, in the other two cases Quinn and Wald [91] give the same results as Mino, Sasaki, and Tanaka [92]. Mino, Sasaki, and Tanaka arrived at the results in two other ways, one of which is referred to as *matched asymptotic expansions*. It is that last method that is considered standard in the gravitational case; Quinn's axioms in [90] are more directly applicable to the scalar case, and we use them here.

Quinn's axioms are as follows:

1. Comparison Axiom: consider two point particles in two possibly different space-times, each particle having scalar charge q. Suppose that, at points x_0 and $\tilde{x}_0$ on their respective trajectories, the magnitude of the particle's 4-accelerations coincide. We may then choose Riemann Normal Coordinate systems about x_0 and $\tilde{x}_0$ for which the components of the 4-velocities and 4-accelerations coincide: $u^\alpha = \tilde{u}^\alpha$ and $a^\alpha = \tilde{a}^\alpha$. Let ψ^{ret} and $\tilde{\psi}^{\mathrm{ret}}$ be the scalar fields of the particles. With the Riemann Normal Coordinates used to identify the neighborhood around x_0 with that around $\tilde{x}_0$ the difference between the renormalized scalar self-forces, $F^{\mathrm{R},\alpha}$ and $\tilde{F}^{\mathrm{R},\alpha}$, is given by the limit as $r \to 0$ of the gradients of the fields averaged over a sphere of geodesic distance r about x_0:

$$F^{\mathrm{R},\alpha} - \tilde{F}^{\mathrm{R},\alpha} = q \lim_{r \to 0} \left\langle \nabla^\alpha \psi^{\mathrm{ret}} - \nabla^\alpha \tilde{\psi}^{\mathrm{ret}} \right\rangle_r . \qquad (3.3.3)$$

2. Flat Spacetime Axiom: let ψ^{adv} be the scalar field with advanced boundary conditions. If, for a uniformly accelerated scalar charge in flat spacetime,

$$\tilde{\psi} = \frac{1}{2} \left(\tilde{\psi}^{\mathrm{ret}} + \tilde{\psi}^{\mathrm{adv}} \right),$$

then

$$\tilde{F}^{\mathrm{R},\alpha} = 0 \qquad (3.3.4)$$

at every point along the particle's path.

These two axioms allow us to write the scalar self-force on a particle in Riemann Normal Coordinates as

$$F^{\mathrm{R},\alpha} = q \lim_{r \to 0} \left\langle \nabla^\alpha \psi^{\mathrm{ret}} - \nabla^\alpha \tilde{\psi} \right\rangle_r. \tag{3.3.5}$$

While a useful starting point, Quinn's axioms are difficult to use for practical calculations. Thankfully, much work has been done to make self-force calculations more tractable. Namely, Detweiler and Whiting showed that ψ can be decomposed into two parts, ψ^{S} and ψ^{R}:

$$\psi = \psi^{\mathrm{S}} + \psi^{\mathrm{R}}, \tag{3.3.6}$$

where ψ^{S} is referred to as the *singular field* and ψ^{R} is called the *renormalized field*. The singular field has many important properties, including:

- The singular field is only defined in a local region of spacetime about the particle.

- The singular field is a solution to the sourced differential equation for ψ: $\nabla_\alpha \nabla^\alpha \psi^{\mathrm{S}} = -4\pi\rho$.

- The singular field reproduces the singular behavior of ψ^{ret} near the particle, so that ψ^{R} is continuous and differentiable at the particle.

- According to Quinn's axioms, the singular field does not contribute to the self-force.

Thus, the Detweiler-Whiting singular field gives us exactly what we need: to find the self-force, we can simply take a derivative of $\psi^{\mathrm{R}} = \psi^{\mathrm{ret}} - \psi^{\mathrm{S}}$:

$$F^{\mathrm{R},\alpha} = q \left. \nabla^\alpha \psi^{\mathrm{R}} \right|_{x=x0}. \tag{3.3.7}$$

We omit any expression for the Detweiler-Whiting singular field here simply because it takes a very simple form once we use *mode-sum renormalization*. The mode-sum renormalization method was first introduced by Barack and Ori [93] for scalar charges following geodesics through Schwarzschild spacetime; eventually, Linz, Friedman, and Wiseman [94] showed that it can be used for any kind (scalar, electromagnetic, or gravitational) of charge following an arbitrary path on any smooth spacetime. The idea is

this: when one decomposes the retarded field into spherical harmonics

$$\psi(t, r, \theta, \phi) = \sum_{\ell=0}^{\infty} \sum_{m=-\ell}^{\ell} \psi_{\ell m}(t, r) \, {}_0Y_{\ell m}(\theta, \phi), \tag{3.3.8}$$

the individual ℓm-modes $\{\psi_{\ell m}\}$ and their derivatives are finite, even in the limit $x \to x_0$. Thus, in this prescription the retarded field is *regularized*—that is, it is decomposed into an infinite set of finite pieces. We can similarly decompose the self-force (allowing it to be defined off the particle's world line):

$$F^{\alpha} = \sum_{\ell=0}^{\infty} \sum_{m=-\ell}^{\ell} F_{\ell m}^{\alpha}(t, r) \, {}_0Y_{\ell m}(\theta, \phi) \tag{3.3.9}$$

$$= \sum_{\ell=0}^{\infty} F_{\ell}^{\alpha}, \tag{3.3.10}$$

where

$$F_{\ell}^{\alpha} = \sum_{m=-\ell}^{\ell} F_{\ell m}^{\alpha} \, {}_0Y_{\ell m}.$$

Because the sum over m is finite, F_{ℓ}^{α} is also finite. Finally, this method shines most brightly when one considers the ℓ-modes of the singular part of the force. It turns out that one can write

$$\lim_{r \to r_0^{\pm}} F_{\ell}^{\mathrm{S},\alpha} = \mp A^{\alpha} \left(\ell + \frac{1}{2} \right) + B^{\alpha}, \tag{3.3.11}$$

where A^{α} and B^{α} are ℓ-independent vectors. That is, the ℓ-modes of the singular part of the force have one term proportional to $\ell + 1/2$ and another that is independent of ℓ. Clearly, these two terms diverge when we do the sum over ℓ. Once one subtracts these two terms from the full force, resulting from the retarded field, we are left with the renormalized force:

$$F^{\mathrm{R},\alpha} = \sum_{\ell=0}^{\infty} F_{\ell}^{\alpha} - F_{\ell}^{\mathrm{S},\alpha}. \tag{3.3.12}$$

In this way, we can renormalize the self-force without directly dealing with any diverging quantities.

As we will show below, Hikida [8, 9] found a way to calculate the *regularization parameters* A^{α} and B^{α}—as well as $F^{\mathrm{R},\alpha}$—analytically, to finite post-Newtonian order. The mode-sum renormalization will therefore be indispensable to us.

49

3.3.2 Description of the system and the resulting scalar perturbation

We now specialize to the specific system considered in this chapter: a scalar point charge in circular orbit around a Schwarzschild black hole of mass M. We use Schwarzschild coordinates (t, r, θ, ϕ), and give the particle naughted coordinates $x_0 = (t_0, r_0, \theta_0, \phi_0)$. We choose our angular coordinates so that $\theta_0 = \pi/2$; because the orbit is circular, the particle's radial coordinate r_0 is constant in t_0. The particle's angular velocity as measured by a stationary observer at infinity is $\Omega = \mathrm{d}\phi_0/\mathrm{d}t_0$. We note that the coordinates of the particle's four-velocity can be written

$$u^\alpha = u^t(1, 0, 0, \Omega)$$

with

$$u^t = \sqrt{\frac{1}{1 - \frac{2M}{r_0} - r_0^2\Omega^2}}.$$

Finally, we emphasize here that we allow the particle to be accelerated; that is, we allow the particle's angular velocity to deviate from the Keplerian value Ω_K obtained from the geodesic equation:

$$\Omega_K = \sqrt{\frac{M}{r_0^3}}. \tag{3.3.13}$$

This is counter to what is normally done in self-force calculations, where the particle's motion to zeroth order in q is taken to be a geodesic. We do not specify what is responsible for the acceleration, but we do assume that its associated stress-energy tensor is small enough that we can still consider the particle to be moving through a Schwarzschild spacetime. Our motivation, beyond academic curiosity, is twofold. First, studying an accelerated particle will allow us to compare our answer to special cases for the self-force on a scalar charge. For example, Wiseman [95] showed that the self-force on a static scalar charge outside a Schwarzschild black hole is zero. We can't compare our result to his if we require the charge to follow a geodesic. Second, Galley and collaborators [96–100] have pioneered the use of effective field theory to solve self-force problems. Since terms proportional to, say, $M^2\Omega^2$ are associated with a different Feynman diagram than terms proportional to $Mr_0^3\Omega^4$, having these terms separated out can be useful points of comparison even though they are identical when the particle follows a geodesic.

Now that we've specified the system we are studying, we can make progress solving for the resulting scalar field ψ. The particle's charge density is given by a delta function spiked at its position:

$$\rho(x) = q \int_{-\infty}^{\infty} d\tau \, \frac{\delta(t-t_0)\delta(r-r_0)\delta(\theta-\theta_0)\delta(\phi-\phi_0)}{\sqrt{-\det(g_{\mu\nu})}}$$

$$= \frac{q}{u^t} \frac{\delta(r-r_0)\delta(\theta-\theta_0)\delta(\phi-\Omega t)}{r^2 \sin\theta},$$

and the resulting scalar field is

$$\psi = -4\pi \int d^4 x' G(x,x')\rho(x')$$

$$= -4\pi \frac{q}{u^t} \int_{-\infty}^{\infty} dt_0 G(x,x_0). \tag{3.3.14}$$

To move forward, it is helpful to look at the form of G given by Eq. (3.2.24):

$$\int_{-\infty}^{\infty} dt_0 G(x,x_0) = \frac{1}{2\pi} \int_{-\infty}^{\infty} dt_0 \int_{-\infty}^{\infty} d\omega \sum_{\ell=0}^{\infty} \sum_{m=-\ell}^{\ell} g_{\ell\omega}(r,r_0)e^{-i\omega(t-t_0)} \, {}_0Y_{\ell m}(\theta,\phi) \, {}_0\overline{Y}_{\ell m}(\theta_0,\phi_0).$$

We note that ${}_0\overline{Y}_{\ell m}(\theta_0,\phi_0) = {}_0\overline{Y}_{\ell m}(\theta_0,\Omega t_0) = {}_0\overline{Y}_{\ell m}(\theta_0,0)e^{-im\Omega t_0}$. Therefore, collecting the terms involving t_0 and performing the integrations,

$$\int_{-\infty}^{\infty} dt_0 G(x,x_0) = \frac{1}{2\pi} \int_{-\infty}^{\infty} dt_0 \int_{-\infty}^{\infty} d\omega \sum_{\ell=0}^{\infty} \sum_{m=-\ell}^{\ell} g_{\ell\omega}(r,r_0)e^{-i\omega t}e^{i(\omega-m\Omega)t_0}$$

$$\times {}_0Y_{\ell m}(\theta,\phi) \, {}_0\overline{Y}_{\ell m}(\theta_0,0)$$

$$= \int_{-\infty}^{\infty} d\omega \sum_{\ell=0}^{\infty} \sum_{m=-\ell}^{\ell} g_{\ell\omega}(r,r_0)e^{-i\omega t}\delta(\omega-m\Omega) \, {}_0Y_{\ell m}(\theta,\phi) \, {}_0\overline{Y}_{\ell m}(\theta_0,0)$$

$$= \sum_{\ell=0}^{\infty} \sum_{m=-\ell}^{\ell} g_{\ell m}(r,r_0)e^{-im\Omega t} \, {}_0Y_{\ell m}(\theta,\phi) \, {}_0\overline{Y}_{\ell m}(\theta_0,0)$$

$$= \sum_{\ell=0}^{\infty} \sum_{m=-\ell}^{\ell} g_{\ell m}(r,r_0) \, {}_0Y_{\ell m}(\theta,\phi-\Omega t) \, {}_0\overline{Y}_{\ell m}(\theta_0,0),$$

where $g_{\ell m}(r,r_0) = g_{\ell\omega}(r,r_0)|_{\omega\to m\Omega}$. Therefore,

$$\psi = -4\pi \frac{q}{u^t} \sum_{\ell=0}^{\infty} \sum_{m=-\ell}^{\ell} g_{\ell m}(r,r_0)e^{-im\Omega t} \, {}_0Y_{\ell m}(\theta,\phi) \, {}_0\overline{Y}_{\ell m}(\theta_0,0) \tag{3.3.15}$$

$$= -4\pi \frac{q}{u^t} \sum_{\ell=0}^{\infty} \sum_{m=-\ell}^{\ell} g_{\ell m}(r,r_0) \, {}_0Y_{\ell m}(\theta,\phi-\Omega t) \, {}_0\overline{Y}_{\ell m}(\theta_0,0). \tag{3.3.16}$$

We report both equations above because, while the first one more explicitly gives the time-dependence, the second more clearly shows that, when one evaluates ψ at $x = x_0$, the resulting summand is proportional to $|_0Y_{\ell m}(\theta_0, 0)|^2$. We note here that the above integrations over t_0 and ω are simple only because of the particle's circular motion; otherwise, r_0 would be a function of t_0.

The way to complete the self-force calculation now seems clear: we know how to calculate $g_{\ell m}$ to finite PN order from Eq. (3.2.3) and MST's method. If we do that and sum over m, we can find the high-ℓ behavior of

$$\psi_\ell \equiv -4\pi \frac{q}{u^t} \sum_{m=-\ell}^{\ell} g_{\ell m}(r, r_0) e^{-im\Omega t} \, _0Y_{\ell m}(\theta, \phi) \, _0Y_{\ell m}(\theta_0, 0) \tag{3.3.17}$$

and therefore of

$$F_\ell^\alpha \equiv P_\beta^\alpha \nabla^\beta \psi_\ell|_{x=x_0} \tag{3.3.18}$$

and recover A^α and B^α. We can then subtract the ℓ-modes of the singular part of the force and recover the renormalized self-force.

There is one difficulty with the above prescription: the sum over m. In particular, the factor of $|2\zeta|^\nu$ in ϕ_c^ν creates difficulty. When expanded in z and ϵ (which are now equal to $m\Omega r$ and $2Mm\omega$, respectively), this factor gives rise to terms proportional to $\ln|z|$. Terms logarithmic in z are challenging to sum over m analytically for generic ℓ. We will therefore need to use a trick discovered by Hikida *et al.* [8, 9], which we discuss in the next subsection.

3.3.3 Hikida's Method

Before we discuss Hikida's method in detail, I wish to write ϕ_c^ν for $s = 0$ in terms of ϵ and z. As we will see, our PN expansions will coincide with a double Taylor series in ϵ and z, and $\zeta \equiv z - \epsilon$ will be less useful to us. Also, ϕ_c^ν is significantly simpler in the $s = 0$ case:

$$\phi_c^\nu = e^{-i(z-\epsilon)}|2z|^\nu \left(1 - \frac{\epsilon}{z}\right)^\nu \sum_{n=-\infty}^{\infty} a_n^\nu \frac{(\nu + 1 + i\epsilon)_n}{(2\nu + 2)_{2n}} [2i(z - \epsilon)]^n$$

$$\times \, _1F_1(n + \nu + 1 + i\epsilon; 2n + 2\nu + 2, 2i(z - \epsilon)). \tag{3.3.19}$$

Here, we have factored out $|2z|^\nu$ from $|2\zeta|^\nu$. We don't need an absolute value sign on $(1 - \epsilon/z) = (1 - 2M/r)$ because it is always positive. Hikida *et al.* noticed that if we define Φ^ν and $\Phi^{-\nu-1}$ by

$$\phi_c^\nu = |2z|^\nu \Phi^\nu, \tag{3.3.20}$$

$$\phi_c^{-\nu-1} = |2z|^{-\nu-1} \Phi^{-\nu-1}, \tag{3.3.21}$$

then Φ^ν and $\Phi^{-\nu-1}$ can be expanded as polynomials in ϵ and z. That is, there are no logarithmic terms in Φ^ν and $\Phi^{-\nu-1}$. The terms that are logarithmic in ω—which are the terms that make the sum over m in Eq. (3.3.17) difficult—are due solely to the factor of $|2z|^\nu$. To see this more explicitly, we write $\nu = \ell + \sum_{n=1}^\infty \nu_{2n}\epsilon^{2n}$. Then

$$
\begin{aligned}
|2z|^\nu &= |2z|^\ell |2z|^{\sum_{n=1}^\infty \nu_{2n}\epsilon^{2n}} \\
&= |2z|^\ell \exp\left(\ln|2z| \sum_{n=1}^\infty \nu_{2n}\epsilon^{2n} \right) \\
&= |2z|^\ell [1 + \nu_2 \epsilon^2 \ln|2z| + \mathcal{O}(\epsilon^4)].
\end{aligned}
$$

Next, Hikida *et al.* write $g_{\ell\omega}$ in terms of ϕ_c^ν and $\phi_c^{-\nu-1}$:

$$
\begin{aligned}
g_{\ell\omega}(r,r') &= \frac{1}{(1 - \beta_c^\nu \gamma_c^\nu)W_{\ell\omega}(\phi_c^\nu, \phi_c^{-\nu-1})} \left[\phi_c^\nu(r_<) + \beta_c^\nu \phi_c^{-\nu-1}(r_<) \right] \left[\gamma_c^\nu \phi_c^\nu(r_>) + \phi_c^{-\nu-1}(r_>) \right] \\
&= \frac{1}{(1 - \beta_c^\nu \gamma_c^\nu)W_{\ell\omega}(\phi_c^\nu, \phi_c^{-\nu-1})} \Big[\phi_c^\nu(r_<)\phi_c^{-\nu-1}(r_>) + \beta_c^\nu \gamma_c^\nu \phi_c^\nu(r_>)\phi_c^{-\nu-1}(r_<) \\
&\qquad\qquad\qquad + \gamma_c^\nu \phi_c^\nu(r_<)\phi_c^\nu(r_>) + \beta_c^\nu \phi_c^{-\nu-1}(r_<)\phi_c^{-\nu-1}(r_>) \Big] \\
&= \frac{1}{(1 - \beta_c^\nu \gamma_c^\nu)W_{\ell\omega}(\phi_c^\nu, \phi_c^{-\nu-1})} \Big\{ (1 - \beta_c^\nu \gamma_c^\nu)\phi_c^\nu(r_<)\phi_c^{-\nu-1}(r_>) \\
&\qquad\qquad + \gamma_c^\nu \phi_c^\nu(r_<)\phi_c^\nu(r_>) + \beta_c^\nu \phi_c^{-\nu-1}(r_<)\phi_c^{-\nu-1}(r_>) \\
&\qquad\qquad + \beta_c^\nu \gamma_c^\nu \left[\phi_c^\nu(r_<)\phi_c^{-\nu-1}(r_>) + \phi_c^\nu(r_>)\phi_c^{-\nu-1}(r_<) \right] \Big\}
\end{aligned}
$$

Let us notice a few things about the terms on the right side of the last equation. First, the first term is the only one whose derivative is discontinuous at the particle. The rest of $g_{\ell\omega}$ is symmetric in $r_<$ and $r_>$ and therefore in r and r'. The first term is also free of terms logarithmic in ω; the factors of $|2z|^\nu$ cancel out. Hikida *et al.*, noticing this, then split $g_{\ell\omega}$ into two parts:

$$g_{\ell\omega}(r,r') = g_{\ell\omega}^{\tilde{S}}(r,r') + g_{\ell\omega}^{\tilde{R}}(r,r'), \tag{3.3.22}$$

with

$$g_{\ell\omega}^{\tilde{S}}(r,r') = \frac{\phi_c^\nu(r_<)\phi_c^{-\nu-1}(r_>)}{W_{\ell\omega}(\phi_c^\nu, \phi_c^{-\nu-1})}, \tag{3.3.23}$$

$$g_{\ell\omega}^{\tilde{R}}(r,r') = \frac{1}{(1-\beta_c^\nu\gamma_c^\nu)W_{\ell\omega}(\phi_c^\nu, \phi_c^{-\nu-1})} \left\{ \gamma_c^\nu\phi_c^\nu(r)\phi_c^\nu(r') + \beta_c^\nu\phi_c^{-\nu-1}(r)\phi_c^{-\nu-1}(r') \right.$$
$$\left. + \beta_c^\nu\gamma_c^\nu \left[\phi_c^\nu(r)\phi_c^{-\nu-1}(r') + \phi_c^\nu(r')\phi_c^{-\nu-1}(r) \right] \right\}. \tag{3.3.24}$$

Let's study $g_{\ell\omega}^{\tilde{R}}$ more closely. We note from the expressions for β_c^ν and γ_c^ν that $\beta_c^\nu = \mathcal{O}(\epsilon^{2\ell+1})$ and $\gamma_c^\nu = \mathcal{O}(\epsilon^{-1})$. Furthermore, for $\ell \neq 0$, Φ^ν and $\Phi^{-\nu-1}$ are $\mathcal{O}(1)$, so $\phi_c^\nu = \mathcal{O}(z^\ell)$ and $\phi_c^{-\nu-1} = \mathcal{O}(z^{-\ell-1})$. Finally, in order to convert expansions in z and ϵ into a Post-Newtonian expansion, we see that $z = \text{PN}(.5)$ and $\epsilon = \text{PN}(1.5)$, where $\text{PN}(x)$ indicates that a term is at x^{th} Post-Newtonian order. Taking all these results together and looking at the terms in $g_{\ell\omega}^{\tilde{R}}$, it becomes clear that for $\ell \neq 0$ the lowest-order term in $g_{\ell\omega}^{\tilde{R}}$ is the first one in Eq. (3.3.24), and $g_{\ell\omega}^{\tilde{R}} = \text{PN}(\ell - 1.5)$. Thus, the PN order of $g_{\ell\omega}^{\tilde{R}}$ increases with ℓ, and to do a finite-PN order calculation, we only need to calculate $g_{\ell\omega}^{\tilde{R}}$ for a finite number of ℓ-values. Making the replacement $\omega \to m\Omega$ and summing over m is therefore not a problem because the sum can be done explicitly.

While we still need to calculate $g_{\ell\omega}^{\tilde{S}}(r,r')$ for all ℓ-values, it turns out that we can: we saw general-ℓ expressions for the coefficients $\{a_n^\nu\}$ in Eq. (3.2.16), and we saw a general-ℓ expression for ν_2 in Eq. (3.2.15). It follows that there are general-ℓ expressions for ϕ_c^ν and $\phi_c^{-\nu-1}$. We also saw that the general-ℓ expressions do not work for all ℓ-values; specifically, we saw that in order to calculate the coefficients and ν to second order in ϵ, we couldn't use the general-ℓ expressions for $\ell = 0, 1$. It turns out that the general-ℓ expressions for ϕ_c^ν and $\phi_c^{-\nu-1}$ are only valid to $(\ell-1)^{\text{th}}$ PN order. Thus, to calculate $g_{\ell\omega}^{\tilde{S}}(r,r')$ accurately to n^{th} PN order, we can use the general-ℓ expressions when $\ell > n + 1$, but we need to calculate $g_{\ell\omega}^{\tilde{S}}(r,r')$ explicitly for lower ℓ-values. Furthermore, since $g_{\ell\omega}^{\tilde{S}}(r,r')$ is polynomial in ω, $g_{\ell m}^{\tilde{S}}(r,r')$ is polynomial in m, and it is possible to do the sum over m indicated in Eq. (3.3.17) for general ℓ analytically using

$$\sum_{m=-\ell}^{\ell} m^{2n} \left| {}_0Y_{\ell m}\left(\frac{\pi}{2}, 0\right) \right|^2 = (-1)^n \frac{2\ell+1}{4\pi} \left. \frac{\mathrm{d}}{\mathrm{d}\phi} P_\ell(\cos\phi) \right|_{\phi=0}. \tag{3.3.25}$$

Therefore, for ℓ-values that are high enough relative to the PN order we calculate to, we can use the general-ℓ expressions to find $g_{\ell m}^{\tilde{S}}(r, r')$ and then do the sum over m using Eq. (3.3.25). For the lower ℓ-values, we must calculate each $g_{\ell m}^{\tilde{S}}(r, r')$ explicitly.

It is now clear that, at least to finite PN order, the field $\psi^{\tilde{S}}$ calculated from $g_{\ell \omega}^{\tilde{S}}(r, r')$ contains the singular field ψ^{S}, while $g_{\ell \omega}^{\tilde{R}}$ produces a regular field $\psi^{\tilde{R}}$. Thus, we only need to renormalize the $\tilde{S}$ part of the force $F^{\tilde{S}}$ resulting from $\psi^{\tilde{S}}$. We can do so using the general-ℓ expression for $\psi^{\tilde{S}}$, computing the sum over m using Eq. (3.3.25), and recovering the regularization parameters analytically from the high-ℓ behavior of the result.

Finally, Hikida *et al.* employ one more trick: they notice that $g^{\tilde{S}}$ can be split into to parts: one that is symmetric in r and r' and one that is antisymmetric. Specifically,

$$g_{\ell \omega}^{\tilde{S}} = g_{\ell \omega}^{\tilde{S}(+)}(r, r') + g_{\ell \omega}^{\tilde{S}(-)}(r, r') \mathrm{Sign}(r - r'), \qquad (3.3.26)$$

and

$$g_{\ell \omega}^{\tilde{S}(\pm)}(r, r') = \frac{1}{2 W_{\ell \omega}(\phi_c^\nu, \phi_c^{-\nu-1})} \left[\phi_c^\nu(r) \phi_c^{-\nu-1}(r') \pm \phi_c^{-\nu-1}(r') \phi_c^\nu(r') \right]. \qquad (3.3.27)$$

When we introduced mode-sum regularization, we saw that the "A-term" $A^\alpha(\ell + 1/2)$ switches sign if one approaches the particle from the opposite radial direction, whereas the "B-term" B^α is unchanged regardless of the the direction from which one approaches the particle. Clearly, then, the antisymmetric part of the Green's function is responsible only for the A-term, and we are free to discard it. This is equivalent to averaging the field outside the particle's orbit with the field inside the orbit, and is standard practice in self-force calculations. This allows us to only have to subtract the B-term when we renormalize.

Our method is therefore as follows:

1. Choose a PN order.

2. Generate the general-ℓ expression for $g_{\ell m}^{\tilde{S}}(r, r')$ to said PN Order.

3. Find the general-ℓ expression for $\psi_\ell^{\tilde{S}(+)}$ using Eq. (3.3.25)

4. Compute the resulting general-ℓ expression for $F_\ell^{\tilde{S}(+),\alpha}$.

5. Get the regularization parameter

$$B^\alpha = \lim_{\ell \to \infty} F_\ell^{\tilde{S}(+),\alpha}$$

6. For low ℓ-values, compute $F_\ell^{\tilde{S}(+),\alpha}$

7. Perform the sum

$$F^{\tilde{S}-S,\alpha} = \sum_{\ell=0}^{\infty} \left[F_\ell^{\tilde{S}(+),\alpha} - B^\alpha \right].$$

8. Compute $F_\ell^{\tilde{R},\alpha}$ explicitly for all ℓ-values needed to be accurate to the given PN order.

9. Perform the sum

$$F^{\tilde{R},\alpha} = \sum_{\ell=0}^{\ell_{\max}} F_\ell^{\tilde{R},\alpha},$$

where $\ell_{\max}$ is the maximum ℓ-value needed for that PN order.

10. Add the $(\tilde{S} - S)$ and $\tilde{R}$ parts of the force:

$$F^{R,\alpha} = F^{\tilde{S}-S,\alpha} + F^{\tilde{R},\alpha}.$$

3.4   Results

We choose to find the self-force to 6th PN order. This means we must explicitly calculate Φ^ν and $\Phi^{-\nu-1}$ for $\ell \in [0, 7]$, and we may use general-ℓ expressions for $\ell \geq 8$. We also note here that for $\ell = 0$, $\Phi^{-\nu-1} = \text{PN}(-1)$, so we need to calculate Φ^ν to 7th PN order, whereas for all other ℓ-values we find both Φ^ν and $\Phi^{-\nu-1}$ to 6th order.[9] We will report intermediate results, including general- and specific-ℓ expressions for Φ^ν, $\Phi^{-\nu-1}$, and $F_{\alpha,\ell}^{\tilde{S}(+)}$, as well as

---

[9]The reason for this is that the specific-ℓ expressions for $\Phi^{-\nu-1}$ have terms proportional to M^{-1}. These terms enter $\Phi^{-\nu-1}$ at $\text{PN}(\ell - 1)$, and are one of the ways that the specific-ℓ expressions deviate from the general-ℓ ones. For $\ell = 0$, then, there is a $\text{PN}(-1)$ term proportional to r/M. After we add the $\tilde{S} - S$ part of the force—which has M^{-1} terms due to the presence of $\Phi^{-\nu-1}$—to the $\tilde{R}$ part—which has these terms both due to $\Phi^{-\nu-1}$ and γ_c^ν, whose leading order term is inversely proportional to M—the terms inversely proportional to M cancel in an apparently miraculous way. However, Hikida *et al.* [8] show that these terms cannot contribute to the force for physical reasons.

$F_{\alpha,\ell}^{\tilde{\text{R}}}$, which only has specific-ℓ expressions. We show these to help the reader understand how the renormalized force is ultimately calculated, but because typesetting the general-ℓ expressions becomes intractable at high PN order, we only give them to 2$^{\text{nd}}$ PN order. We give quantities that are calculated from the intermediate results to 6$^{\text{th}}$ PN order; these include the regularization parameter B_α, the renormalized $\tilde{\text{S}}$ part of the force $F_\alpha^{\tilde{\text{S}}-\text{S}}$, the $\tilde{\text{R}}$ part of the force, and the total renormalized force F_α^{R}.

Before we get to more complicated results, we mention that, in the scalar case, ϕ_c^ν and $\phi_c^{-\nu-1}$ are real, and because of Eq. (3.2.18), even in ω. After the replacement $\omega \to m\Omega$, they are even in m. Therefore, $g_{\ell m}^{\tilde{\text{S}}}$ is also even in m. When we take a time derivative of $\psi^{\tilde{\text{S}}}$, this introduces a factor of $-im\Omega$ to its corresponding summand in Eq. (3.3.15), causing the summand to be odd in m. The sum over m is therefore zero, with the end result that

$$F_{t,\ell}^{\tilde{\text{S}}(+)} = 0 \qquad (3.4.1)$$

for all values of ℓ, and therefore

$$F_t^{\tilde{\text{S}}} = 0. \qquad (3.4.2)$$

Since the motion is circular, $F_\phi^{\tilde{\text{S}}} \propto F_t^{\tilde{\text{S}}}$, and

$$F_\phi^{\tilde{\text{S}}} = 0. \qquad (3.4.3)$$

The t- (or ϕ-) component of the force modifies the energy of the particle, and this energy is carried away by the resulting scalar radiation. Since the t-component of the $\tilde{\text{S}}$ part of the force is zero, it must be that the $\tilde{\text{R}}$ part of the field carries the radiative information. This is an unexpected benefit of the otherwise unphysical $\tilde{\text{R}}$-$\tilde{\text{S}}$ decomposition.

We also note that, since the quantity $\partial_\theta \, _0Y_{\ell m}(\theta,0)|_{\theta=\theta_0} \, _0Y_{\ell m}(\theta_0,0) = 0$,

$$F_\theta^{\tilde{\text{S}}} = F_\theta^{\tilde{\text{R}}} = F_\theta^{\text{R}} = 0. \qquad (3.4.4)$$

3.4.1   Intermediate Results

All expressions in this section will be accurate through 2$^{\text{nd}}$ PN order. The general-ℓ expressions will therefore be true for all $\ell > 3$. We start with the general-ℓ expressions

for Φ^ν and $\Phi^{-\nu-1}$. We manually insert factors of c so that the reader can easily distinguish between different PN orders.

$$\begin{aligned}
\Phi^\nu =1+ &\left[-\frac{M}{r}\ell - \frac{(r\omega)^2}{2}\frac{1}{2\ell+3}\right]\frac{1}{c^2} + \left[\frac{M^2}{r^2}\frac{\ell(\ell-1)^2}{2\ell-1}\right.\\
&\left.+\frac{M}{r}\frac{(r\omega)^2}{2}\frac{\ell^2-5\ell-10}{(\ell+1)(2\ell+3)} + \frac{(r\omega)^4}{8}\frac{1}{(2\ell+3)(2\ell+5)}\right]\frac{1}{c^4} + \text{PN}(3)
\end{aligned} \qquad (3.4.5)$$

$$\begin{aligned}
\Phi^{-\nu-1} =1+ &\left[\frac{M}{r}(\ell+1) + \frac{(r\omega)^2}{2}\frac{1}{2\ell-1}\right]\frac{1}{c^2} + \left[\frac{M^2}{r^2}\frac{(\ell+1)(\ell+2)^2}{2\ell+3}\right.\\
&\left.+\frac{M}{r}\frac{(r\omega)^2}{2}\frac{\ell^2+7\ell-4}{\ell(2\ell-1)} + \frac{(r\omega)^4}{8}\frac{1}{(2\ell-1)(2\ell-3)}\right]\frac{1}{c^4} + \text{PN}(3)
\end{aligned} \qquad (3.4.6)$$

Now for the specific-ℓ expressions for the same quantities. For $\ell = 0$, we report Φ^ν through PN(3) because that is required to find the force through PN(2). For $\ell = 0$:

$$\begin{aligned}
\Phi^\nu =\frac{7}{9}+ &\left[-\frac{14}{27}\frac{M}{r} - \frac{7}{54}(r\omega)^2\right]\frac{1}{c^2} + \left[-\frac{14}{27}\frac{M^2}{r^2} - \frac{28}{27}\frac{M}{r}(r\omega)^2 + \frac{7}{1080}(r\omega)^4\right]\frac{1}{c^4}\\
&+\left[-\frac{56}{81}\frac{M^3}{r^3} + \frac{7601}{2835}\frac{M^2}{r^2}(r\omega)^2 + \frac{203}{1620}\frac{M}{r}(r\omega)^4 - \frac{1}{6480}(r\omega)^6\right]\frac{1}{c^6} + \text{PN}(4)
\end{aligned} \qquad (3.4.7)$$

$$\begin{aligned}
\Phi^{-\nu-1} = -&\frac{1}{3}\frac{r}{M}c^2 + \left[1 + \frac{1}{18}\frac{r}{M}(r\omega)^2\right] + \left[\frac{M}{r} + \frac{1}{18}(r\omega)^2 - \frac{1}{360}\frac{r}{M}(r\omega)^4\right]\frac{1}{c^2}\\
&+\left[\frac{4}{3}\frac{M^2}{r^2} + \frac{2243}{1890}\frac{M}{r}(r\omega)^2 - \frac{23}{1080}(r\omega)^4 + \frac{1}{15120}\frac{r}{M}(r\omega)^6\right]\frac{1}{c^4} + \text{PN}(3)
\end{aligned} \qquad (3.4.8)$$

For $\ell = 1$:

$$\Phi^\nu =1+ \left[-\frac{M}{r} - \frac{1}{10}(r\omega)^2\right]\frac{1}{c^2} + \left[-\frac{7}{10}\frac{M}{r}(r\omega)^2 + \frac{1}{280}(r\omega)^4\right]\frac{1}{c^4} + \text{PN}(3) \qquad (3.4.9)$$

$$\begin{aligned}
\Phi^{-\nu-1} =&\left[1 - \frac{5}{19}\frac{r}{M}(r\omega)^2\right] + \left[2\frac{M}{r} + \frac{29}{38}(r\omega)^2 + \frac{1}{38}\frac{r}{M}(r\omega)^4\right]\frac{1}{c^2}\\
&+\left[\frac{18}{5}\frac{M^2}{r^2} + 2\frac{M}{r}(r\omega)^2 + \frac{9}{152}(r\omega)^4 - \frac{1}{1064}\frac{r}{M}(r\omega)^6\right]\frac{1}{c^4} + \text{PN}(3)
\end{aligned} \qquad (3.4.10)$$

For $\ell = 2$:

$$\Phi^\nu =1+ \left[-2\frac{M}{r} - \frac{1}{14}(r\omega)^2\right]\frac{1}{c^2} + \left[\frac{2}{3}\frac{M^2}{r^2} - \frac{8}{21}\frac{M}{r}(r\omega)^2 + \frac{1}{504}(r\omega)^4\right]\frac{1}{c^4} + \text{PN}(3)$$

$$(3.4.11)$$

$$\Phi^{-\nu-1} = 1 + \left[3\frac{M}{r} + \frac{1}{6}(r\omega)^2 - \frac{7}{237}\frac{r}{M}(r\omega)^4\right]\frac{1}{c^2}$$
$$+ \left[\frac{48}{7}\frac{M^2}{r^2} + \frac{7}{6}\frac{M}{r}(r\omega)^2 + \frac{191}{1896}(r\omega)^4 + \frac{1}{474}\frac{r}{M}(r\omega)^6\right]\frac{1}{c^4} + \mathrm{PN(3)} \qquad (3.4.12)$$

For $\ell = 3$:

$$\Phi^{\nu} = 1 + \left[-3\frac{M}{r} - \frac{1}{18}(r\omega)^2\right]\frac{1}{c^2} + \left[\frac{12}{5}\frac{M^2}{r^2} - \frac{2}{9}\frac{M}{r}(r\omega)^2 + \frac{1}{792}(r\omega)^4\right]\frac{1}{c^4} + \mathrm{PN(3)} \qquad (3.4.13)$$

$$\Phi^{-\nu-1} = 1 + \left[4\frac{M}{r} + \frac{1}{10}(r\omega)^2\right]\frac{1}{c^2}$$
$$+ \left[\frac{100}{9}\frac{M^2}{r^2} + \frac{13}{15}\frac{M}{r}(r\omega)^2 + \frac{1}{120}(r\omega)^4 - \frac{1}{845}\frac{r}{M}(r\omega)^6\right]\frac{1}{c^4} + \mathrm{PN(3)} \qquad (3.4.14)$$

The functions Φ^{ν} and $\Phi^{-\nu-1}$ are used to construct the radial Green's function and its $\tilde{\mathrm{R}}$ and $\tilde{\mathrm{S}}$ parts. These give rise to the respective parts of the scalar field ψ, and then to the force. The general-ℓ expression for $F_{r,\ell}^{\tilde{\mathrm{S}}(+)}$ is

$$F_{r,\ell}^{\tilde{\mathrm{S}}(+)} = \frac{q^2}{r_0^2}\left\{\left[-\frac{1}{2}\right] + \left[-\frac{1}{2}\frac{M}{r_0} + \frac{3(-1+2\ell+2\ell^2)}{4(-1+2\ell)(3+2\ell)}(r_0\omega)^2\right]\frac{1}{c^2}\right.$$
$$+ \left[-\frac{-9+16\ell+16\ell^2}{4(-1+2\ell)(3+2\ell)}\frac{M^2}{r_0^2} + \frac{-9+10\ell+10\ell^2}{4(-1+2\ell)(3+2\ell)}\frac{M}{r_0}(r_0\omega)\right.$$
$$\left.\left.+ \frac{3(15-16\ell+2\ell^2+36\ell^3+18\ell^4)}{16(-3+2\ell)(-1+2\ell)(3+2\ell)(5+2\ell)}(r_0\omega)^4\right]\frac{1}{c^4} + \mathrm{PN(3)}\right\} \qquad (3.4.15)$$

To get $F_r^{\tilde{\mathrm{S}}(+)}$ through 2$^{\mathrm{nd}}$ PN order, we need to calculate the ℓ-modes explicitly up through $\ell = 3$. These explicit ℓ-modes are as follows.

$$F_{r,0}^{\tilde{\mathrm{S}}(+)} = \frac{q^2}{r_0^2}\left[-\frac{11}{14} + \left(\frac{M}{14r_0} + \frac{11}{28}\Omega^2 r_0^2\right)\frac{1}{c^2} + \left(\frac{15M^2}{28r_0^2} + \frac{3}{4}M\Omega^2 r_0 + \frac{11}{112}\Omega^4 r_0^4\right)\frac{1}{c^4}\right.$$
$$+\mathrm{PN(3)}] \qquad (3.4.16)$$

$$F_{r,1}^{\tilde{\mathrm{S}}(+)} = \frac{q^2}{r_0^2}\left[\left(-\frac{1}{2} - \frac{5\Omega^2 r_0^3}{19M}\right) + \left(-\frac{M}{2r_0} + \frac{371}{380}\Omega^2 r_0^2 + \frac{9\Omega^4 r_0^5}{38M}\right)\frac{1}{c^2}\right.$$
$$\left.+ \left(-\frac{23M^2}{20r_0^2} + \frac{159}{380}M\Omega^2 r_0 + \frac{157\Omega^4 r_0^4}{2128} - \frac{177\Omega^6 r_0^7}{5320M}\right)\frac{1}{c^4} + \mathrm{PN(3)}\right] \qquad (3.4.17)$$

$$F_{r,2}^{\tilde{\mathrm{S}}(+)} = \frac{q^2}{r_0^2}\left[-\frac{1}{2} + \left(-\frac{M}{2r_0} + \frac{11}{28}\Omega^2 r_0^2 - \frac{56\Omega^4 r_0^5}{79M}\right)\frac{1}{c^2}\right.$$
$$\left.+ \left(-\frac{29M^2}{28r_0^2} + \frac{17}{28}M\Omega^2 r_0 + \frac{4295\Omega^4 r_0^4}{1264} + \frac{76\Omega^6 r_0^7}{79M}\right)\frac{1}{c^4} + \mathrm{PN(3)}\right] \qquad (3.4.18)$$

$$F_{r,3}^{\tilde{S}(+)} = \frac{q^2}{r_0^2} \left[-\frac{1}{2} + \left(-\frac{M}{2r_0} + \frac{23}{60}\Omega^2 r_0^2 \right) \frac{1}{c^2} \right.$$
$$\left. + \left(-\frac{61M^2}{60r_0^2} + \frac{37}{60}M\Omega^2 r_0 + \frac{161}{528}\Omega^4 r_0^4 - \frac{1368\Omega^6 r_0^7}{845M} \right) \frac{1}{c^4} + \text{PN}(3) \right] \qquad (3.4.19)$$

We will now report the expressions for the ℓ-modes of the $\tilde{R}$ part of the force, accurate through 2$^{\text{nd}}$ PN Order. We will first show these for the radial component.

$$F_{r,0}^{\tilde{R}} = \frac{q^2}{r_0^2} \left[-\frac{9}{7} + \left(-\frac{3}{7}\frac{M}{r_0} + \frac{9}{14}(r_0\Omega)^2 \right) \frac{1}{c^2} + \left(-\frac{3}{14}\frac{M^2}{r_0^2} + \frac{3}{2}\frac{M}{r_0}(r_0\Omega)^2 + \frac{9}{56}(r_0\Omega)^4 \right) \right.$$
$$\left. + \text{PN}(3) \right] \qquad (3.4.20)$$

$$F_{r,1}^{\tilde{R}} = \frac{q^2}{r_0^2} \left[\frac{5}{19}\frac{r_0}{M}(r_0\Omega)^2 + \left(-\frac{10}{19}(r_0\Omega)^2 - \frac{9}{38}\frac{r_0}{M}(r_0\Omega)^4 \right) \frac{1}{c^2} \right.$$
$$\left. + \left(\frac{5}{38}\frac{M}{r_0}(r_0\Omega)^2 - \frac{7}{19}(r_0\Omega)^4 + \frac{177}{5320}\frac{r_0}{M}(r_0\Omega)^6 \right) \frac{1}{c^4} + \text{PN}(3) \right] \qquad (3.4.21)$$

$$F_{r,2}^{\tilde{R}} = \frac{q^2}{r_0^2} \left[\left(\frac{56}{79}\frac{r_0}{M}(r_0\Omega)^4 \right) \frac{1}{c^2} + \left(-\frac{224}{79}(r_0\Omega)^4 - \frac{76}{79}\frac{r_0}{M}(r_0\Omega)^6 \right) \frac{1}{c^4} + \text{PN}(3) \right] \qquad (3.4.22)$$

$$F_{r,3}^{\tilde{R}} = \frac{q^2}{r_0^2} \left[\left(\frac{1368}{845}\frac{r_0}{M}(r_0\Omega)^6 \right) \frac{1}{c^4} + \text{PN}(3) \right] \qquad (3.4.23)$$

As mentioned in the last section, each ℓ-mode of the $\tilde{R}$ part of the force enters at a higher PN order than the previous ℓ-mode.

Finally, we show the ℓ-modes of the temporal component of the $\tilde{R}$ part of the force. Again, since the $\tilde{S}$ part doesn't contribute to the temporal component, these are all one needs to compute the damping force F_t^R.

$$F_{t,0}^{\tilde{R}} = 0 \qquad (3.4.24)$$

$$F_{t,1}^{\tilde{R}} = \frac{q^2}{r_0^2}\frac{r_0\Omega}{c} \left[\left(\frac{1}{3}(r_0\Omega)^3 \right) \frac{1}{c^3} + \left(-\frac{M}{r_0}(r_0\Omega)^3 - \frac{7}{30}(r_0\Omega)^5 \right) \frac{1}{c^5} + \text{PN}(3) \right] \qquad (3.4.25)$$

$$F_{t,2}^{\tilde{R}} = \frac{q^2}{r_0^2}\frac{r_0\Omega}{c} \left[\left(\frac{16}{15}(r_0\Omega)^5 \right) \frac{1}{c^5} + \text{PN}(3.5) \right] \qquad (3.4.26)$$

To reiterate from the last section, in order to calculate the full renormalized force F_α^R, we first need to take the high-ℓ limit of $F_{\alpha,\ell}^{\tilde{S}(+)}$. This gives us the regularization parameter

B_α. We then subtract B_α from $F_{\alpha,\ell}^{\tilde{\mathrm{S}}(+)}$ for all ℓ-values, and sum from $\ell = 0$ to ∞. Because we have general-ℓ expressions for $F_{\alpha,\ell}^{\tilde{\mathrm{S}}(+)}$ that are valid for $\ell > \mathrm{PN} + 1$, we can do this sum analytically. After that, we add the ℓ-modes of the $\tilde{\mathrm{R}}$ part of the force, which does not need to be renormalized. Only a finite number of the $\tilde{\mathrm{R}}$ ℓ-modes contributes to finite PN order, so no infinite sum is needed for that part.

3.4.2 B_α and $F_\alpha^{\tilde{\mathrm{S}}-\mathrm{S}}$

We now report the regularization parameter B_r, obtained by taking the high-ℓ limit of the general-ℓ expression for $F_{r,\ell}^{\tilde{\mathrm{S}}(+)}$. To 6th PN order, it is

$$
\begin{aligned}
B_r =& \frac{q^2}{r_0^2}\left[-\frac{1}{2} + \left(-\frac{M}{2r_0} + \frac{3}{8}\Omega^2 r_0^2\right)\left(\frac{1}{c}\right)^2 + \left(-\frac{M^2}{r_0^2} + \frac{5}{8}M\Omega^2 r_0 + \frac{27}{128}\Omega^4 r_0^4\right)\left(\frac{1}{c}\right)^4 \right.\\
&+ \left(M^2\Omega^2 - \frac{2M^3}{r_0^3} + \frac{95}{128}M\Omega^4 r_0^3 + \frac{79}{512}\Omega^6 r_0^6\right)\left(\frac{1}{c}\right)^6 \\
&+ \left(-\frac{4M^4}{r_0^4} + \frac{3M^3\Omega^2}{2r_0} + \frac{123}{64}M^2\Omega^4 r_0^2 + \frac{429}{512}M\Omega^6 r_0^5 + \frac{4095\Omega^8 r_0^8}{32768}\right)\left(\frac{1}{c}\right)^8 \\
&+ \left(-\frac{8M^5}{r_0^5} + \frac{2M^4\Omega^2}{r_0^2} + \frac{69}{16}M^3\Omega^4 r_0 + 3M^2\Omega^6 r_0^4 + \frac{30183M\Omega^8 r_0^7}{32768}\right. \\
&\left.+ \frac{13995\Omega^{10} r_0^{10}}{131072}\right)\left(\frac{1}{c}\right)^{10} \\
&+ \left(\frac{35M^4\Omega^4}{4} - \frac{16M^6}{r_0^6} + \frac{2M^5\Omega^2}{r_0^3} + \frac{565}{64}M^3\Omega^6 r_0^3 + \frac{69015M^2\Omega^8 r_0^6}{16384}\right. \\
&\left.\left.+ \frac{130533M\Omega^{10} r_0^9}{131072} + \frac{197659\Omega^{12} r_0^{12}}{2097152}\right)\left(\frac{1}{c}\right)^{12} + \mathrm{PN}(7)\right],
\end{aligned}
$$

where we have manually re-added factors of $1/c$ so that one can easily demarcate terms of different PN orders. We write the resulting renormalized $\tilde{\mathrm{S}}$ force as

$$
F_r^{\tilde{\mathrm{S}}-\mathrm{S}} = \frac{q^2}{r_0^2}\sum_{n=0}^{6} C_{r,n}^{\tilde{\mathrm{S}}-\mathrm{S}}, \tag{3.4.27}
$$

where n refers to the PN order of the term, and

$$
C_{r,0}^{\tilde{\mathrm{S}}-\mathrm{S}} = -\frac{2}{7} - \frac{5r_0^3\Omega^2}{19M} \tag{3.4.28}
$$

$$
C_{r,1}^{\tilde{\mathrm{S}}-\mathrm{S}} = \frac{4M}{7r_0} + \frac{89r_0^2\Omega^2}{133} - \frac{1417r_0^5\Omega^4}{3002M} \tag{3.4.29}
$$

$$C_{r,2}^{\tilde{\text{S}}-\text{S}} = \frac{9M^2}{7r_0^2} - \frac{5}{38}Mr_0\Omega^2 + \frac{136153r_0^4\Omega^4}{42028} - \frac{9804331r_0^7\Omega^6}{14205464M} \tag{3.4.30}$$

$$C_{r,3}^{\tilde{\text{S}}-\text{S}} = \frac{482M^3}{133r_0^3} - \frac{3949M^2\Omega^2}{5054} + \frac{7}{64}M^2\pi^2\Omega^2 - \frac{866709919Mr_0^3\Omega^4}{97534980} + \frac{1243509067r_0^6\Omega^6}{127849176}$$
$$- \frac{1015083323057r_0^9\Omega^8}{1108452355920M} \tag{3.4.31}$$

$$C_{r,4}^{\tilde{\text{S}}-\text{S}} = \frac{4919M^4}{532r_0^4} - \frac{13687M^3\Omega^2}{20216r_0} + \frac{7M^3\pi^2\Omega^2}{64r_0} + \frac{1634173681M^2r_0^2\Omega^4}{195069960} - \frac{83M^2\pi^2r_0^2\Omega^4}{1024}$$
$$- \frac{710943482539363Mr_0^5\Omega^6}{12153768834480} + \frac{94836548674327r_0^8\Omega^8}{4433809423680}$$
$$- \frac{342957264845834411r_0^{11}\Omega^{10}}{299752119897310080M} \tag{3.4.32}$$

$$C_{r,5}^{\tilde{\text{S}}-\text{S}} = \frac{2355447M^5}{105070r_0^5} - \frac{57835M^4\Omega^2}{20216r_0^2} + \frac{11M^4\pi^2\Omega^2}{256r_0^2} - \frac{4498242521M^3r_0\Omega^4}{2730979440}$$
$$- \frac{141M^3\pi^2r_0\Omega^4}{1024} + \frac{5779923174043661M^2r_0^4\Omega^6}{36461306503440} + \frac{1529M^2\pi^2r_0^4\Omega^6}{2048}$$
$$- \frac{4480789140704780813 6653Mr_0^7\Omega^8}{205683170492936256120} + \frac{19645812110644890187r_0^{10}\Omega^{10}}{4995868664955168 00}$$
$$- \frac{18934621312338701702 5r_0^{13}\Omega^{12}}{13783458907506595507 2M} \tag{3.4.33}$$

$$C_{r,6}^{\tilde{\text{S}}-\text{S}} = \frac{22121093M^6}{420280r_0^6} - \frac{5515976489M^5\Omega^2}{2730979440r_0^3} - \frac{23M^5\pi^2\Omega^2}{256r_0^3} - \frac{5027838304339M^4\Omega^4}{546560018592}$$
$$+ \frac{5221M^4\pi^2\Omega^4}{2048} - \frac{76585M^4\pi^4\Omega^4}{524288} - \frac{17575679246803750626521M^3r_0^3\Omega^6}{82923949380773592000}$$
$$- \frac{857101M^3\pi^2r_0^3\Omega^6}{276480} + \frac{21750282723232026898 92893M^2r_0^6\Omega^8}{1974558436732188058752}$$
$$+ \frac{423951M^2\pi^2r_0^6\Omega^8}{131072} - \frac{6744910273910089717 5124383220723Mr_0^9\Omega^{10}}{112731391541992244040866246400}$$
$$+ \frac{16796339394328549334797373r_0^{12}\Omega^{12}}{260507373351874655086080}$$
$$- \frac{381008986372827393765 13402669r_0^{15}\Omega^{14}}{2375566737595744979729 9635200M} \tag{3.4.34}$$

3.4.3 $F_\alpha^{\tilde{\text{R}}}$

Unlike the $\tilde{\text{S}}$ part of the force, the $\tilde{\text{R}}$ part doesn't need to be regularized and is fully responsible for the temporal component of the force. It is still true that

$$F_\theta^{\tilde{\text{R}}} = 0, \tag{3.4.35}$$

but $F_t^{\tilde{R}}$, $F_r^{\tilde{R}}$, and $F_\phi^{\tilde{R}}$ are all nonzero. We start with the radial component, and again we write

$$F_r^{\tilde{R}} = \frac{q^2}{r_0^2} \sum_{p=0}^{12} C_{r,p/2}^{\tilde{R}}, \tag{3.4.36}$$

where p denotes the PN order divided by two. The coefficients are

$$C_{r,0}^{\tilde{R}} = \frac{2}{7} + \frac{5\Omega^2 r_0^3}{19M} \tag{3.4.37}$$

$$C_{r,1}^{\tilde{R}} = -\frac{4M}{7r_0} - \frac{89}{133}\Omega^2 r_0^2 + \frac{1417\Omega^4 r_0^5}{3002M} \tag{3.4.38}$$

$$C_{r,2}^{\tilde{R}} = -\frac{9M^2}{7r_0^2} + \frac{5}{38}M\Omega^2 r_0 - \frac{136153\Omega^4 r_0^4}{42028} + \frac{9804331\Omega^6 r_0^7}{14205464M} \tag{3.4.39}$$

$$C_{r,3}^{\tilde{R}} = \frac{3949M^2\Omega^2}{5054} - \frac{482M^3}{133r_0^3} + \frac{93892831M\Omega^4 r_0^3}{10837220} - \frac{4}{3}\gamma M\Omega^4 r_0^3 - \frac{4}{3}M\Omega^4 \ln|2\Omega r_0| \, r_0^3$$
$$- \frac{1243509067\Omega^6 r_0^6}{127849176} + \frac{1015083323057\Omega^8 r_0^9}{1108452355920M} \tag{3.4.40}$$

$$C_{r,4}^{\tilde{R}} = -\frac{4919M^4}{532r_0^4} + \frac{54119M^3\Omega^2}{20216r_0} - \frac{494150867M^2\Omega^4 r_0^2}{65023320} + \frac{8}{3}\gamma M^2\Omega^4 r_0^2$$
$$+ \frac{8}{3}M^2\Omega^4 \ln|2\Omega r_0| \, r_0^2 + \frac{2520940799065817M\Omega^6 r_0^5}{36461306503440} - \frac{22}{3}\gamma M\Omega^6 r_0^5$$
$$+ \frac{6}{5}M\Omega^6 \ln|2\Omega r_0| \, r_0^5 - \frac{128}{15}M\Omega^6 \ln|4\Omega r_0| \, r_0^5 - \frac{94836548674327\Omega^8 r_0^8}{4433809423680}$$
$$+ \frac{3429572648458344411\Omega^{10} r_0^{11}}{299752119897310080M} \tag{3.4.41}$$

$$C_{r,4.5}^{\tilde{R}} = -\frac{38}{45}M^2\pi|\Omega|^5 r_0^3 \tag{3.4.42}$$

$$C_{r,5}^{\tilde{R}} = -\frac{2355447M^5}{105070r_0^5} + \frac{138699M^4\Omega^2}{20216r_0^2} - \frac{140795391M^3\Omega^4 r_0}{303442160} - \frac{2}{3}\gamma M^3\Omega^4 r_0$$
$$- \frac{2}{3}M^3\Omega^4 \ln|2\Omega r_0| \, r_0 - \frac{7036622871528893M^2\Omega^6 r_0^4}{36461306503440} + 36\gamma M^2\Omega^6 r_0^4$$
$$+ \frac{28}{15}M^2\Omega^6 \ln|2\Omega r_0| \, r_0^4 + \frac{512}{15}M^2\Omega^6 \ln|4\Omega r_0| \, r_0^4$$
$$+ \frac{5372850110381565542 8867M\Omega^8 r_0^7}{205683170492936256120} - \frac{119}{6}\gamma M\Omega^8 r_0^7 - \frac{6}{35}M\Omega^8 \ln|2\Omega r_0| \, r_0^7$$
$$+ \frac{1216}{105}M\Omega^8 \ln|4\Omega r_0| \, r_0^7 - \frac{2187}{70}M\Omega^8 \ln|6\Omega r_0| \, r_0^7$$
$$- \frac{196458121106448 90187\Omega^{10} r_0^{10}}{499586866495516800} + \frac{18934621312338701702 5\Omega^{12} r_0^{13}}{137834589075065955072M} \tag{3.4.43}$$

63

$$C_{r,5.5}^{\tilde{R}} = \frac{76}{45}M^3\pi|\Omega|^5 r_0^2 - \frac{1783}{315}M^2\pi|\Omega|^7 r_0^5 \tag{3.4.44}$$

$$
\begin{aligned}
C_{r,6}^{\tilde{R}} = {} & \frac{11348688119305 M^4\Omega^4}{1639680055776} - \frac{22121093 M^6}{420280 r_0^6} + \frac{26210731801 M^5\Omega^2}{2730979440 r_0^3} \\
& + \frac{16M^5\Omega^2}{3r_0^3}\ln\left|\frac{2M}{r_0}\right| + \frac{18610404287177043507497 M^3\Omega^6 r_0^3}{82923949380773592000} - \frac{49207}{675}\gamma M^3\Omega^6 r_0^3 \\
& + \frac{152}{45}[\gamma + \ln|2\Omega r_0|]^2 M^3\Omega^6 r_0^3 - \frac{38}{27}M^3\pi^2\Omega^6 r_0^3 - \frac{19447}{675}M^3\Omega^6\ln|2\Omega r_0|\, r_0^3 \\
& - \frac{1984}{45}M^3\Omega^6\ln|4\Omega r_0|\, r_0^3 + \frac{8}{3}M^3\Omega^6\psi^{(2)}(2)r_0^3 \\
& - \frac{14021972419142980434311137 M^2\Omega^8 r_0^6}{9872792183660940293760} + \frac{5131}{27}\gamma M^2\Omega^8 r_0^6 \\
& - \frac{1786}{945}M^2\Omega^8\ln|2\Omega r_0|\, r_0^6 + \frac{1408}{315}M^2\Omega^8\ln|4\Omega r_0|\, r_0^6 + \frac{6561}{35}M^2\Omega^8\ln|6\Omega r_0|\, r_0^6 \\
& + \frac{7957658645318333255309314421 2243 M\Omega^{10} r_0^9}{1127313915419992244040866246400} - \frac{161}{4}\gamma M\Omega^{10} r_0^9 \\
& + \frac{65 M\Omega^{10}\ln|2\Omega r_0|\, r_0^9}{1134} - \frac{14512 M\Omega^{10}\ln|4\Omega r_0|\, r_0^9}{2835} + \frac{8019}{140}M\Omega^{10}\ln|6\Omega r_0|\, r_0^9 \\
& - \frac{262144 M\Omega^{10}\ln|8\Omega r_0|\, r_0^9}{2835} - \frac{167963339432854933479737 3\Omega^{12} r_0^{12}}{260507373351874655086080} \\
& + \frac{3810089863728273937651340266 9\Omega^{14} r_0^{15}}{2375566737595744979729963520 0 M}, \tag{3.4.45}
\end{aligned}
$$

where γ is the Euler-Mascheroni constant and $\psi^{(2)}$ is the second derivative of the digamma function. As expected, there are logarithmic terms in the $\tilde{R}$ part of the force, and there are also terms at half-integer PN order.

We now report $F_t^{\tilde{R}}$. Because the $\tilde{S}$ part of the force doesn't contribute to the time component, the $\tilde{R}$ part is the full renormalized force. We write

$$F_t^{\tilde{R}} = F_t^{R} = \frac{q^2}{r_0^2}(r_0\Omega)\sum_{p=3}^{12} C_{p/2}^{R}, \tag{3.4.46}$$

with

$$C_{1.5}^{R} = \frac{1}{3}\Omega^3 r_0^3 \tag{3.4.47}$$

$$C_{2.5}^{R} = -M\Omega^3 r_0^2 + \frac{5}{6}\Omega^5 r_0^5 \tag{3.4.48}$$

$$C_3^{R} = \frac{2}{3}M\pi\Omega^3\,\mathrm{Abs}[\Omega]r_0^3 \tag{3.4.49}$$

$$C_{3.5}^{\mathrm{R}} = \frac{5}{6}M^2\Omega^3 r_0 - \frac{11}{2}M\Omega^5 r_0^4 + \frac{35}{24}\Omega^7 r_0^7 \tag{3.4.50}$$

$$C_4^{\mathrm{R}} = -2M^2\pi\Omega^3\mathrm{Abs}[\Omega]r_0^2 + \frac{19}{5}M\pi\Omega^5\mathrm{Abs}[\Omega]r_0^5 \tag{3.4.51}$$

$$C_{4.5}^{\mathrm{R}} = -\frac{1}{6}M^3\Omega^3 + \frac{4M^4\Omega}{3r_0^3} + \frac{46537M^2\Omega^5 r_0^3}{2700} - \frac{76}{45}\gamma M^2\Omega^5 r_0^3 + \frac{4}{9}M^2\pi^2\Omega^5 r_0^3$$
$$- \frac{76}{45}M^2\Omega^5\ln|2\Omega r_0|\,r_0^3 - \frac{19201M\Omega^7 r_0^6}{1080} + \frac{35}{16}\Omega^9 r_0^9 \tag{3.4.52}$$

$$C_5^{\mathrm{R}} = \frac{5}{3}M^3\pi\Omega^3|\Omega|r_0 - \frac{65}{3}M^2\pi\Omega^5|\Omega|r_0^4 + \frac{4639}{420}M\pi\Omega^7|\Omega|r_0^7 \tag{3.4.53}$$

$$C_{5.5}^{\mathrm{R}} = \frac{4M^5\Omega}{r_0^4} + \frac{5M^4\Omega^3}{8r_0} - \frac{20417}{900}M^3\Omega^5 r_0^2 + \frac{76}{15}\gamma M^3\Omega^5 r_0^2 - \frac{4}{3}M^3\pi^2\Omega^5 r_0^2$$
$$+ \frac{76}{15}M^3\Omega^5\ln|2\Omega r_0|\,r_0^2 + \frac{335959619M^2\Omega^7 r_0^5}{2646000} - \frac{18362\gamma M^2\Omega^7 r_0^5}{1575}$$
$$+ \frac{242}{45}M^2\pi^2\Omega^7 r_0^5 - \frac{20224M^2\Omega^7\ln|2\Omega r_0|\,r_0^5}{1575} + \frac{266M^2\Omega^7\ln|4\Omega r_0|\,r_0^5}{225}$$
$$- \frac{3215311M\Omega^9 r_0^8}{75600} + \frac{385}{128}\Omega^{11}r_0^{11} \tag{3.4.54}$$

$$C_6^{\mathrm{R}} = -\frac{1}{3}M^4\pi\Omega^3|\Omega| + \frac{71977M^3\pi\Omega^5|\Omega|r_0^3}{1350} - \frac{152}{45}\gamma M^3\pi\Omega^5|\Omega|r_0^3$$
$$- \frac{152}{45}M^3\pi\Omega^5|\Omega|\ln|2\Omega r_0|\,r_0^3 - \frac{11675}{108}M^2\pi\Omega^7|\Omega|r_0^6 + \frac{546307M\pi\Omega^9|\Omega|r_0^9}{22680}. \tag{3.4.55}$$

The ϕ-component of the force F_ϕ^{R} is proportional to the t-component:

$$F^{\mathrm{R},\phi} = \Omega F^{\mathrm{R},t}. \tag{3.4.56}$$

Here we note that the 1.5-PN term is proportional to the particle's jerk and was first predicted by Gal'tsov [101]. Furthermore, in the limit $\Omega \to 0$, $F_t^{\mathrm{R}} \to 0$; as one should expect, a static particle does not feel a force in the temporal direction and does not radiate. However, F_t^{R} remains non-zero when the mass of the black hole goes to zero, which is also unsurprising: a particle undergoing circular motion in flat spacetime radiates. These are limits we could not check if we forced the scalar charge to follow a geodesic.

To allow for easy comparison to other Post-Newtonian work, we also report the force when the particle does follow a geodesic. To do this, we will use the usual gauge-invariant

Post-Newtonian expansion parameter $x \equiv (M\Omega_K)^{2/3} = (r_0\Omega_K)^2$, where $\Omega_K = \sqrt{M/r_0^3}$ is the Keplerian angular velocity. The result is

$$
\begin{aligned}
F_{t,\text{geo}}^{\text{R}} =& \frac{q^2}{r_0} x^{1/2} \left[\frac{1}{3} x^{3/2} - \frac{1}{6} x^{5/2} + \frac{2\pi}{3} x^3 - \frac{77}{24} x^{7/2} + \frac{9\pi}{5} x^4 \right. \\
&+ \left(\frac{10121}{3600} + \frac{4\pi^2}{9} - \frac{76}{45}\gamma - \frac{38}{45}\ln(4x) \right) x^{9/2} - \frac{3761\pi}{420} x^5 \\
&+ \left(\frac{163194823}{2352000} + \frac{182\pi^2}{45} - \frac{10382}{1575}\gamma + \frac{20224}{1575}\ln(2x) - \frac{5083}{315}\ln(4x) \right) x^{11/2} \\
&\left. + \left(-\frac{3518947\pi}{113400} - \frac{152\pi}{45}\gamma - \frac{76\pi}{45}\ln(4x) \right) x^6 + \mathcal{O}(x^{13/2}) \right].
\end{aligned}
\tag{3.4.57}
$$

This agrees with Hikida $et\ al.$ [9], who report the above through 4$^{\text{th}}$ PN order.

3.4.4 F_r^{R}

Here, we finally report the radial component of the renormalized force. Similarly to before, we write

$$
F_r^{\text{R}} = F_r^{\tilde{\text{S}}-\text{S}} + F_r^{\tilde{\text{R}}} = \frac{q^2}{r_0^2} \sum_{p=6}^{12} C_{r,p/2}^{\text{R}}.
\tag{3.4.58}
$$

Then the coefficients are given by

$$
C_{r,3}^{\text{R}} = \frac{7}{64} M^2\pi^2\Omega^2 - \frac{2}{9} M\Omega^4 r_0^3 - \frac{4}{3}\gamma M\Omega^4 r_0^3 - \frac{4}{3} M\Omega^4 \ln|2\Omega r_0| r_0^3
\tag{3.4.59}
$$

$$
\begin{aligned}
C_{r,4}^{\text{R}} =& \frac{2M^3\Omega^2}{r_0} + \frac{7M^3\pi^2\Omega^2}{64 r_0} + \frac{7}{9} M^2\Omega^4 r_0^2 + \frac{8}{3}\gamma M^2\Omega^4 r_0^2 - \frac{83 M^2\pi^2\Omega^4 r_0^2}{1024} \\
&+ \frac{8}{3} M^2\Omega^4 \ln|2\Omega r_0| r_0^2 + \frac{479}{45} M\Omega^6 r_0^5 - \frac{22}{3}\gamma M\Omega^6 r_0^5 + \frac{6}{5} M\Omega^6 \ln|2\Omega r_0| r_0^5 \\
&- \frac{128}{15} M\Omega^6 \ln|4\Omega r_0| r_0^5
\end{aligned}
\tag{3.4.60}
$$

$$
C_{r,4.5}^{\text{R}} = -\frac{38}{45} M^2\pi|\Omega|^5 r_0^3
\tag{3.4.61}
$$

$$
\begin{aligned}
C_{r,5}^{\text{R}} =& \frac{4M^4\Omega^2}{r_0^2} + \frac{11M^4\pi^2\Omega^2}{256 r_0^2} - \frac{19}{9} M^3\Omega^4 r_0 - \frac{2}{3}\gamma M^3\Omega^4 r_0 - \frac{141 M^3\pi^2\Omega^4 r_0}{1024} \\
&- \frac{2}{3} M^3\Omega^4 \ln|2\Omega r_0| r_0 - \frac{517}{15} M^2\Omega^6 r_0^4 + 36\gamma M^2\Omega^6 r_0^4 + \frac{1529 M^2\pi^2\Omega^6 r_0^4}{2048} \\
&+ \frac{28}{15} M^2\Omega^6 \ln|2\Omega r_0| r_0^4 + \frac{512}{15} M^2\Omega^6 \ln|4\Omega r_0| r_0^4 + \frac{54647 M\Omega^8 r_0^7}{1260} - \frac{119}{6}\gamma M\Omega^8 r_0^7 \\
&- \frac{6}{35} M\Omega^8 \ln|2\Omega r_0| r_0^7 + \frac{1216}{105} M\Omega^8 \ln|4\Omega r_0| r_0^7 - \frac{2187}{70} M\Omega^8 \ln|6\Omega r_0| r_0^7
\end{aligned}
\tag{3.4.62}
$$

$$C^{\mathrm{R}}_{r,5.5} = \frac{76}{45}M^3\pi|\Omega|^5 r_0^2 - \frac{1783}{315}M^2\pi|\Omega|^7 r_0^5 \tag{3.4.63}$$

$$
\begin{aligned}
C^{\mathrm{R}}_{r,6} = &-\frac{41}{18}M^4\Omega^4 + \frac{5221M^4\pi^2\Omega^4}{2048} - \frac{76585M^4\pi^4\Omega^4}{524288} + \frac{341M^5\Omega^2}{45r_0^3} - \frac{23M^5\pi^2\Omega^2}{256r_0^3} \\
&+ \frac{16M^5\Omega^2}{3r_0^3}\ln\left|\frac{2M}{r_0}\right| + \frac{6239}{500}M^3\Omega^6 r_0^3 - \frac{49207}{675}\gamma M^3\Omega^6 r_0^3 \\
&+ \frac{152}{45}[\gamma + \ln|2\Omega r_0|]^2 M^3\Omega^6 r_0^3 - \frac{138469M^3\pi^2\Omega^6 r_0^3}{30720} + -\frac{19447}{675}M^3\Omega^6\ln|2\Omega r_0|\,r_0^3 \\
&- \frac{1984}{45}M^3\Omega^6\ln|4\Omega r_0|\,r_0^3 + \frac{8}{3}M^3\Omega^6\psi^{(2)}(2)r_0^3 - \frac{803219M^2\Omega^8 r_0^6}{2520} \\
&+ \frac{5131}{27}\gamma M^2\Omega^8 r_0^6 + \frac{423951M^2\pi^2\Omega^8 r_0^6}{131072} - \frac{1786}{945}M^2\Omega^8\ln|2\Omega r_0|\,r_0^6 \\
&+ \frac{1408}{315}M^2\Omega^8\ln|4\Omega r_0|\,r_0^6 + \frac{6561}{35}M^2\Omega^8\ln|6\Omega r_0|\,r_0^6 + \frac{7319647M\Omega^{10}r_0^9}{68040} \\
&- \frac{161}{4}\gamma M\Omega^{10}r_0^9 + \frac{65M\Omega^{10}\ln|2\Omega r_0|\,r_0^9}{1134} - \frac{14512M\Omega^{10}\ln|4\Omega r_0|\,r_0^9}{2835} \\
&+ \frac{8019}{140}M\Omega^{10}\ln|6\Omega r_0|\,r_0^9 - \frac{262144M\Omega^{10}\ln|8\Omega r_0|\,r_0^9}{2835}. \tag{3.4.64}
\end{aligned}
$$

Because we allowed the scalar charge to be accelerated, we can easily see that the radial component of the self force both for a static particle outside a black hole (corresponding to $\Omega \to 0$) and for a particle undergoing circular motion in flat spacetime (corresponding to $M \to 0$).

For non-accelerated motion, the radial component of the force reduces to

$$
\begin{aligned}
F^{\mathrm{R}}_{r,\mathrm{geo}} = \frac{q^2}{r_0^2}\Bigg\{ &\left[-\frac{2}{9} + \frac{7\pi^2}{64} - \frac{4}{3}\gamma - \frac{2}{3}\ln(4x)\right]x^3 + \left[\frac{604}{45} + \frac{29\pi^2}{1024} - \frac{14}{3}\gamma + \frac{128}{15}\ln(2x)\right. \\
&\left. - \frac{163}{15}\ln(4x)\right]x^4 + \frac{38}{45}\pi x^{9/2} + \left[\frac{1511}{140} + \frac{1335\pi^2}{2048} + \frac{31}{2}\gamma - \frac{1013}{70}\ln(2x)\right. \\
&\left. + \frac{1497}{28}\ln(4x) - \frac{2187}{70}\ln(6x)\right]x^5 - \frac{139}{45}\pi x^{11/2} + \left[-\frac{41117659}{212625} + \frac{2332769\pi^2}{1966080}\right. \\
&- \frac{76585}{524288\pi^4} + \frac{152}{45}\left(\gamma + \frac{1}{2}\ln(4x)\right)^2 + \frac{69199}{900}\gamma - \frac{36781}{3780}\ln(2x) - \frac{7228421}{37800}\ln(4x) \\
&\left. + \frac{34263}{140}\ln(6x) + \frac{8}{3}\psi^{(2)}(2)\right]x^6 + \mathcal{O}(x^{13/2})\Bigg\}. \tag{3.4.65}
\end{aligned}
$$

This is again in agreement with Hikida *et al.* [9], who report the above expression through 4th PN order.

3.4.5 Comparisons to Other Work

Our results are consistent with those of Hikida *et al.* [9], who calculate the self-force for geodesic motion to 4th PN order. Accelerated scalar charges are rarely studied due to their doubly non-physical nature, but Heffernan *et al.* [10] recently studied them numerically. Niels Warburton, one of the coauthors of that work, graciously shared some of the numerical data with us. In Fig. 12 and Fig. 13, one can see how our results compare. In both figures, a dimensionless quantity proportional to the radial component of the force is plotted against the ratio between the particle's angular velocity and it's Keplerian angular velocity Ω_K for constant radial coordinate r_0. In Fig. 12, $r_0 = 50M$, whereas for Fig. 13, $r_0 = 6M$. The numerical data is plotted in blue dots, where as our analytical results are plotted in curves of successively higher accuracy. In Fig. 12, one can see how curves accurate to higher PN orders stick with the numerical results to higher angular velocities. However, even our results accurate to 6th PN order no longer accurately describe the force when $\Omega \gtrsim 3\Omega_K$.

In Fig. 13, the particle is at its innermost stable circular orbit, $r_0 = 6M$. Remarkably, our 6th PN-accurate expression still correctly gives the force for geodesic motion, although it becomes inaccurate for faster-moving particles.

3.5 Conclusion

In this chapter, we have successfully calculated the self-force on an accelerated scalar charge in circular orbit around a Schwarzschild black hole to 6th PN order. We used a method developed by Hikida *et al.* [8, 9], which allowed us to compute only a handful of the field's ℓ-modes, along with general-ℓ expressions that are valid for high ℓ-values. Our results are compatible with previous PN calculations, as well as numerical results found in [10].

We do not expect scalar charges to be astrophysically relevant; instead we have used the scalar field as a toy model for the gravitational field, with the intention of eventually applying Hikida's method to finding the gravitational self-force. We do just that in the
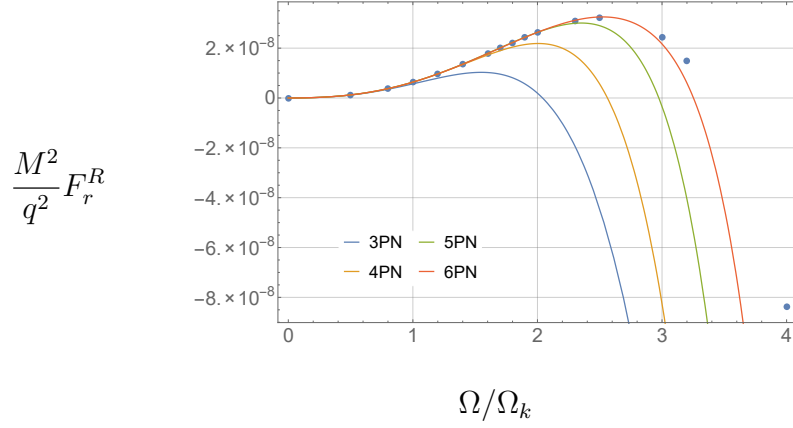
Figure 12 : The radial component of the self-force on an accelerated scalar charge at $r_0 = 50M$ as a function of angular velocity. The blue dots are numerical results obtained from Warburton and reported in [10]. The curves are our analytical results, accurate to 3rd, 4th, 5th, and 6th PN order. As the particle's angular velocity increases, it becomes more relativistic, and PN expansions become less useful. Here, when the particle's angular velocity exceeds thrice the Keplerian velocity, even our results accurate to 6th PN order become inaccurate.
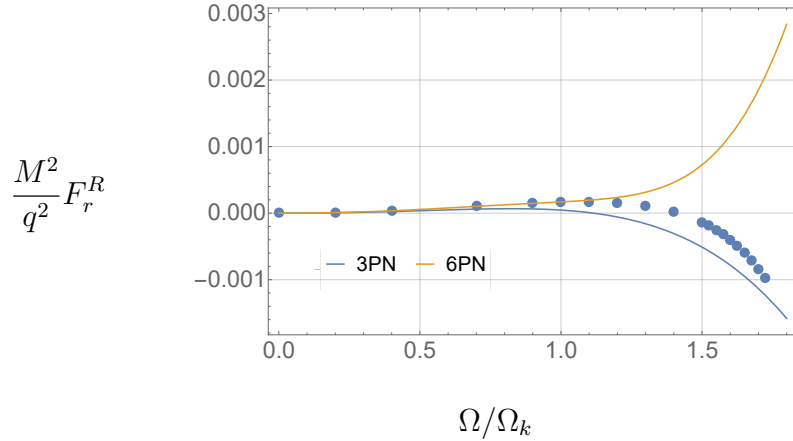
Figure 13 : The radial component of the self-force on an accelerated scalar charge at $r_0 = 6M$ as a function of angular velocity. Once again, the dots are numerical results given by Warburton and reported in [10]. For clarity, we only show our results accurate to 3rd and 6th PN order. Remarkably, our analytical results at 6th PN order still accurately compute the self-force for geodesic motion at $r_0 = 6M$, otherwise known as the innermost stable circular orbit.

69

next chapter.

Chapter 4

Gravitational Self-Force

4.1 Introduction

This chapter will discuss work I did under the supervision of Alan Wiseman. It is a continuation of the last chapter, and discusses how the methods of the last chapter can be extended to the gravitational case.

To be more specific, in this chapter we consider the gravitational self-force on a massive point particle in circular orbit around a Schwarzschild black hole. As with the last chapter, we describe the particle's position with a radial coordinate r_0 and angular coordinates $\theta_0 = \pi/2$ and ϕ_0; the angular velocity as measured by a stationary observer at infinity is Ω. This system is much more astrophysically motivated than that of the last chapter; it models an extreme mass ratio inspiral (EMRI), where a supermassive black hole is orbited by a stellar-mass black hole. EMRIs are expected to produce gravitational waves that are too low in frequency to be detected by terrestrial detectors like LIGO; instead, we will need space-based gravitational-wave observatories to study EMRIs observationally.

This chapter begins by discussing the spin-weighted spherical harmonics, because their identities and relationships to ordinary spherical harmonics will be needed for the calculations in the rest of the chapter. We then discuss the tetrad formalism of Newman and Penrose [102] and the resulting description of gravitational perturbations to Schwarzschild spacetimes. Next, we explain how gravitational self-force differs from scalar self-force and

71

introduce Detweiler's [11] gauge-invariant redshift factor. Finally, we show how to apply the method discovered by Hikida *et al.* [8, 9] to find the redshift factor, and report the results we thereby obtain. To our knowledge, this is the first time Hikida's method has been successfully applied to the gravitational case.

4.2   Properties of the Spin-Weighted Spherical Harmonics

This chapter will make extensive use of the spin-weighted spherical harmonics $_sY_{\ell m}(\theta, \phi)$, and we consider their properties here. We stated the differential equation they satisfy in Eq. (3.2.3). Along with the harmonics we have the spin-weight raising operator $\hat{\eth}^{(s)}$ and the spin-weight lowering operator $\check{\eth}^{(s)}$.[1] These operators are given by

$$\hat{\eth}^{(s)} = -\partial_\theta - i \csc\theta \partial_\phi + s \cot\theta, \tag{4.2.1}$$

$$\check{\eth}^{(s)} = -\partial_\theta + i \csc\theta \partial_\phi - s \cot\theta, \tag{4.2.2}$$

and when they act on a spin-weighted spherical harmonic, they have the properties

$$\hat{\eth}^{(s)}{}_sY_{\ell m}(\theta, \phi) = \sqrt{(\ell - s)(\ell + s + 1)} \; _{s+1}Y_{\ell m}(\theta, \phi),$$

$$\check{\eth}^{(s)}{}_sY_{\ell m}(\theta, \phi) = -\sqrt{(\ell + s)(\ell - s + 1)} \; _{s-1}Y_{\ell m}(\theta, \phi).$$

Like the usual spherical harmonics, the spin-weighted spherical harmonics of a particular spin-weight form a complete orthonormal basis on $\mathcal{S}^2$:

$$\int \mathrm{d}\Omega \; _sY_{\ell m}(\theta, \phi) {}_s\overline{Y}_{\ell' m'}(\theta, \phi) = \delta_{\ell\ell'}\delta_{mm'} \tag{4.2.3}$$

$$\sum_{\ell=|s|}^{\infty} \sum_{m=-\ell}^{\ell} {}_sY_{\ell m}(\theta, \phi) {}_sY_{\ell m}(\theta', \phi') = \delta(\cos\theta - \cos\theta')\delta(\phi - \phi') \tag{4.2.4}$$

We choose the spin-weighted spherical harmonics to satisfy the phase conventions

$$_sY_{\ell m}(\theta, \phi) = (-1)^{s+m} {}_{-s}\overline{Y}_{\ell,-m}(\theta, \phi), \tag{4.2.5}$$

$$_sY_{\ell m}(\theta, \phi) = (-1)^{\ell} {}_{-s}Y_{\ell m}(\pi - \theta, \phi + \pi); \tag{4.2.6}$$

---

[1]Note that this is counter to the usual and simpler notation, with $\eth$ as the spin-weight raising operator and $\overline{\eth}$ as the spin-weight lowering operator. The notation here will be useful because it will allow us to have operators corresponding to different spin weights in the same equation without confusion. Also, this notation allows us to continue using an overline to exclusively denote complex conjugation.

they then can be explicitly written [103]

$$sY_{\ell m}(\theta, \phi) = (-1)^m \sqrt{\frac{2\ell+1}{4\pi} \frac{(\ell+m)!(\ell-m)!}{(\ell+s)!(\ell-s)!}} \sin^{2\ell}\left(\frac{\theta}{2}\right)$$

$$\times \sum_{r=0}^{\ell-s} \binom{\ell-s}{r} \binom{\ell+s}{r+s-m} (-1)^{\ell-r-s} \cot^{2r+s-m}\left(\frac{\theta}{2}\right) e^{im\phi}. \qquad (4.2.7)$$

Our two phase conventions, along with the explicit ϕ-dependence shown above, have implications when we evaluate $_sY_{\ell m}$ at the angular position $(\theta_0, 0)$ of the particle:

$$_sY_{\ell m}(\theta_0, 0) = (-1)^{\ell+m} {}_{-s}Y_{\ell m}(\theta_0, 0) \qquad (4.2.8)$$

$$_sY_{\ell m}(\theta_0, 0) = (-1)^{\ell+s} {}_s\overline{Y}_{\ell,-m}(\theta_0, 0). \qquad (4.2.9)$$

Since the factor of $e^{im\phi}$ is the only complex term in the explicit expression for $_sY_{\ell m}(\theta, \phi)$,

$$_sY_{\ell m}(\theta, 0) = {}_s\overline{Y}_{\ell m}(\theta, 0). \qquad (4.2.10)$$

Finally, when evaluated at $(\theta_0, 0)$ the spin-weighted spherical harmonics can be written simply in terms of ℓ and m. First, we define $\mathbb{0}_n$:

$$\mathbb{0}_n = \begin{cases} 1, & n \text{ even} \\ \\ 0, & n \text{ odd} \end{cases}$$

Then the expressions for the spin-weighted harmonics with $|s| \leq 2$ are [104]

$$_0Y_{\ell m}(\theta_0, 0) = i^{\ell+m} \sqrt{\frac{2\ell+1}{4\pi}} \frac{\sqrt{(\ell+m)!(\ell-m)!}}{(\ell+m)!!(\ell-m)!!} \mathbb{0}_{\ell+m}$$

$$_{\pm 1}Y_{\ell m}(\theta_0, 0) = i^{\ell+m} \sqrt{\frac{2\ell+1}{4\pi}} \sqrt{\frac{(\ell+m)!(\ell-m)!}{\ell(\ell+1)}} \left[\frac{m}{(\ell+m)!!(\ell-m)!!} \mathbb{0}_{\ell+m} \right.$$

$$\left. \mp \frac{i}{(\ell+m-1)!!(\ell-m-1)!!} \mathbb{0}_{\ell+m-1} \right]$$

$$_{\pm 2}Y_{\ell m}(\theta_0, 0) = i^{\ell+m} \sqrt{\frac{2\ell+1}{4\pi}} \sqrt{\frac{(\ell+m)!(\ell-m)!}{(\ell+2)(\ell+1)\ell(\ell-1)}} \left[\frac{2m^2-\ell(\ell+1)}{(\ell+m)!!(\ell-m)!!} \mathbb{0}_{\ell+m} \right.$$

$$\left. \mp \frac{2im}{(\ell+m-1)!!(\ell-m-1)!!} \mathbb{0}_{\ell+m-1} \right].$$

4.3 Gravitational Perturbations to Schwarzschild Spacetimes

In this chapter, we make use of the tetrad formalism developed by Newman and Penrose [102]. In particular, we use the Kinnersley tetrad [105] $\{e_{\mathbf{a}}^\alpha\} = \{l^\alpha, n^\alpha, m^\alpha, \overline{m}^\alpha\}$, where

the tetrad vectors in Schwarzschild have components

$$\ell^\alpha = \left(\frac{1}{f(r)}, 1, 0, 0 \right) \tag{4.3.1}$$

$$n^\alpha = \frac{1}{2} (1, -f(r), 0, 0) \tag{4.3.2}$$

$$m^\alpha = \frac{1}{\sqrt{2}} \left(0, 0, \frac{1}{r}, \frac{i}{r \sin \theta} \right) \tag{4.3.3}$$

and throughout this chapter we use an overline to denote a complex conjugate. These vectors are each associated with a directional derivative:

$$\boldsymbol{D} = \ell^\alpha \nabla_\alpha \tag{4.3.4}$$

$$\boldsymbol{\Delta} = n^\alpha \nabla_\alpha \tag{4.3.5}$$

$$\boldsymbol{\delta} = m^\alpha \nabla_\alpha. \tag{4.3.6}$$

The tetrad formalism gives rise to spin coefficients; in Schwarzschild, the non-zero spin coefficients are

$$\alpha = -\beta = -\frac{\cot \theta}{2\sqrt{2}r}$$

$$\gamma = \frac{M}{2r^2}$$

$$\rho = -\frac{1}{r}$$

$$\mu = -\frac{f(r)}{2r}.$$

The Bardeen-Press equation, given in the last chapter as Eq. (3.2.2), gives information about gravitational perturbations for $s = \pm 2$. In this chapter, we specialize to $s = -2$. The solution to Eq. (3.2.2) is then

$$\psi_{-2} \equiv \frac{\psi_4}{\rho^4}, \tag{4.3.7}$$

where $\psi_4 \equiv C_{\alpha\beta\gamma\delta} n^\alpha \overline{m}^\beta n^\gamma \overline{m}^\delta$ is one of the Weyl scalars. Meanwhile, while the stress-energy $T^{\alpha\beta}$ that sources the metric is proportional to a three-dimensional delta function,

$$T^{\alpha\beta} = \frac{\mathrm{m}}{u^t r_0^2} u^\alpha u^\beta \delta(r - r_0) \delta(\theta - \theta_0) \delta(\phi - \phi_0),$$

the source T_{-2} of ψ_{-2} is no longer so simple. Defining the tetrad components of the stress-energy tensor,

$$T_{\boldsymbol{ab}} = T_{\alpha\beta} e_{\boldsymbol{a}}^\alpha e_{\boldsymbol{b}}^\beta,$$

the source is given by [85, 106]

$$T_{-2} = 2\rho^{-4} \left\{ (\mathbf{\Delta} + 2\gamma + 5\mu) \left[\left(\overline{\boldsymbol{\delta}} + 2\alpha \right) T_{\mathbf{24}} - (\mathbf{\Delta} + \mu) T_{\mathbf{44}} \right] \right.$$

$$\left. + \left(\overline{\boldsymbol{\delta}} + 2\alpha \right) \left[(\mathbf{\Delta} + 2\gamma + 2\mu) T_{\mathbf{24}} - \overline{\boldsymbol{\delta}} T_{\mathbf{22}} \right] \right\}. \tag{4.3.8}$$

Since we will be integrating a Green's function against this source, it is convenient to write it in terms of Dirac delta functions and their derivatives. The result is

$$T_{-2}(x, x_0) = \frac{m u^t}{4} \left\{ \left[2 \left(1 - \frac{2M}{r_0} \right)^2 - 2 r_0^2 \Omega^2 \left(1 - \frac{4M}{r_0} \right) \right] \delta(r - r_0) \delta(\cos\theta - \cos\theta_0) \right.$$

$$\times \delta(\phi - \phi_0)$$

$$-2 \left(1 - \frac{4M^2}{r_0^2} \right) r_0^3 \Omega^2 \delta'(r - r_0) \delta(\cos\theta - \cos\theta_0) \delta(\phi - \phi_0)$$

$$-\frac{8iM}{r_0} \left(1 - \frac{2M}{r_0} \right) r_0 \Omega \delta(r - r_0) \delta'(\cos\theta - \cos\theta_0) \delta(\phi - \phi_0)$$

$$+ \left[\frac{8M}{r_0} \left(1 - \frac{2M}{r_0} \right) - 2 r_0^2 \Omega^2 \left(1 + \frac{M}{r_0} \right) \right] r_0 \Omega \delta(r - r_0) \delta(\cos\theta - \cos\theta_0)$$

$$\times \delta'(\phi - \phi_0)$$

$$+2i \left(1 - \frac{2M}{r_0} \right)^2 r_0^2 \Omega \delta'(r - r_0) \delta'(\cos\theta - \cos\theta_0) \delta(\phi - \phi_0)$$

$$-2 \left(1 - \frac{2M}{r_0} \right) \left(1 - \frac{2M}{r_0} - r_0^2 \Omega^2 \right) r_0^2 \Omega \delta'(r - r_0) \delta(\cos\theta - \cos\theta_0) \delta'(\phi - \phi_0)$$

$$-2i \left(1 - \frac{2M}{r_0} \right) \left(1 - \frac{2M}{r_0} - r_0^2 \Omega^2 \right) \delta(r - r_0) \delta'(\cos\theta - \cos\theta_0) \delta'(\phi - \phi_0)$$

$$+ \left(1 - \frac{2M}{r_0} \right)^2 r_0^4 \Omega^2 \delta''(r - r_0) \delta(\cos\theta - \cos\theta_0) \delta(\phi - \phi_0)$$

$$- \left(1 - \frac{2M}{r_0} \right)^2 \delta(r - r_0) \delta''(\cos\theta - \cos\theta_0) \delta(\phi - \phi_0)$$

$$+ \left. \left(1 - \frac{2M}{r_0} - r_0^2 \Omega^2 \right)^2 \delta(r - r_0) \delta(\cos\theta - \cos\theta_0) \delta''(\phi - \phi_0) \right\}.$$

As outlined in the last chapter, we now integrate our Green's function $G(x, x')$ against $4\pi (r'^2 f(r'))^{-2} T_{-2}(x', x_0)$. The result is

$$\psi_{-2} = \frac{\pi m}{r_0^2} \sum_{\ell=2}^{\infty} \sum_{m=-\ell}^{\ell} {}_{-2}Y_{\ell m}(\theta, \phi - \phi_0) \left[{}_{-2}\overline{Y}_{\ell m}(\theta_0, 0) \psi_{-2,\ell m}^{(-2)} \right.$$

$$+ \sqrt{(\ell + 2)(\ell - 1)} \, {}_{-1}\overline{Y}_{\ell m}(\theta_0, 0) \psi_{-2,\ell m}^{(-1)}$$

$$+ \left. \sqrt{(\ell + 2)(\ell + 1)(\ell)(\ell - 1)} \, {}_{0}\overline{Y}_{\ell m}(\theta_0, 0) \psi_{-2,\ell m}^{(0)} \right], \tag{4.3.9}$$

with

$$\psi_{-2,\ell m}^{(-2)} = \left(\frac{r_0\Omega}{f_0}\right)^2 \left\{ g_{\ell m}(r,r_0) \left[2imr_0\Omega\left(1-\frac{M}{r_0}\right) - m^2r_0^2\Omega^2\right] \right.$$

$$\left. -2r_0f_0\partial_{r_0}g_{\ell m}(r,r_0)\left[imr_0\Omega + f_0\right] + r_0^2f_0^2\partial_{r_0}^2 g_{\ell m}(r,r_0) \right\}, \quad (4.3.10)$$

$$\psi_{-2,\ell m}^{(-1)} = \frac{r_0\Omega}{f_0}\{2g_{\ell m}(r,r_0)[mr_0\Omega - 2if_0] + 2ir_0f_0\partial_{r_0}g_{\ell m}(r,r_0), \quad (4.3.11)$$

and

$$\psi_{-2,\ell m}^{(0)} = -g_{\ell m}(r,r_0), \quad (4.3.12)$$

where $g_{\ell m}$ is the same radial Green's function defined in the last chapter but for $s = -2$, $f_0 = f(r_0)$, and $\partial_{r_0}g(r,r_0) = [\partial_{r'}g(r,r')]|_{r'=r_0}$. The quantities ψ_{-2}, $\psi_{-2,\ell m}^{(-2)}$, $\psi_{-2,\ell m}^{(-1)}$, and $\psi_{-2,\ell m}^{(0)}$ all have $\tilde{S}$ and $\tilde{R}$ parts, and Eqns. (4.3.9)-(4.3.12) all hold for both parts as long as the relevant label is placed on $g_{\ell m}$. While we are free to absorb terms proportional to $_s\overline{Y}_{\ell m}(\theta_0, 0)$, which are constant in r, into the radial functions $\psi_{-2,\ell m}^{(s)}$, we will see later that factoring out their dependence on ℓ and m will be useful.

Our goal in this section is to find the linear perturbation $h_{\alpha\beta}$ to the background metric $g_{\alpha\beta}$. Of course, ψ_{-2} is a scalar quantity, and finding it is not equivalent to calculating the tensor $h_{\alpha\beta}$. However, it turns out that ψ_{-2} contains all of the radiative information about the metric perturbation. That is, we can construct the radiative part of $h_{\alpha\beta}$ from ψ_{-2}; then we can add the contributions due to the particle's mass and angular momentum separately. In doing so, we use a method originally discovered by Chrzanowski [107] and Cohen and Kegeles [108], called the CCK metric reconstruction procedure. Our choice of $s = -2$ means we specialize to the ingoing radiation gauge, where

$$h_{\alpha\beta}l^\alpha = 0 \quad (4.3.13)$$

$$h_\alpha^\alpha = 0. \quad (4.3.14)$$

The first step in CCK metric reconstruction is finding the *Hertz Potential* Ψ, which satisfies a differential equation sourced by ψ_{-2}:

$$12M\partial_t\Psi - \breve{\eth}^{(-1)}\breve{\eth}^{(0)}\breve{\eth}^{(1)}\breve{\eth}^{(2)}\overline{\Psi} = -8\psi_{-2}. \quad (4.3.15)$$

If we decompose Ψ into spin-weighted spherical harmonics

$$\Psi = \sum_{\ell=2}^{\infty} \sum_{m=-\ell}^{\ell} \Psi_{\ell m \, -2} Y_{\ell m}(\theta, \phi - \phi_0)$$

and use Eq. (4.2.5), then we can write the ℓm modes of Ψ algebraically in terms of the ℓm modes of ψ_{-2}:

$$\Psi_{\ell m} = 8 \frac{(\ell+2)(\ell+1)\ell(\ell-1)(-1)^m \overline{\psi}_{2,\ell,-m} - 12 i M m \Omega \psi_{-2,\ell m}}{(\ell+2)^2(\ell+1)^2\ell^2(\ell-1)^2 + (12 M m \Omega)^2}, \qquad (4.3.16)$$

where $\psi_{-2,\ell m}$ is everything contained in the square brackets in Eq. (4.3.9). The radiative part of the metric is follows directly from Ψ:

$$h_{\alpha\beta}^{\pm} = \left\{ \frac{-1}{2r^2} \ell_\alpha \ell_\beta \hat{\eth}^{(-1)} \hat{\eth}^{(-2)} - \ell_{(\alpha} m_{\beta)} \left[\mathbf{D} \left(\frac{1}{\sqrt{2}r} \hat{\eth}^{(-2)} \right) + \frac{1}{\sqrt{2}r} \hat{\eth}^{(-2)}(\mathbf{D} + 3\rho) \right] \right.$$
$$\left. - m_\alpha m_\beta (\mathbf{D} - \rho)(\mathbf{D} + 3\rho) \right\} \Psi \pm \text{c.c.}, \qquad (4.3.17)$$

where the $\pm$ refers to the two polarizations of $h_{\alpha\beta}$. We point out here that Ψ and $h_{\alpha\beta}$ have $\tilde{\mathrm{S}}$ and $\tilde{\mathrm{R}}$ parts that are calculated from the corresponding parts of ψ_{-2}, and ultimately constructed from the corresponding parts of $g_{\ell m}$.

We still need to obtain the contributions to $h_{\alpha\beta}$ due to the energy and angular momentum that the particle adds to the spacetime. As we will see later, the only relevant components of the metric perturbation are the tt, $t\phi$, and $\phi\phi$ components. In Schwarzschild, the added energy and angular momentum do not contribute anything to $h_{\phi\phi}$. The contributions to h_{tt} and $h_{\phi\phi}$ are [104]

$$h_{tt}^{(\text{nonrad})} = -\frac{2\mathrm{m} u_t}{r} \qquad (4.3.18)$$

$$h_{\phi\phi}^{(\text{nonrad})} = \frac{2M\mathrm{m} u_\phi}{r}. \qquad (4.3.19)$$

4.4 Gravitational Self-Force

In many ways, gravitational self-force calculations are analogous to those of scalar self-force. As in the scalar case, the perturbation to the gravitational field can be decomposed into singular and renormalized parts [109]:

$$h_{\alpha\beta} = h_{\alpha\beta}^{\mathrm{S}} + h_{\alpha\beta}^{\mathrm{R}} \qquad (4.4.1)$$

such that $h^{\mathrm{R}}_{\alpha\beta}$ is continuous and differentiable at the particle and is solely responsible for the modification to the particle's motion. The renormalized gravitational "self-force" relative to geodesics on the background metric is given by [91, 92]

$$F^{\mathrm{R},\alpha} = -\mathrm{m}(g^{\alpha\beta} + u^\alpha u^\beta) \left(\nabla_\mu h^{\mathrm{R}}_{\nu\beta} - \frac{1}{2} \nabla_\beta h^{\mathrm{R}}_{\mu\nu} \right) u^\mu u^\nu, \qquad (4.4.2)$$

and similarly for the singular part of the force, where ∇_α is the covariant derivative that is compatible with the background metric. The scare quotes around the term self-force appear here for two reasons. First, gravity is not thought of as a force in General Relativity; instead, freely-falling objects are considered inertial. Second, the motion resulting from the "force" given above is that of a geodesic on the renormalized perturbed spacetime with metric $g_{\alpha\beta} + h^{\mathrm{R}}_{\alpha\beta}$. It is tempting, then, to say that the gravitational self-force is completely fictitious and results simply from the fact that we stubbornly measure the motion of the particle relative to geodesics on the background spacetime. However, this is also not quite right because while the massive particle follows a geodesic on the metric $g_{\alpha\beta} + h^{\mathrm{R}}_{\alpha\beta}$, nearby test particles follow geodesics on the full perturbed metric $g_{\alpha\beta} + h_{\alpha\beta}$. Thus, there is something unique about the effect of the particle's own field on its motion; this effect is referred to as the gravitational self-force, regardless of interpretive difficulties.

However, there is one remaining difficulty with the gravitational self-force: the renormalized metric perturbation $h^{\mathrm{R}}_{\alpha\beta}$ is gauge-dependent, and therefore so is $F^{\mathrm{R},\alpha}$, in sharp contrast to the scalar case. This makes it impossible to compare two self-force results if the calculations are done in different gauges. To remedy this, Detweiler [11] found a gauge-invariant[2] quantity[3]

$$H \equiv \frac{1}{2} h_{\alpha\beta} u^\alpha u^\beta. \qquad (4.4.3)$$

Thus, in this chapter we choose to compute H^{R}, called the renormalized *redshift factor*, instead of the self-force. This will allow us to compare our results with those of other authors who worked in different gauges.

---

[2]That is, for any gauge that preserves the helical symmetry of the system.

[3]Alternatively, some compute $\Delta U = -u^t H$, and others compute $h_{kk} = H/(u^t)^2$.

In order to take the limits required to renormalize H, we need to define it such that it has well-defined values away from the particle, which means we need to extend the particle's four-velocity off its worldline. We are free to do this in any way we like, and we choose the components of u^α to be constant as we move away from the particle. With that choice, we can speak of H as a function of the Schwarzschild coordinates and decompose it into spherical harmonics:

$$H = \sum_{\ell=0}^{\infty} \sum_{m=-\ell}^{\ell} H_{\ell m} \, {}_0Y_{\ell m}(\theta, \phi). \tag{4.4.4}$$

Similarly to the scalar case, the ℓm-modes of H are finite, and we can define the ℓ-modes

$$H_\ell = \lim_{x \to x_0} \sum_{m=-\ell}^{\ell} H_{\ell m} \, {}_0Y_{\ell m}(\theta, \phi). \tag{4.4.5}$$

The limit of H_ℓ as $\ell \to \infty$ is a constant B_H:

$$\lim_{\ell \to \infty} H_\ell = B_H. \tag{4.4.6}$$

To renormalize the redshift factor, we need only to subtract B_H from H_ℓ and then sum to infinity:

$$H_\ell^{\mathrm{S}} = B_H, \tag{4.4.7}$$

so

$$H^{\mathrm{R}} = \sum_{\ell=0}^{\infty} (H_\ell - B_H). \tag{4.4.8}$$

Finally, we note here that the time rate of change of the particle's energy $E \equiv \mathrm{m} u_t$ is related to the time derivative of H^{R}:

$$\frac{\mathrm{d}E}{\mathrm{d}t} = -\frac{\mathrm{m}}{u^t} \partial_t H^{\mathrm{R}}. \tag{4.4.9}$$

This in turn is the opposite of the gravitational power radiated by the particle.

4.5   Using Hikida's Method to Find the Redshift Factor

As in the scalar case, we split our radial Green's function into $\tilde{\mathrm{S}}$ and $\tilde{\mathrm{R}}$ parts, defined in the same way as the last chapter. The $\tilde{\mathrm{S}}$ part of $g_{\ell m}$ is still polynomial in m, and it

follows immediately that the $\tilde{\text{S}}$ part of $\psi_{-2,\ell m}$ is also polynomial in m. In the scalar case, it followed immediately that $\psi_{\ell m}^{\tilde{\text{S}}}$, when evaluated at the particle, was equal to the sum of a polynomial in m multiplied by $|_0Y_{\ell m}(\theta_0, 0)|^2$. This is what allowed us to do the sum over m analytically for general ℓ-values. In this chapter, it is clear that the $\tilde{\text{S}}$ parts of $\psi_{-2,\ell m}^{(-2)}$, $\psi_{-2,\ell m}^{(-1)}$, and $\psi_{-2,\ell m}^{(0)}$ are polynomials in m. It is not clear at this point whether H can be written as the sum of a polynomial in m multiplied by $|_0Y_{\ell m}(\theta_0, 0)|^2$. There are two reasons for the uncertainty here: first, it is not obvious that the polynomial nature of $\psi_{-2,\ell m}^{\tilde{\text{S}}(-2)}$, $\psi_{-2,\ell m}^{\tilde{\text{S}}(-1)}$, and $\psi_{-2,\ell m}^{\tilde{\text{S}}(0)}$ will meaningfully translate to the Hertz potential Ψ and then the metric perturbation $h_{\alpha\beta}$. Second, $\psi_{-2,\ell m}$ is decomposed into spin-weighted spherical harmonics of spin-weight -2, but the mode-sum renormalization needs to be done with respect to the non-spin-weighted basis $_0Y_{\ell m}$. We expect that decomposing H into the usual spherical harmonics will affect our expressions non-trivially.

We start by calculating Ψ, and we will try to keep terms polynomial in m factored from terms with a more complicated m-dependence. All of the equations in the rest of this section are true whether they refer to the full perturbation, the $\tilde{\text{S}}$ part, the $\tilde{\text{R}}$ part, or the renormalized perturbation, as long as the relevant labels are placed on the quantities involved. The challenge here is dealing with the factor of $(-1)^m\overline{\psi}_{2,\ell,-m}$ in Eq. (4.3.16). As mentioned in the last chapter, $g_{\ell m} = \overline{g}_{\ell,-m}$. It follows from expressions (4.3.10)-(4.3.12) that

$$\psi_{-2,\ell m}^{(-2)} = \overline{\psi}_{-2,\ell,-m}^{(-2)}$$

$$\psi_{-2,\ell m}^{(-1)} = -\overline{\psi}_{-2,\ell,-m}^{(-1)}$$

$$\psi_{-2,\ell m}^{(0)} = \overline{\psi}_{-2,\ell,-m}^{(0)}.$$

We can then use Eq. (4.2.8), Eq. (4.2.9), and Eq. (4.2.10) to show that

$$(-1)^m\overline{\psi}_{2,\ell,-m} = {}_2Y_{\ell m}(\theta_0, 0)\psi_{-2,\ell m}^{(-2)} + \sqrt{(\ell+2)(\ell-1)}\ {}_1Y_{\ell m}(\theta_0, 0)\psi_{-2,\ell m}^{(-1)}$$
$$+ \sqrt{(\ell+2)(\ell+1)\ell(\ell-1)}\ {}_0Y_{\ell m}(\theta_0, 0)\psi_{-2,\ell m}^{(0)}.$$

We now define

$$\Psi^{(2)}_{\ell m} = \frac{8}{[(\ell+2)(\ell+1)\ell(\ell-1)]^2 + (12Mm\Omega)^2} \psi^{(-2)}_{-2,\ell m},$$

$$\Psi^{(1)}_{\ell m} = \frac{8}{[(\ell+2)(\ell+1)\ell(\ell-1)]^2 + (12Mm\Omega)^2} \psi^{(-1)}_{-2,\ell m},$$

$$\Psi^{(0)}_{\ell m} = \frac{8}{[(\ell+2)(\ell+1)\ell(\ell-1)]^2 + (12Mm\Omega)^2} \psi^{(0)}_{-2,\ell m},$$

and we can then write

$$\begin{aligned}
\Psi_{\ell m} =& [(\ell+2)(\ell+1)\ell(\ell-1) \; {}_2Y_{\ell m}(\theta_0,0) - 12iMm\Omega \; {}_{-2}Y_{\ell m}(\theta_0,0)]\Psi^{(2)}_{\ell m} \\
&+ [(\ell+2)(\ell+1)\ell(\ell-1) \; {}_1Y_{\ell m}(\theta_0,0) - 12iMm\Omega \; {}_{-1}Y_{\ell m}(\theta_0,0)]\Psi^{(1)}_{\ell m} \\
&+ [(\ell+2)(\ell+1)\ell(\ell-1) - 12iMm\Omega] \; {}_0Y_{\ell m}(\theta_0,0)\Psi^{(0)}_{\ell m}.
\end{aligned} \tag{4.5.1}$$

It should be clear that $\Psi^{\tilde{S}(2)}_{\ell m}$, $\Psi^{\tilde{S}(1)}_{\ell m}$, and $\Psi^{\tilde{S}(0)}_{\ell m}$ are polynomial in m when written as a PN expansion.

Finally, we need to see what happens with h_{tt}, $h_{t\phi}$, and $h_{\phi\phi}$. We start with h_{tt}. From Eq. (4.3.17), and summing over both polarizations, we see that the radiative part of h_{tt} is

$$h_{tt} = -\frac{1}{r^2} \sum_{\ell=2}^{\infty} \sum_{m=-\ell}^{\ell} \Psi_{\ell m} \sqrt{(\ell+2)(\ell+1)\ell(\ell-1)} \; {}_0Y_{\ell m}(\theta, \phi - \phi_0), \tag{4.5.2}$$

where we are helped by the fact that the angular derivatives acting on Ψ are two successive spin-weight raising operators. Similarly,

$$h_{t\phi} = \frac{1}{2r} \sin\theta \sum_{\ell=2}^{\infty} \sum_{m=-\ell}^{\ell} D^{(t\phi)}_m \Psi_{\ell m} \sqrt{(\ell+2)(\ell-1)} \; {}_{-1}Y_{\ell m}(\theta, \phi - \phi_0), \tag{4.5.3}$$

$$h_{\phi\phi} = -\sin^2\theta \sum_{\ell=-2}^{\infty} \sum_{m=-\ell}^{\ell} D^{(\phi\phi)}_m \Psi_{\ell m} \; {}_{-2}Y_{\ell m}(\theta, \phi - \phi_0), \tag{4.5.4}$$

where $D^{(t\phi)}_m$ and $D^{(\phi\phi)}_m$ are radial derivatives:

$$D^{(t\phi)}_m = \frac{r_0 m\Omega}{f_0} - 2i + ir_0\partial_r$$

and

$$D^{(\phi\phi)}_m = \frac{1}{f_0^2}\left[-r_0^2 m^2\Omega^2 + 2ir_0 m\Omega\left(1 - \frac{M}{r_0}\right)\right] - \left(\frac{2ir_0 m\Omega}{f_0} + 2\right)r_0\partial_r + r_0^2\partial_r^2.$$

As mentioned before, H needs to be decomposed into spherical harmonics, which means we need to express $h_{t\phi}$ and $h_{\phi\phi}$ in terms of spherical harmonics. We use the expressions in Appendix C of [110] to show that

$$\sin\theta \,\, _{-1}Y_{\ell m}(\theta,\phi) = \frac{1}{\sqrt{\ell(\ell+1)}}[\ell\sqrt{C_{\ell+1,m}}\,\, _0Y_{\ell+1,m}(\theta,\phi) + m\,\, _0Y_{\ell m}(\theta,\phi)$$
$$- (\ell+1)\sqrt{C_{\ell m}}\,\, _0Y_{\ell-1,m}(\theta,\phi)],$$

$$\sin^2\theta \,\, _{-2}Y_{\ell m}(\theta,\phi) = \frac{1}{\sqrt{(\ell+2)(\ell+1)\ell(\ell-1)}}\{\ell(\ell-1)\sqrt{C_{\ell+1,m}C_{\ell+2,m}}\,\, _0Y_{\ell+2m}(\theta,\phi)$$
$$+ 2m(\ell-1)\sqrt{C_{\ell+1,m}}\,\, _0Y_{\ell+1,m}$$
$$+ [\ell(\ell-1)C_{\ell+1,m} + (\ell+1)(\ell+2)C_{\ell,m} + 2m^2 - \ell(\ell+1)]\,\, _0Y_{\ell m}(\theta,\phi)$$
$$- 2m(\ell+2)\sqrt{C_{\ell m}}\,\, _{-1}Y_{\ell-1,m}(\theta,\phi)$$
$$+ (\ell+1)(\ell+2)\sqrt{C_{\ell m}C_{\ell-1,m}}\,\, _0Y_{\ell-2,m}(\theta,\phi)\},$$

where
$$C_{\ell m} = \frac{(\ell+m)(\ell-m)}{(2\ell+1)(2\ell-1)}. \tag{4.5.5}$$

We can then plug these expressions into our equations for $h_{t\phi}$ and $h_{\phi\phi}$. Before we do, we make the following definitions:

$$X_{\ell m} = (\ell+2)(\ell+1)\ell(\ell-1) - 12iMm\Omega$$
$$Z_{\ell m}^{(1)} = \frac{2m^2 - \ell(\ell+1)}{(\ell+2)(\ell+1)\ell(\ell-1)}\Psi_{\ell m}^{(2)} + \frac{m}{\ell(\ell+1)}\Psi_{\ell m}^{(1)} + \Psi_{\ell m}^{(0)}$$
$$Z_{\ell m}^{(2)} = 2m\Psi_{\ell m}^{(2)} + (\ell+2)(\ell-1)\Psi_{\ell m}^{(1)}.$$

Finally, evaluating the components of the metric perturbation at the position of the particle and using the explicit expressions for $_sY_{\ell m}(\theta_0,0)$, we find that

$$h_{tt}|_{x=x_0} = -\frac{1}{r_0^2}\sum_{\ell=2}^{\infty}\sum_{m=-\ell}^{\ell}(\ell+2)(\ell+1)\ell(\ell-1)X_{\ell m}Z_{\ell m}^{(1)}|_0Y_{\ell m}(\theta_0,0)|^2, \tag{4.5.6}$$

$$h_{t\phi}|_{x=x_0} = -\frac{1}{r_0} \sum_{\ell=3}^{\infty} \sum_{m=-\ell}^{\ell} D_m^{(t\phi)} \left[m(\ell+2)(\ell-1) X_{\ell m} Z_{\ell m}^{(1)} - \frac{2\ell-1}{\ell} C_{\ell m} \overline{X}_{\ell-1,m} Z_{\ell-1,m}^{(2)} \right.$$

$$\left. -\frac{2\ell+3}{\ell+1} C_{\ell+1,m} \overline{X}_{\ell+1,m} Z_{\ell+1,m}^{(2)} \right] |{}_0 Y_{\ell m}(\theta_0,0)|^2$$

$$-\frac{1}{r_0} \sum_{m=-2}^{2} D_m^{(t\phi)} \left[4m X_{2,m} Z_{2,m}^{(1)} - \frac{7}{3} C_{3,m} \overline{X}_{3,m} Z_{3,m}^{(2)} \right] |{}_0 Y_{2,m}(\theta_0,0)|^2$$

$$-\frac{1}{r_0} \sum_{m=-1}^{1} D_m^{(t\phi)} \left[-\frac{5}{2} C_{2,m} \overline{X}_{2,m} Z_{2,m}^{(2)} \right] |{}_0 Y_{1,m}(\theta_0,0)|^2, \tag{4.5.7}$$

and

$$h_{\phi\phi}|_{x=x_0} = \sum_{\ell=4}^{\infty} \sum_{m=-\ell}^{\ell} D_m^{(\phi\phi)} \left[-(\ell-2)(\ell-3) C_{\ell m} X_{\ell-2,m} Z_{\ell-2,m}^{(1)} \right.$$

$$-\frac{2m(2\ell-1)}{(\ell+1)\ell(\ell-1)} C_{\ell m} \overline{X}_{\ell-1,m} Z_{\ell-1,m}^{(2)} + (\ell(\ell-1) C_{\ell+1,m}$$

$$+(\ell+1)(\ell+2) C_{\ell m} + 2m^2 - \ell(\ell+1)) X_{\ell m} Z_{\ell m}^{(1)}$$

$$-\frac{2m(2\ell+3)}{(\ell+2)(\ell+1)\ell} C_{\ell+1,m} \overline{X}_{\ell+1,m} Z_{\ell+1,m}^{(2)}$$

$$\left. -(\ell+4)(\ell+3) C_{\ell+1,m} X_{\ell+2,m} Z_{\ell+2,m}^{(1)} \right] |{}_0 Y_{\ell m}(\theta_0,0)|^2$$

$$+\sum_{m=-3}^{3} D_m^{(\phi\phi)} \left[-\frac{10m}{24} C_{3,m} \overline{X}_{2,m} Z_{2,m}^{(2)} + (6C_{4,m} + 20C_{3,m} + 2m^2 - 12) X_{3,m} Z_{3,m}^{(1)} \right.$$

$$\left. -\frac{3m}{10} C_{4,m} \overline{X}_{4,m} Z_{4,m}^{(2)} - 42 C_{4,m} X_{5,m} Z_{5,m}^{(1)} \right] |{}_0 Y_{3,m}(\theta_0,0)|^2$$

$$+\sum_{m=-2}^{2} D_m^{(\phi\phi)} \left[(2C_{3,m} + 12C_{2,m} + 2m^2 - 6) X_{2,m} Z_{2,m}^{(1)} - \frac{7m}{12} C_{3,m} \overline{X}_{3,m} Z_{3,m}^{(2)} \right.$$

$$\left. -30 C_{3,m} X_{4,m} Z_{4,m}^{(1)} \right] |{}_0 Y_{2,m}(\theta_0,0)|^2$$

$$+\sum_{m=-1}^{1} D_m^{(\phi\phi)} \left[-\frac{5m}{3} C_{2,m} \overline{X}_{2,m} Z_{2,m}^{(2)} - 20 C_{2,m} X_{3,m} Z_{3,m}^{(1)} \right] |{}_0 Y_{1,m}(\theta_0,0)|^2$$

$$+ D_0^{(\phi\phi)} \left[-12 C_{1,0} X_{2,0} Z_{2,0}^{(1)} \right] |{}_0 Y_{0,m}(\theta_0,0)|^2. \tag{4.5.8}$$

Remarkably, our final expressions are free of square roots. Noting that $C_{\ell m}$, $X_{\ell m}$, and the $\tilde{\mathbb{S}}$ parts of $Z_{\ell m}^{(1)}$ and $Z_{\ell m}^{(2)}$ are all polynomial in m, it follows that $H^{\tilde{\mathbb{S}}}$ is a sum over polynomials in m times $|{}_0 Y_{0,m}(\theta_0,0)|^2$. Thus, we can once again do the renormalization analytically, and Hikida's method still works in the gravitational case. Notice, however, that $\Psi_{\ell-2}$ contributes to H_ℓ, so we need to compute the ℓ-modes explicitly through $\ell = 9$

to get an expression for H that is accurate through 6th PN Order.

Finally, we note here that

$$\partial_t H = \sum_{\ell=0}^{\infty} \sum_{m=-\ell}^{\ell} im\Omega H_{\ell m} \, {}_0Y_{\ell m}(\theta, \phi - \phi_0); \tag{4.5.9}$$

that is, to get $\partial_t H$ and therefore the power radiated by the particle, we simply need to multiply the ℓm-modes of H by $im\Omega$.

4.6 Results

Following the format of the last chapter, we will first report several intermediate results: general- and specific-ℓ expressions for Φ^ν and $\Phi^{-\nu-1}$; general- and specific-ℓ expressions for $H_\ell^{\tilde{\text{S}}}$ and $(\mathrm{d}E/\mathrm{d}t)_\ell^{\tilde{\text{S}}}$; and expressions for $H_\ell^{\tilde{\text{R}}}$ and $(\mathrm{d}E/\mathrm{d}t)_\ell^{\tilde{\text{R}}}$. Unlike the last chapter, the expressions for Φ^ν, $\Phi^{-\nu-1}$, and the ℓ-modes of both parts of H will be given through 1st PN order, and the ℓ-modes of both parts of $\mathrm{d}E/\mathrm{d}t$ will be given through 1.5^{th} order. Higher-order expressions are too complicated to easily typeset.

We will then report the primary results of the chapter: the renormalized $\tilde{\text{S}}$ part of H and $\mathrm{d}E/\mathrm{d}t$; the $\tilde{\text{R}}$ parts of the same quantities; and finally, the full renormalized redshift factor H^{R} and the power radiated by the particle, $(\mathrm{d}E/\mathrm{d}t)^{\text{R}}$. All results will be given through 6th PN order.

For all results, we will treat the particle's angular velocity Ω as independent of its radial coordinate r_0. In this chapter, we cannot interpret these results as corresponding to an accelerated particle. The reason is that whatever force was responsible for the acceleration would have a stress-energy tensor associated with it and would therefore source its own perturbation to the gravitational field. This is in contrast to the scalar case, where you could accelerate the particle with something other than a scalar field. Still, we will learn interesting things from keeping factors of $r_0\Omega$ and factors of M/r_0 separated. We also remind the reader here of the effective field theory work of Galley [96–100], which calculates terms of different powers of M/r_0 separately. The results here are therefore useful as intermediate points of comparison.

4.6.1 Intermediate Results

We begin with general-ℓ expressions for Φ^ν and $\Phi^{-\nu-1}$. They are as follows.

$$\Phi^\nu = (r\omega)^2 \left[1 + \left(\frac{2i}{\ell+1}r\omega\right)\frac{1}{c} + \left(-(\ell+2)\frac{M}{r} - \frac{\ell+9}{2(\ell+1)(2\ell+3)}(r\omega)^2\right)\frac{1}{c^2} + \text{PN}(1.5)\right]$$

(4.6.1)

$$\Phi^{-\nu-1} = (r\omega)^2 \left[1 + \left(-\frac{2i}{\ell}r\omega\right)\frac{1}{c} + \left((\ell-1)\frac{M}{r} + \frac{\ell-8}{2\ell(2\ell-1)}\right)\frac{1}{c^2} + \text{PN}(1.5)\right] \quad (4.6.2)$$

Now, we show the $\ell = 2$ expressions for these two functions. Remember that they are solutions to a radial differential equation that resulted from the Bardeen-Press equation. We used spin-weighted spherical harmonics with spin-weight -2, so $\ell \geq 2$. At 1st PN order, the general-ℓ expressions are sufficient for $\ell \geq 3$. For $\ell = 2$:

$$\Phi^\nu = (r\omega)^2 \left[1 + \left(\frac{2i}{3}r\omega\right)\frac{1}{c} + \left(-4\frac{M}{r} - \frac{11}{42}(r\omega)^2\right)\frac{1}{c^2} + \text{PN}(1.5)\right]$$

(4.6.3)

$$\Phi^{-\nu-1} = (r\omega)^2 \left[1 - (ir\omega)\frac{1}{c} + \left(\frac{M}{r} - \frac{1}{2}(r\omega)^2 - \frac{14}{107}\frac{r}{M}(r\omega)^4\right)\frac{1}{c^2} + \text{PN}(1.5)\right] \quad (4.6.4)$$

Now for the general-ℓ expressions for $H_\ell^{\tilde{\text{S}}}$ and $(\mathrm{d}E/\mathrm{d}t)_\ell^{\tilde{\text{S}}}$:

$$H_\ell^{\tilde{\text{S}}} = \frac{\mathrm{m}}{r_0} \left[1 - \left(\frac{8\ell^4 + 16\ell^3 + 46\ell^2 + 38\ell - 147}{2(2\ell+5)(2\ell+3)(2\ell-1)(2\ell-3)}(r_0\Omega)^2\right)\frac{1}{c^2} + \text{PN}(2)\right]$$

(4.6.5)

$$\left(\frac{\mathrm{d}E}{\mathrm{d}t}\right)_\ell^{\tilde{\text{S}}} = \frac{\mathrm{m}^2}{r_0^2}\frac{r_0\Omega}{c}\left[\left(\frac{2(\ell^2+\ell+1)}{(\ell+2)(\ell-1)}\frac{M}{r_0}r_0\Omega\right.\right.$$
$$\left.\left. - \frac{\ell(\ell+1)(32\ell^4 + 64\ell^3 - 80\ell^2 - 112\ell - 9)}{(\ell+2)(\ell-1)(2\ell+5)(2\ell+3)(2\ell-1)(2\ell-3)}(r_0\Omega)^3\right)\frac{1}{c^3} + \text{PN}(2.5)\right]$$

(4.6.6)

Because the ℓ-modes of H and $\mathrm{d}E/\mathrm{d}t$ are expressed with respect to the usual spherical harmonics (which have spin-weight 0), they start at $\ell = 0$. The expression shown for $H_\ell^{\tilde{\text{S}}}$ above is true for $\ell \geq 3$, while that for $(\mathrm{d}E/\mathrm{d}t)_\ell^{\tilde{\text{S}}}$ is true for $\ell \geq 4$. We show the low-ℓ expressions for $H_\ell^{\tilde{\text{S}}}$ below.

$$H_0^{\tilde{\text{S}}} = \frac{\mathrm{m}}{r_0}\left[1 + \left(\frac{M}{r_0} + \frac{49}{30}(r_0\Omega)^2\right)\frac{1}{c^2} + \text{PN}(2)\right]$$

(4.6.7)

$$H_1^{\tilde{\text{S}}} = \frac{\mathrm{m}}{r_0}\left[\left(-\frac{107}{35}(r_0\Omega)^2\right)\frac{1}{c^2} + \text{PN}(2)\right]$$

(4.6.8)

$$H_2^{\tilde{S}} = \frac{m}{r_0}\left[1 + \left(\frac{1}{42}(r_0\Omega)^2 - \frac{168}{107}\frac{r_0}{M}(r_0\Omega)^4\right)\frac{1}{c^2} + \text{PN}(2)\right] \tag{4.6.9}$$

Next are the low-ℓ expressions for $(\mathrm{d}E/\mathrm{d}t)_\ell^{\tilde{S}}$.

$$\left(\frac{\mathrm{d}E}{\mathrm{d}t}\right)_0^{\tilde{S}} = 0 \tag{4.6.10}$$

$$\left(\frac{\mathrm{d}E}{\mathrm{d}t}\right)_1^{\tilde{S}} = \frac{m^2}{r_0^2}\frac{r_0\Omega}{c}\left[\left(-\frac{9}{140}(r_0\Omega)^3\right)\frac{1}{c^3} + \text{PN}(2.5)\right] \tag{4.6.11}$$

$$\left(\frac{\mathrm{d}E}{\mathrm{d}t}\right)_2^{\tilde{S}} = \frac{m^2}{r_0^2}\frac{r_0\Omega}{c}\left[\left(\frac{7}{2}\frac{M}{r_0}r_0\Omega - \frac{293}{84}(r_0\Omega)^3\right)\frac{1}{c^3} + \text{PN}(2.5)\right] \tag{4.6.12}$$

$$\left(\frac{\mathrm{d}E}{\mathrm{d}t}\right)_3^{\tilde{S}} = \frac{m^2}{r_0^2}\frac{r_0\Omega}{c}\left[\left(\frac{13}{5}\frac{M}{r_0}r_0\Omega - \frac{167}{66}(r_0\Omega)^3\right)\frac{1}{c^3} + \text{PN}(2.5)\right] \tag{4.6.13}$$

For every ℓ-value other than 2, $H_\ell^{\tilde{R}} = \text{PN}(4)$ or higher. For $\ell = 2$,

$$H_2^{\tilde{R}} = \frac{m}{r_0}\left[\left(\frac{168}{107}\frac{r_0}{M}(r_0\Omega)^4\right)\frac{1}{c^2} + \text{PN}(4)\right]. \tag{4.6.14}$$

Meanwhile, for all ℓ-values, $(\mathrm{d}E/\mathrm{d}t)_\ell^{\tilde{R}} = \text{PN}(2.5)$ or higher.

We remind the reader here that in order to find the full renormalized quantities H^R and $(\mathrm{d}E/\mathrm{d}t)^\text{R}$, we need to take the high-ℓ limit of $H_\ell^{\tilde{S}}$ and $(\mathrm{d}E/\mathrm{d}t)_\ell^{\tilde{S}}$ to get their respective B-terms, which are reported to 6th PN order in the next subsection. To renormalize the $\tilde{S}$ parts of these quantities, we subtract these B-terms from them and them sum the result form $\ell = 0$ to infinity. Finally, we can add the respective $\tilde{R}$ parts, which do not need to be renormalized.

4.6.2 B_H, $H^{\tilde{S}-\text{S}}$, $B_{\mathrm{d}E/\mathrm{d}t}$, and $(\mathrm{d}E/\mathrm{d}t)^{\tilde{S}-\text{S}}$

The regularization parameter B_H was found analytically by Detweiler [11]:

$$B_H = \frac{m}{r_0}\sqrt{\frac{1 - \frac{3M}{r_0}}{f_0}}\,_2F_1\left(\frac{1}{2}, \frac{1}{2}, 1, \frac{M}{r_0 f_0}\right). \tag{4.6.15}$$

This expression is true once we have enforced geodesic motion: $\Omega = \Omega_K = \sqrt{M/r_0^3}$.
Treating Ω and r_0 as independent, we find, to 6th PN order,

$$
\begin{aligned}
B_H =\frac{\mathrm{m}}{r_0} & \left[1 - \frac{1}{4}\left(r_0^2\Omega^2\right)\left(\frac{1}{c}\right)^2 + \left(-\frac{1}{2}Mr_0\Omega^2 - \frac{7r_0^4\Omega^4}{64}\right)\left(\frac{1}{c}\right)^4 \right. \\
& + \left(-M^2\Omega^2 - \frac{7}{16}Mr_0^3\Omega^4 - \frac{17r_0^6\Omega^6}{256}\right)\left(\frac{1}{c}\right)^6 \\
& + \left(-\frac{2M^3\Omega^2}{r_0} - \frac{21}{16}M^2r_0^2\Omega^4 - \frac{51}{128}Mr_0^5\Omega^6 - \frac{759r_0^8\Omega^8}{16384}\right)\left(\frac{1}{c}\right)^8 \\
& + \left(-\frac{4M^4\Omega^2}{r_0^2} - \frac{7}{2}M^3r_0\Omega^4 - \frac{51}{32}M^2r_0^4\Omega^6 - \frac{759Mr_0^7\Omega^8}{2048} - \frac{2289r_0^{10}\Omega^{10}}{65536}\right)\left(\frac{1}{c}\right)^{10} \\
& + \left(-\frac{8M^5\Omega^2}{r_0^3} - \frac{35M^4\Omega^4}{4} - \frac{85}{16}M^3r_0^3\Omega^6 - \frac{3795M^2r_0^6\Omega^8}{2048} - \frac{11445Mr_0^9\Omega^{10}}{32768} \right. \\
& \left.\left. - \frac{29023r_0^{12}\Omega^{12}}{1048576}\right)\left(\frac{1}{c}\right)^{12} + \mathrm{PN}(7) \right],
\end{aligned}
$$

(4.6.16)

which is consistent with

$$
B_H = \frac{\mathrm{m}}{r_0}\sqrt{\frac{1 - \frac{2M}{r_0} - r_0^2\Omega^2}{1 - \frac{2M}{r_0}}}\, {}_2F_1\left(\frac{1}{2},\frac{1}{2},1,\frac{r_0^2\Omega^2}{1 - \frac{2M}{r_0}}\right).
$$

(4.6.17)

Now that we have B_H, we can calculate

$$
H^{\tilde{\mathrm{S}}-\mathrm{S}} = \sum_{\ell=0}^{\infty}(H_\ell^{\tilde{\mathrm{S}}} - B_H).
$$

The result is

$$
H^{\tilde{\mathrm{S}}-\mathrm{S}} = \frac{\mathrm{m}}{r_0}\sum_{n=0}^{6}C_{H,n}^{\tilde{\mathrm{S}}-\mathrm{S}},
$$

with

$$
C_{H,0}^{\tilde{\mathrm{S}}-\mathrm{S}} = -1
$$

(4.6.18)

$$
C_{H,1}^{\tilde{\mathrm{S}}-\mathrm{S}} = \frac{M}{r_0} - \frac{3}{2}\Omega^2r_0^2 - \frac{168\Omega^4r_0^5}{107M}
$$

(4.6.19)

$$
C_{H,2}^{\tilde{\mathrm{S}}-\mathrm{S}} = \frac{M^2}{2r_0^2} - \frac{3}{2}M\Omega^2r_0 + \frac{6827}{856}\Omega^4r_0^4 - \frac{27396\Omega^6r_0^7}{6955M}
$$

(4.6.20)

$$
\begin{aligned}
C_{H,3}^{\tilde{\mathrm{S}}-\mathrm{S}} = & -\frac{221}{36}M^2\Omega^2 - \frac{5}{96}M^2\pi^2\Omega^2 + \frac{M^3}{2r_0^3} - \frac{276151M\Omega^4r_0^3}{7704} + \frac{4}{3}M\pi^2\Omega^4r_0^3 + \frac{9010381\Omega^6r_0^6}{333840} \\
& - \frac{540816331\Omega^8r_0^9}{98336745M}
\end{aligned}
$$

(4.6.21)

87

$$C_{H,4}^{\tilde{S}-S} = \frac{5M^4}{8r_0^4} - \frac{173M^3\Omega^2}{12r_0} + \frac{6032429M^2\Omega^4r_0^2}{385200} - \frac{6041M^2\pi^2\Omega^4r_0^2}{1536} - \frac{130815307817M\Omega^6r_0^5}{750138480}$$
$$+ \frac{10}{3}M\pi^2\Omega^6r_0^5 + \frac{13088784257\Omega^8r_0^8}{279713408} - \frac{17355718782469\Omega^{10}r_0^{11}}{2701431414990M} \tag{4.6.22}$$

$$C_{H,5}^{\tilde{S}-S} = -\frac{147M^5}{856r_0^5} - \frac{1699M^4\Omega^2}{48r_0^2} + \frac{31M^4\pi^2\Omega^2}{128r_0^2} + \frac{84704899M^3\Omega^4r_0}{128400} - \frac{57619}{768}M^3\pi^2\Omega^4r_0$$
$$+ \frac{27101275436783M^2\Omega^6r_0^4}{52509693600} - \frac{11995M^2\pi^2\Omega^6r_0^4}{1024}$$
$$- \frac{10867515234509729328 1M\Omega^8r_0^7}{235929203926416000} + \frac{9}{2}M\pi^2\Omega^8r_0^7 + \frac{6520327683660 53603\Omega^{10}r_0^{10}}{10216322442144000}$$
$$- \frac{2564553670549760739 43\Omega^{12}r_0^{13}}{35258079439638198000M} \tag{4.6.23}$$

$$C_{H,6}^{\tilde{S}-S} = -\frac{53038469341M^4\Omega^4}{59351616} - \frac{1110607M^4\pi^2\Omega^4}{27648} + \frac{130233589M^4\pi^4\Omega^4}{11796480} - \frac{6713M^6}{1712r_0^6}$$
$$- \frac{832519M^5\Omega^2}{15408r_0^3} - \frac{419M^5\pi^2\Omega^2}{192r_0^3} + \frac{2012925308063017M^3\Omega^6r_0^3}{472587242400}$$
$$- \frac{2395843M^3\pi^2\Omega^6r_0^3}{4608} - \frac{16}{45}M^3\pi^4\Omega^6r_0^3 + \frac{1228617042491149185 7937M^2\Omega^8r_0^6}{5460075862297056000}$$
$$- \frac{58085759M^2\pi^2\Omega^8r_0^6}{1769472} - \frac{413234948225737252798734 16799M\Omega^{10}r_0^9}{4641436314118720029513 6000}$$
$$+ \frac{553}{108}M\pi^2\Omega^{10}r_0^9 + \frac{18730900383696291572893\Omega^{12}r_0^{12}}{243009532137814041600}$$
$$- \frac{52190812805755179821585 17\Omega^{14}r_0^{15}}{648745841042987672144160M} \tag{4.6.24}$$

Now for $(\mathrm{d}E/\mathrm{d}t)^{\tilde{S}-S}$. Detweiler [11] reported that $\mathrm{d}E/\mathrm{d}t$ doesn't need to be renormalized. This is true for geodesic motion. If we don't enforce geodesic motion, we find a non-zero B-term:

$$B_{\mathrm{d}E/\mathrm{d}t} = \mathrm{m}^2\left[\left(\frac{2M\Omega^2}{r_0} - 2\Omega^4r_0^2\right)\left(\frac{1}{c}\right)^3 + \left(\frac{2M^2\Omega^2}{r_0^2} - \frac{1}{4}M\Omega^4r_0 - \frac{7}{4}\Omega^6r_0^4\right)\left(\frac{1}{c}\right)^5\right.$$
$$+ \left(\frac{9M^2\Omega^4}{4} + \frac{3M^3\Omega^2}{r_0^3} - \frac{113}{32}M\Omega^6r_0^3 - \frac{55}{32}\Omega^8r_0^6\right)\left(\frac{1}{c}\right)^7$$
$$+ \left(\frac{5M^4\Omega^2}{r_0^4} + \frac{65M^3\Omega^4}{8r_0} - \frac{145}{32}M^2\Omega^6r_0^2 - \frac{3525}{512}M\Omega^8r_0^5 - \frac{875}{512}\Omega^{10}r_0^8\right)\left(\frac{1}{c}\right)^9$$
$$+ \left(\frac{35M^5\Omega^2}{4r_0^5} + \frac{175M^4\Omega^4}{8r_0^2} - \frac{35}{64}M^3\Omega^6r_0 - \frac{9275}{512}M^2\Omega^8r_0^4 - \frac{84035M\Omega^{10}r_0^7}{8192}\right.$$
$$\left.\left. - \frac{13965\Omega^{12}r_0^{10}}{8192}\right)\left(\frac{1}{c}\right)^{11} + \mathrm{PN}(6.5)\right]. \tag{4.6.25}$$

As soon as we require $\Omega = \Omega_K$, the above is zero. Meanwhile,

$$
\begin{aligned}
\left(\frac{\mathrm{d}E}{\mathrm{d}t}\right)^{\tilde{\mathrm{S}}-\mathrm{S}} = {} & \left(-\frac{M\Omega^2}{3r_0} + \frac{1}{3}\Omega^4 r_0^2\right)\left(\frac{1}{c}\right)^3 \\
& + \left(-\frac{23M^2\Omega^2}{3r_0^2} + \frac{57}{5}M\Omega^4 r_0 - \frac{9352\Omega^6 r_0^4}{1605} + \frac{224\Omega^8 r_0^7}{107M}\right)\left(\frac{1}{c}\right)^5 \\
& + \left(\frac{17M^2\Omega^4}{15} - \frac{22M^3\Omega^2}{3r_0^3} + \frac{225088M\Omega^6 r_0^3}{11235} - \frac{13169981\Omega^8 r_0^6}{730275}\right. \\
& \left. + \frac{146046\Omega^{10} r_0^9}{34775M}\right)\left(\frac{1}{c}\right)^7 \\
& + \left(-\frac{8M^4\Omega^2}{r_0^4} - \frac{3098M^3\Omega^4}{45r_0} + \frac{487M^3\pi^2\Omega^4}{96r_0} + \frac{25412}{315}M^2\Omega^6 r_0^2\right. \\
& - \frac{1205}{288}M^2\pi^2\Omega^6 r_0^2 + \frac{605529446M\Omega^8 r_0^5}{19717425} - \frac{8}{9}M\pi^2\Omega^8 r_0^5 \\
& \left. - \frac{1238833072684\Omega^{10} r_0^8}{30976074675} + \frac{8045342788\Omega^{12} r_0^{11}}{1475051175M}\right)\left(\frac{1}{c}\right)^9 \\
& + \left(-\frac{8M^5\Omega^2}{r_0^5} + \frac{6694M^4\Omega^4}{45r_0^2} - \frac{1901M^4\pi^2\Omega^4}{96r_0^2} - \frac{4984166M^3\Omega^6 r_0}{7875}\right. \\
& + \frac{796979M^3\pi^2\Omega^6 r_0}{11520} + \frac{4264013536816M^2\Omega^8 r_0^4}{10548822375} - \frac{184841M^2\pi^2\Omega^8 r_0^4}{3840} \\
& + \frac{18449132889161543M\Omega^{10} r_0^7}{121529466308250} - \frac{56}{45}M\pi^2\Omega^{10} r_0^7 \\
& \left. - \frac{259409565425251607\Omega^{12} r_0^{10}}{3687453881461350} + \frac{1194501181991071023\Omega^{14} r_0^{13}}{1843726940730675M}\right)\left(\frac{1}{c}\right)^{11} + \\
& \mathrm{PN}(6.5). \qquad\qquad (4.6.26)
\end{aligned}
$$

Remarkably, when we enforce geodesic motion,

$$
\left(\frac{\mathrm{d}E}{\mathrm{d}t}\right)^{\tilde{\mathrm{S}}-\mathrm{S}} = 0. \qquad\qquad (4.6.27)
$$

This means that, as in the scalar case, the $\tilde{\mathrm{R}}$ part of the field contains all of the radiative information—but this is only apparent when we make the replacement $\Omega \to \Omega_K$.

4.6.3 $H^{\tilde{\mathrm{R}}}$ and $(\mathrm{d}E/\mathrm{d}t)^{\tilde{\mathrm{R}}}$

The $\tilde{\mathrm{R}}$ part of the redshift factor can be written

$$
H^{\tilde{\mathrm{R}}} = \frac{\mathrm{m}}{r_0}\sum_{p=0}^{12} C_{H,p/2}^{\tilde{\mathrm{R}}}, \qquad\qquad (4.6.28)
$$

89

with

$$C_{H,1}^{\tilde{R}} = \frac{168\Omega^4 r_0^5}{107M} \tag{4.6.29}$$

$$C_{H,2}^{\tilde{R}} = -\frac{840}{107}\Omega^4 r_0^4 + \frac{27396\Omega^6 r_0^7}{6955M} \tag{4.6.30}$$

$$C_{H,3}^{\tilde{R}} = \frac{1260}{107}M\Omega^4 r_0^3 - \frac{546196\Omega^6 r_0^6}{20865} + \frac{540816331\Omega^8 r_0^9}{98336745M} \tag{4.6.31}$$

$$C_{H,4}^{\tilde{R}} = -\frac{420}{107}M^2\Omega^4 r_0^2 + \frac{13670721634M\Omega^6 r_0^5}{78139425} - \frac{128}{5}\gamma M\Omega^6 r_0^5 - \frac{128}{5}M\Omega^6 \ln(4|\Omega|r_0) r_0^5$$
$$- \frac{1631444539\Omega^8 r_0^8}{32778915} + \frac{17355718782469\Omega^{10} r_0^{11}}{2701431414990M} \tag{4.6.32}$$

$$C_{H,5}^{\tilde{R}} = \frac{112M^5}{107r_0^5} - \frac{105}{107}M^3\Omega^4 r_0 - \frac{2753696702M^2\Omega^6 r_0^4}{5209295} + 128\gamma M^2\Omega^6 r_0^4$$
$$+ 128M^2\Omega^6 \ln(4|\Omega|r_0) r_0^4 + \frac{2021293463103094699M\Omega^8 r_0^7}{3686393811350250} - \frac{7496}{105}\gamma M\Omega^8 r_0^7$$
$$- \frac{5}{7}M\Omega^8 \ln(2|\Omega|r_0) - \frac{3776}{105}M\Omega^8 \ln(4|\Omega|r_0)r_0^7 - \frac{243}{7}M\Omega^8 \ln(6|\Omega|r_0)r_0^7$$
$$- \frac{56352759493226671\Omega^{10} r_0^{10}}{79815019079250} + \frac{2564553670549760739943\Omega^{12} r_0^{13}}{35258079439638198000M} \tag{4.6.33}$$

$$C_{H,5.5}^{\tilde{R}} = \frac{3072}{175}M^2\pi|\Omega|^7 r_0^5 - \frac{128}{15}M\pi|\Omega|^9 r_0^8 \tag{4.6.34}$$

$$C_{H,6}^{\tilde{R}} = -\frac{44373M^4\Omega^4}{11449} + \frac{560M^6}{107r_0^6} + \frac{392M^5\Omega^2}{107r_0^3} + \frac{5565517751M^3\Omega^6 r_0^3}{10418590} - 192\gamma M^3\Omega^6 r_0^3$$
$$- 192M^3\Omega^6 \ln(4|\Omega|r_0) r_0^3 - \frac{4164919900017694087M^2\Omega^8 r_0^6}{1579883062007250} + \frac{4408}{9}\gamma M^2\Omega^8 r_0^6$$
$$+ \frac{11}{15}M^2\Omega^8 \ln(2|\Omega|r_0)r_0^6 + \frac{11072}{45}M^2\Omega^8 \ln(4|\Omega|r_0)r_0^6 + 243M^2\Omega^8 \ln(6|\Omega|r_0)r_0^6$$
$$+ \frac{878596259017569091295972 09M\Omega^{10} r_0^9}{8058049156456111 1623500} - \frac{327428\gamma M\Omega^{10} r_0^9}{2835}$$
$$+ \frac{322439}{5670}M\Omega^{10} \ln(2|\Omega|r_0)r_0^9 - \frac{2926}{189}M\Omega^{10} \ln(4|\Omega|r_0)r_0^9 - \frac{243}{14}M\Omega^{10} \ln(6|\Omega|r_0)r_0^9$$
$$- \frac{1401983999029191802 61\Omega^{12} r_0^{12}}{1627295974137147600} + \frac{521908128057551798215 8517\Omega^{14} r_0^{15}}{6487458410429876721441 60M}. \tag{4.6.35}$$

90

Now, $(\mathrm{d}E/\mathrm{d}t)^{\tilde{\mathrm{R}}}$ can be written

$$\left(\frac{\mathrm{d}E}{\mathrm{d}t}\right)^{\tilde{\mathrm{R}}} = \mathrm{m}^2 \sum_{p=0}^{12} C_{\mathrm{d}E/\mathrm{d}t,p/2}^{\tilde{\mathrm{R}}}, \tag{4.6.36}$$

with

$$C_{\mathrm{d}E/\mathrm{d}t,2.5}^{\tilde{\mathrm{R}}} = -\frac{2304}{535} r_0^4 \Omega^6 - \frac{224 r_0^7 \Omega^8}{107 M} \tag{4.6.37}$$

$$C_{\mathrm{d}E/\mathrm{d}t,3.5}^{\tilde{\mathrm{R}}} = \frac{18304}{535} M r_0^3 \Omega^6 - \frac{4572224 r_0^6 \Omega^8}{730275} - \frac{146046 r_0^9 \Omega^{10}}{34775 M} \tag{4.6.38}$$

$$C_{\mathrm{d}E/\mathrm{d}t,4}^{\tilde{\mathrm{R}}} = -\frac{128}{5} \pi r_0^4 M |\Omega|^7 \tag{4.6.39}$$

$$C_{\mathrm{d}E/\mathrm{d}t,4.5}^{\tilde{\mathrm{R}}} = -\frac{384}{5} M^2 r_0^2 \Omega^6 + \frac{25503564 M r_0^5 \Omega^8}{243425} + \frac{279612756734 r_0^8 \Omega^{10}}{30976074675}$$
$$- \frac{8045342788 r_0^{11} \Omega^{12}}{1475051175 M} \tag{4.6.40}$$

$$C_{\mathrm{d}E/\mathrm{d}t,5}^{\tilde{\mathrm{R}}} = \frac{768}{5} M \pi r_0^3 M |\Omega|^7 - \frac{3328}{105} \pi r_0^6 M |\Omega|^9 - \frac{4609}{105} \pi r_0^6 M |\Omega|^9 \tag{4.6.41}$$

$$C_{\mathrm{d}E/\mathrm{d}t,5.5}^{\tilde{\mathrm{R}}} = \frac{256}{5} M^3 r_0 \Omega^6 - \frac{5824767162556 M^2 r_0^4 \Omega^8}{8204639625} + \frac{12288}{175} \gamma M^2 r_0^4 \Omega^8 - \frac{512}{15} M^2 \pi^2 r_0^4 \Omega^8$$
$$+ \frac{65605444274612 M r_0^7 \Omega^{10}}{3314439990225} + \frac{512}{15} \gamma M r_0^7 \Omega^{10} + \frac{15047672593787723 r_0^{10} \Omega^{12}}{409717097940150}$$
$$- \frac{11945011819910723 r_0^{13} \Omega^{14}}{1843726940730675 M} + \frac{12288}{175} M^2 r_0^4 \Omega^8 \ln(4|\Omega|r_0)$$
$$+ \frac{512}{15} M r_0^7 \Omega^{10} \ln(4|\Omega|r_0) \tag{4.6.42}$$

$$C_{\mathrm{d}E/\mathrm{d}t,6}^{\tilde{\mathrm{R}}} = -\frac{1536}{5} M^2 \pi r_0^2 M |\Omega|^7 + \frac{15616}{63} M \pi r_0^5 M |\Omega|^9 - \frac{20992}{945} \pi r_0^8 M |\Omega|^{11}$$
$$+ \frac{14008}{35} M \pi r_0^5 M |\Omega|^9 - \frac{21148}{189} \pi r_0^8 M |\Omega|^{11}. \tag{4.6.43}$$

4.6.4 H^{R} and $(\mathrm{d}E/\mathrm{d}t)^{\mathrm{R}}$

Finally, we can add the renormalized $\tilde{\mathrm{S}}$ and $\tilde{\mathrm{R}}$ parts of H and $\mathrm{d}E/\mathrm{d}t$ to find the full, renormalized expressions for each. We start with H:

$$H^{\mathrm{R}} = \frac{\mathrm{m}}{r_0} \sum_{p=0}^{12} C_{H,p/2}^{\mathrm{R}}, \tag{4.6.44}$$

91

with

$$C_{H,0}^{\mathrm{R}} = -1 \tag{4.6.45}$$

$$C_{H,1}^{\mathrm{R}} = \frac{M}{r_0} - \frac{3}{2}\Omega^2 r_0^2 \tag{4.6.46}$$

$$C_{H,2}^{\mathrm{R}} = \frac{M^2}{2r_0^2} - \frac{3}{2}M\Omega^2 r_0 + \frac{1}{8}\Omega^4 r_0^4 \tag{4.6.47}$$

$$C_{H,3}^{\mathrm{R}} = -\frac{221}{36}M^2\Omega^2 - \frac{5}{96}M^2\pi^2\Omega^2 + \frac{M^3}{2r_0^3} - \frac{1733}{72}M\Omega^4 r_0^3 + \frac{4}{3}M\pi^2\Omega^4 r_0^3 + \frac{13}{16}\Omega^6 r_0^6 \tag{4.6.48}$$

$$\begin{aligned}
C_{H,4}^{\mathrm{R}} =& \frac{5M^4}{8r_0^4} - \frac{173M^3\Omega^2}{12r_0} + \frac{42247M^2\Omega^4 r_0^2}{3600} - \frac{6041M^2\pi^2\Omega^4 r_0^2}{1536} + \frac{2033M\Omega^6 r_0^5}{3600} \\
& - \frac{128}{5}\gamma M\Omega^6 r_0^5 + \frac{10}{3}M\pi^2\Omega^6 r_0^5 - \frac{128}{5}M\Omega^6 \ln(4r_0|\Omega|)r_0^5 - \frac{5717\Omega^8 r_0^8}{1920}
\end{aligned} \tag{4.6.49}$$

$$\begin{aligned}
C_{H,5}^{\mathrm{R}} =& \frac{7M^5}{8r_0^5} - \frac{1699M^4\Omega^2}{48r_0^2} + \frac{31M^4\pi^2\Omega^2}{128r_0^2} + \frac{790457M^3\Omega^4 r_0}{1200} - \frac{57619}{768}M^3\pi^2\Omega^4 r_0 \\
& - \frac{4407421M^2\Omega^6 r_0^4}{352800} + 128\gamma M^2\Omega^6 r_0^4 - \frac{11995M^2\pi^2\Omega^6 r_0^4}{1024} + 128M^2\Omega^6 \ln(4r_0|\Omega|)r_0^4 \\
& + \frac{41247377M\Omega^8 r_0^7}{470400} - \frac{7496}{105}\gamma M\Omega^8 r_0^7 + \frac{9}{2}M\pi^2\Omega^8 r_0^7 - \frac{5}{7}M\Omega^8 \ln(2|\Omega|r_0) \\
& - \frac{3776}{105}M\Omega^8 \ln(4|\Omega|r_0)r_0^7 - \frac{243}{7}M\Omega^8 \ln(6|\Omega|r_0)r_0^7 - \frac{911441\Omega^{10}r_0^{10}}{134400}
\end{aligned} \tag{4.6.50}$$

$$C_{H,5.5}^{\mathrm{R}} = \frac{128}{15}M^2\pi\Omega^6|\Omega|r_0^5 - \frac{13696}{525}M^2\pi|\Omega|^7 r_0^5 - \frac{128}{15}M\pi\Omega^8|\Omega|r_0^8 \tag{4.6.51}$$

$$\begin{aligned}
C_{H,6}^{\mathrm{R}} =& -\frac{4652677M^4\Omega^4}{5184} - \frac{1110607M^4\pi^2\Omega^4}{27648} + \frac{130233589M^4\pi^4\Omega^4}{11796480} + \frac{21M^6}{16r_0^6} - \frac{7253M^5\Omega^2}{144r_0^3} \\
& - \frac{419M^5\pi^2\Omega^2}{192r_0^3} + \frac{15220524421M^3\Omega^6 r_0^3}{3175200} - 192\gamma M^3\Omega^6 r_0^3 - \frac{2395843M^3\pi^2\Omega^6 r_0^3}{4608} \\
& - \frac{16}{45}M^3\pi^4\Omega^6 r_0^3 - 192M^3\Omega^6 \ln(4r_0|\Omega|)r_0^3 - \frac{1801095461M^2\Omega^8 r_0^6}{4665600} + \frac{4408}{9}\gamma M^2\Omega^8 r_0^6 \\
& - \frac{58085759M^2\pi^2\Omega^8 r_0^6}{1769472} + \frac{11}{15}M^2\Omega^8 \ln(2|\Omega|r_0)r_0^6 + \frac{11072}{45}M^2\Omega^8 \ln(4|\Omega|r_0)r_0^6 \\
& + 243M^2\Omega^8 \ln(6|\Omega|r_0)r_0^6 + \frac{45726707459M\Omega^{10}r_0^9}{228614400} - \frac{327428\gamma M\Omega^{10}r_0^9}{2835} \\
& + \frac{553}{108}M\pi^2\Omega^{10}r_0^9 + \frac{322439}{5670}M\Omega^{10} \ln(2r_0|\Omega|)r_0^9 - \frac{29296}{189}M\Omega^{10} \ln(4r_0|\Omega|)r_0^9 \\
& - \frac{243}{14}M\Omega^{10} \ln(6r_0|\Omega|)r_0^9 - \frac{395191103\Omega^{12}r_0^{12}}{43545600}.
\end{aligned} \tag{4.6.52}$$

For when we enforce geodesic motion, the redshift factor reduces to

$$
\begin{aligned}
H^{\mathrm{R}} ={} & \frac{\mathrm{m}}{r_0}\left[-1 - \frac{1}{2}x - \frac{7}{8}x^2 + \left(-\frac{1387}{48} + \frac{41\pi^2}{32}\right)x^3 + \left(-\frac{8581}{1920} - \frac{307\pi^2}{512} - \frac{128}{5}\gamma\right.\right. \\
& \left. - \frac{64}{5}\ln(16x)\right)x^4 + \left(\frac{279258271}{403200} - \frac{251893\pi^2}{3072} + \frac{5944}{105}\gamma - \frac{6019}{105}\ln(2x)\right. \\
& \left. + \frac{4212}{35}\ln(4x) - \frac{243}{7}\ln(6x)\right)x^5 - \frac{13696\pi}{525}x^{11/2} + \left(\frac{10601627591}{2903040}\right. \\
& - \frac{1043969471\pi^2}{1769472} + \frac{2800873\pi^4}{262144} + \frac{516772}{2835}\gamma - \frac{235649}{1890}\ln(2x) - \frac{27838}{2835}\ln(4x) \\
& \left.\left. + \frac{3159}{14}\ln(6x)\right)x^6 + \mathcal{O}(x^{13/2})\right].
\end{aligned}
\tag{4.6.53}
$$

This agrees with previous PN expansions of the redshift factor, including those of Bini and Damour [12], who report it to PN(6), and Kavanagh *et al.* [13], who report it to PN(21.5).

Finally, we write a similar expression for $\mathrm{d}E/\mathrm{d}t$:

$$
\left(\frac{\mathrm{d}E}{\mathrm{d}t}\right)^{\mathrm{R}} = \mathrm{m}^2 \sum_{p=0}^{12} C^{\mathrm{R}}_{\mathrm{d}E/\mathrm{d}t,p/2},
$$

with

$$
C^{\mathrm{R}}_{\mathrm{d}E/\mathrm{d}t,1.5} = -\frac{M\Omega^2}{3r_0} + \frac{1}{3}\Omega^4 r_0^2
\tag{4.6.54}
$$

$$
C^{\mathrm{R}}_{\mathrm{d}E/\mathrm{d}t,2.5} = -\frac{23M^2\Omega^2}{3r_0^2} + \frac{57}{5}M\Omega^4 r_0 - \frac{152}{15}\Omega^6 r_0^4
\tag{4.6.55}
$$

$$
C^{\mathrm{R}}_{\mathrm{d}E/\mathrm{d}t,3.5} = \frac{17M^2\Omega^4}{15} - \frac{22M^3\Omega^2}{3r_0^3} + \frac{5696}{105}M\Omega^6 r_0^3 - \frac{2551}{105}\Omega^8 r_0^6
\tag{4.6.56}
$$

$$
C^{\mathrm{R}}_{\mathrm{d}E/\mathrm{d}t,4} = -\frac{128}{5}\pi M|\Omega|^7 r_0^4
\tag{4.6.57}
$$

$$
\begin{aligned}
C^{\mathrm{R}}_{\mathrm{d}E/\mathrm{d}t,4.5} ={} & -\frac{8M^4\Omega^2}{r_0^4} - \frac{3098M^3\Omega^4}{45r_0} + \frac{487M^3\pi^2\Omega^4}{96r_0} + \frac{244}{63}M^2\Omega^6 r_0^2 - \frac{1205}{288}M^2\pi^2\Omega^6 r_0^2 \\
& + \frac{384086M\Omega^8 r_0^5}{2835} - \frac{8}{9}M\pi^2\Omega^8 r_0^5 - \frac{17558}{567}\Omega^{10}r_0^8
\end{aligned}
\tag{4.6.58}
$$

$$
C^{\mathrm{R}}_{\mathrm{d}E/\mathrm{d}t,5} = \frac{768}{5}M^2\pi|\Omega|^7 r_0^3 - \frac{3328}{105}\pi M|\Omega|^9 r_0^6 - \frac{4609}{105}\pi M|\Omega|^9 r_0^6
\tag{4.6.59}
$$

93

$$C_{\mathrm{d}E/\mathrm{d}t,5.5}^{\mathrm{R}} = -\frac{8M^5\Omega^2}{r_0^5} + \frac{6694M^4\Omega^4}{45r_0^2} - \frac{1901M^4\pi^2\Omega^4}{96r_0^2} - \frac{4580966M^3\Omega^6 r_0}{7875}$$
$$+ \frac{796979M^3\pi^2\Omega^6 r_0}{11520} - \frac{151674716M^2\Omega^8 r_0^4}{496125} + \frac{12288}{175}\gamma M^2\Omega^8 r_0^4$$
$$- \frac{315913M^2\pi^2\Omega^8 r_0^4}{3840} + \frac{12288}{175}M^2\Omega^8\ln(4|\Omega|r_0)r_0^4 + \frac{267569987M\Omega^{10}r_0^7}{1559250}$$
$$+ \frac{512}{15}\gamma M\Omega^{10}r_0^7 - \frac{56}{45}M\pi^2\Omega^{10}r_0^7 + \frac{512}{15}M\Omega^{10}\ln(4|\Omega|r_0)r_0^7 - \frac{209702\Omega^{12}r_0^{10}}{6237}$$

$$(4.6.60)$$

$$C_{\mathrm{d}E/\mathrm{d}t,6}^{\mathrm{R}} = -\frac{1536}{5}M^3\pi|\Omega|^7 r_0^2 + \frac{15616}{63}M^2\pi|\Omega|^9 r_0^5 + \frac{14008}{35}M^2\pi|\Omega|^9 r_0^5$$
$$- \frac{20992}{945}\pi M|\Omega|^{11}r_0^8 - \frac{21148}{189}\pi M|\Omega|^{11}r_0^8 \qquad (4.6.61)$$

After we set $\Omega = \Omega_K$, $(\mathrm{d}E/\mathrm{d}t)^{\mathrm{R}}$ reduces to

$$\left(\frac{\mathrm{d}E}{\mathrm{d}t}\right)^{\mathrm{R}} = \frac{\mathrm{m}^2}{r_0^2}x^{1/2}\left[-\frac{32}{5}x^{5/2} + \frac{2494}{105}x^{7/2} - \frac{128\pi}{5}x^4 + \frac{89422}{2835}x^{9/2} + \frac{8191\pi}{105}x^5 +\right.$$
$$\left(-\frac{6643739519}{10914750} - \frac{512\pi^2}{15} + \frac{54784}{525}\gamma + \frac{54784}{525}\ln(16x)\right)x^{11/2}$$
$$\left.+ \frac{13028\pi}{63}x^6 + \mathcal{O}(x^{13/2})\right] \qquad (4.6.62)$$

This agrees with previous high-PN-order calculations of the gravitational wave flux, like that of Fujita [111].

We note here how terms simplify after adding the $\tilde{\mathrm{R}}$ and renormalized $\tilde{\mathrm{S}}$ parts of the quantities. In particular, all of the terms proportional to M^{-1} again went away, even though in this case we can't take the limit as $M \to 0$ independently of the limit as $\Omega \to 0$. Furthermore, there are no terms independent of Ω in $(\mathrm{d}E/\mathrm{d}t)^{\mathrm{R}}$.

Interestingly, there is a PN(1.5) term in $(\mathrm{d}E/\mathrm{d}t)^{\mathrm{R}}$. This suggests dipolar radiation. Of course, gravitational radiation is quadrupolar. We do see that, when we enforce geodesic motion, $C_{\mathrm{d}E/\mathrm{d}t,1.5}^{\mathrm{R}} = 0$. Still, this is interesting because it suggests that if freely-falling particles did not follow geodesics—that is, if the Equivalence Principle did not hold— dipolar radiation would exist. This comports with alternate theories of gravity that do not respect the Equivalence Principle, like Rosen's bimetric theory of gravity, which predicted dipolar gravitational radiation [112].

When we enforce geodesic motion, our results agree with previous Post-Newtonian calculations [12, 13]. In particular, the 2.5 PN term in $\mathrm{d}E/\mathrm{d}t$ is exactly what one obtains by applying the quadrupole formula to our system.

4.7 Conclusion

In this section, we successfully applied the method of Hikida *et al.* [8, 9] to find Detweiler's [11] redshift factor and the power radiated by a massive point particle in circular orbit around a Schwarzschild black hole. As in chapter 3, we treated the particle's angular velocity Ω as independent from its radial coordinate r_0 and black hole mass M. Unlike in chapter 3, we cannot interpret our expressions to be accurate for an accelerated particle, because whatever accelerated the particle would also perturb the spacetime. Nevertheless, this gave interesting results. First, we found that if the Equivalence Principle is violated—that is, if a freely falling particle does not follow a geodesic—dipolar gravitational radiation can result. We also found that the resulting expressions agree with what one would expect of expressions that do describe an accelerated particle. In particular, our expressions have no terms proportional to M^{-1}, despite the fact that the $\tilde{\mathrm{S}}$ and $\tilde{\mathrm{R}}$ parts individually have such terms. We also saw that our Post-Newtonian expression for the power radiated by the particle is free of terms independent of Ω, which we would also expect if it correctly described an accelerated particle.

To our knowledge, this is the first time that Hikida's method has been successfully applied to the gravitational case. Knowing that Hikida's method allows for the analytical renormalization of a particle following an arbitrary path, we hope that Hikida's method is eventually applied to more complicated orbits in the future.

Bibliography

[1] B. Abbott *et al.*, Physical review letters **116**, 061102 (2016).

[2] B. Abbott *et al.*, Physical Review Letters **116**, 241103 (2016).

[3] B. Abbott *et al.*, Physical Review Letters **118**, 221101 (2017).

[4] B. Abbott *et al.*, The Astrophysical Journal Letters **851**, L35 (2017).

[5] B. P. Abbott *et al.*, Physical review letters **119**, 141101 (2017).

[6] B. P. Abbott *et al.*, Physical Review Letters **119**, 161101 (2017).

[7] B. Abbott *et al.*, arXiv preprint arXiv:1805.11581 (2018).

[8] W. Hikida *et al.*, Progress of theoretical physics **111**, 821 (2004).

[9] W. Hikida *et al.*, Progress of theoretical physics **113**, 283 (2005).

[10] A. Heffernan, A. C. Ottewill, N. Warburton, B. Wardell, and P. Diener, arXiv preprint arXiv:1712.01098 (2017).

[11] S. Detweiler, Physical Review D **77**, 124026 (2008).

[12] D. Bini and T. Damour, Physical Review D **91**, 064050 (2015).

[13] C. Kavanagh, A. C. Ottewill, and B. Wardell, Physical Review D **92**, 084025 (2015).

[14] A. Einstein, Sitzungsber. Preuss. Akad. Wiss. Berlin (Math. Phys.) **1916**, 688 (1916).

[15] A. Buonanno and T. Damour, Phys. Rev. D **59**, 084006 (1999).

[16] T. Damour, International Journal of Modern Physics A **23**, 1130 (2008).

[17] R. Arnowitt, S. Deser, and C. W. Misner, *Gravitation: an introduction to current research* .

[18] M. Shibata and T. Nakamura, Physical Review D **52**, 5428 (1995).

[19] T. W. Baumgarte and S. L. Shapiro, Physical Review D **59**, 024007 (1998).

[20] L. Blanchet, Living Reviews in Relativity **17**, 2 (2014).

[21] E. Poisson, A. Pound, and I. Vega, Living Reviews in Relativity **14**, 7 (2011).

[22] E. D. Van Oeveren and J. L. Friedman, Physical Review D **95**, 083014 (2017).

[23] C. S. Kochanek, The Astrophysical Journal **398**, 234 (1992).

[24] D. Lai and A. G. Wiseman, Physical Review D **54**, 3958 (1996).

[25] F. Pannarale, E. Berti, K. Kyutoku, B. D. Lackey, and M. Shibata, Phys. Rev. D **92**, 084050 (2015).

[26] K. Chatziioannou, K. Yagi, A. Klein, N. Cornish, and N. Yunes, Physical Review D **92**, 104008 (2015), 1508.02062.

[27] X. Zhuge, J. M. Centrella, and S. L. W. McMillan, Physical Review D **54**, 7261 (1996).

[28] K. Uryū, M. Shibata, and Y. Eriguchi, Physical Review D **62**, 104015 (2000).

[29] J. A. Faber, P. Grandclément, F. A. Rasio, and K. Taniguchi, Physical review letters **89**, 231102 (2002).

[30] J. A. Faber, P. Grandclément, and F. A. Rasio, Physical Review D **69**, 124036 (2004).

[31] M. Bejger *et al.*, Astronomy & Astrophysics **431**, 297 (2005).

[32] D. Gondek-Rosińska *et al.*, Advances in Space Research **39**, 271 (2007).

[33] M. Shibata, K. Taniguchi, and K. Uryū, Physical Review D **71**, 084021 (2005).

[34] M. Shibata and K. Uryū, Progress of Theoretical Physics **107**, 265 (2002).

[35] R. Oechslin and H.-T. Janka, Physical review letters **99**, 121102 (2007).

[36] K. Taniguchi and E. Gourgoulhon, Physical Review D **68**, 124025 (2003).

[37] M. Shibata, Physical Review D **60**, 104052 (1999).

[38] M. Shibata and K. Uryū, Physical Review D **61**, 064001 (2000).

[39] M. Shibata and K. Taniguchi, Physical Review D **73**, 064027 (2006).

[40] M. Shibata, K. Taniguchi, and K. Uryū, Physical Review D **68**, 084020 (2003).

[41] M. Miller, P. Gressman, and W.-M. Suen, Physical Review D **69**, 064026 (2004).

[42] P. Marronetti, M. D. Duez, S. L. Shapiro, and T. W. Baumgarte, Physical review letters **92**, 141101 (2004).

[43] Y. T. Liu, S. L. Shapiro, Z. B. Etienne, and K. Taniguchi, Physical Review D **78**, 024012 (2008).

[44] J. Vines, É. É. Flanagan, and T. Hinderer, Physical Review D **83**, 084051 (2011).

[45] T. Hinderer *et al.*, Physical review letters **116**, 181101 (2016).

[46] S. Bernuzzi, T. Dietrich, and A. Nagar, Physical Review Letters **115**, 091101 (2015), 1504.01764.

[47] S. Bernuzzi, A. Nagar, T. Dietrich, and T. Damour, Physical Review Letters **114**, 161103 (2015), 1412.4553.

[48] K. Hotokezaka, K. Kyutoku, Y.-i. Sekiguchi, and M. Shibata, Physical Review D **93**, 064082 (2016), 1603.01286.

[49] T. Damour, A. Nagar, and L. Villain, Physical Review D **85**, 123007 (2012).

[50] W. Del Pozzo, T. G. F. Li, M. Agathos, C. Van Den Broeck, and S. Vitale, Physical review letters **111**, 071101 (2013).

[51] M. Agathos *et al.*, Physical Review D **92**, 023012 (2015), 1503.05405.

[52] L. Wade *et al.*, Physical Review D **89**, 103012 (2014).

[53] C. Moustakidis, T. Gaitanos, C. Margaritis, and G. Lalazissis, (2016), 1608.00344.

[54] B. D. Lackey, K. Kyutoku, M. Shibata, P. R. Brady, and J. L. Friedman, Physical Review D **89**, 043009 (2014).

[55] C. E. Rhoades Jr and R. Ruffini, Physical Review Letters **32**, 324 (1974).

[56] K. Brecher and G. Caporaso, Nature **259**, 377 (1976).

[57] J. M. Lattimer, Annual Review of Nuclear and Particle Science **62**, 485 (2012), 1305.3510.

[58] R. Geroch and L. Lindblom, Annals of Physics **207**, 394 (1991).

[59] H. Mueller and B. D. Serot, Nuclear Physics A **606**, 508 (1996).

[60] P. Pani, L. Gualtieri, A. Maselli, and V. Ferrari, Physical Review D **92**, 024010 (2015), 1503.07365.

[61] R. Essick, S. Vitale, and N. N. Weinberg, Physical Review D **94**, 103012 (2016), 1609.06362.

[62] J. R. Oppenheimer and G. M. Volkoff, Physical Review **55**, 374 (1939).

[63] É. É. Flanagan and T. Hinderer, Physical Review D **77**, 021502 (2008).

[64] T. Hinderer, The Astrophysical Journal **677**, 1216 (2008).

[65] T. Regge and J. A. Wheeler, Physical Review **108**, 1063 (1957).

[66] S. Postnikov, M. Prakash, and J. M. Lattimer, Phys. Rev. D **82**, 024016 (2010).

[67] L. Lindblom and N. M. Indik, Physical Review D **89**, 064003 (2014).

[68] B. D. Lackey, K. Kyutoku, M. Shibata, P. R. Brady, and J. L. Friedman, Physical Review D **85**, 044061 (2012), 1109.3402.

[69] J. S. Read *et al.*, Physical Review D **88**, 044042 (2013), 1306.4065.

[70] C. Markakis *et al.*, (in preparation).

[71] S. Koranda, N. Stergioulas, and J. L. Friedman, The Astrophysical Journal **488**, 799 (1997).

[72] P. Haensel and J. Zdunik, Nature **340**, 617 (1989).

[73] J. M. Lattimer and M. Prakash, From Nuclei to Stars: Festschrift in Honor of Gerald E. Brown , 275 (2011).

[74] F. Douchin and P. Haensel, Astronomy & Astrophysics **380**, 151 (2001).

[75] H. Müther, M. Prakash, and T. Ainsworth, Physics Letters B **199**, 469 (1987).

[76] B. D. Lackey, M. Nayyar, and B. J. Owen, Physical Review D **73**, 024021 (2006).

[77] A. Lichnerowicz, **17**, 189 (1965).

[78] W. Israel, Annals of Physics **100**, 310 (1976).

[79] W. Israel and J. M. Stewart, Annals of Physics **118**, 341 (1979).

[80] I.-S. Liu, I. Müller, and T. Ruggeri, Annals of Physics **169**, 191 (1986).

[81] S. A. Bludman and M. A. Ruderman, Physical Review D **1**, 3243 (1970).

[82] A. Reisenegger and P. Goldreich, The Astrophysical Journal **395**, 240 (1992).

[83] T. M. Linz, *Self-Force on Accelerated Particles*, PhD thesis, University of Wisconsin-Milwaukee, 2015.

[84] S. Mano, H. Suzuki, and E. Takasugi, Progress of Theoretical Physics **95**, 1079 (1996).

[85] S. A. Teukolsky, Physical Review Letters **29**, 1114 (1972).

[86] J. M. Bardeen and W. H. Press, Journal of Mathematical Physics **14**, 7 (1973).

[87] M. Shuhei and T. Eiichi, Progress of theoretical physics **97**, 213 (1997).

[88] G. B. Arfken and H. J. Weber, *Mathematical methods for physicists* (AAPT, 1999).

[89] F. W. Olver, D. W. Lozier, R. F. Boisvert, and C. W. Clark, *NIST handbook of mathematical functions hardback and CD-ROM* (Cambridge University Press, 2010).

[90] T. C. Quinn, Physical Review D **62**, 064029 (2000).

[91] T. C. Quinn and R. M. Wald, Phys. Rev. D **56**, 3381 (1997).

[92] Y. Mino, M. Sasaki, and T. Tanaka, Phys. Rev. D **55**, 3457 (1997).

[93] L. Barack and A. Ori, Phys. Rev. D **61**, 061502 (2000).

[94] T. M. Linz, J. L. Friedman, and A. G. Wiseman, Physical Review D **90**, 024064 (2014).

[95] A. G. Wiseman, Physical Review D **61**, 084014 (2000).

[96] C. R. Galley and M. Tiglio, Physical Review D **79**, 124027 (2009).

[97] C. R. Galley and B. Hu, Physical Review D **79**, 064002 (2009).

[98] C. R. Galley, Classical and Quantum Gravity **29**, 015010 (2011).

[99] C. R. Galley, Classical and Quantum Gravity **29**, 015011 (2011).

[100] C. R. Galley and A. K. Leibovich, Physical Review D **86**, 044029 (2012).

[101] D. Gal'tsov, Journal of Physics A: Mathematical and General **15**, 3737 (1982).

101

[102] E. Newman and R. Penrose, Journal of Mathematical Physics **3**, 566 (1962).

[103] J. N. Goldberg, A. J. MacFarlane, E. T. Newman, F. Rohrlich, and E. G. Sudarshan, Journal of Mathematical Physics **8**, 2155 (1967).

[104] A. G. Shah, J. L. Friedman, and T. S. Keidl, Physical Review D **86**, 084059 (2012).

[105] W. M. Kinnersley, *Type D gravitational fields*, PhD thesis, California Institute of Technology, 1968.

[106] C. Merlin and A. G. Shah, Physical Review D **91**, 024005 (2015).

[107] P. L. Chrzanowski, Physical Review D **11**, 2042 (1975).

[108] J. M. Cohen and L. S. Kegeles, Physical Review D **10**, 1070 (1974).

[109] S. Detweiler and B. F. Whiting, Phys. Rev. D **67**, 024025 (2003).

[110] L. Barack and N. Sago, Physical Review D **75**, 064021 (2007).

[111] R. Fujita, Progress of theoretical physics **128**, 971 (2012).

[112] C. M. Will and D. M. Eardley, The Astrophysical Journal **212**, L91 (1977).

CURRICULUM VITAE

Eric D. Van Oeveren
Place of birth: Grand Rapids, MI

EDUCATION

8/2012–8/2018 **Doctor of Philosophy in Physics**
University of Wisconsin – Milwaukee, Milwaukee, WI
Advisor: Dr. Alan Wiseman

8/2008–5/2012 **Bachelor of Science in Physics**
Grand Valley State University, Allendale, MI

RESEARCH EXPERIENCE

5/2013–present **Graduate Research Assistant**
University of Wisconsin - Milwaukee, Milwaukee, WI
Advisor: Dr. Alan Wiseman

6/2011 – 8/2011 **NSF REU Fellow**
Baylor University, Waco, TX
Advisor: Dr. Ke Qiao

6/2010 – 8/2010 **Undergraduate Research Assistant**
Grand Valley State University, Allendale, MI
Advisor: Dr. Harold Schnyders

TEACHING EXPERIENCE

8/2012–present **Teaching Assistant and Lecturer**
University of Wisconsin – Milwaukee, Milwaukee, WI
Discussion section leader, tutor, and grader

FELLOWSHIPS & AWARDS

2016, 2017	CGSA	University of Wisconsin-Milwaukee
2016	Research Excellence Award	University of Wisconsin-Milwaukee
2012	Outstanding Student — Physics	Grand Valley State University
2008-2012	Presidential Scholarship	Grand Valley State University
2011	REU Fellowship	National Science Foundation

CONFERENCES AND PRESENTATIONS

Midwest Relativity Meeting, October 2016
Perimeter Institute, Waterloo, ON
"A Constraint on the Tidal Deformability of Neutron Stars"

21st International Conference on General Relativity and Gravitation, July 2016
Columbia University, New York, NY
"Limits set by causality on neutron-star deformability and on the tidally induced change in inspiral waveform"

Midwest Relativity Meeting, October 2015
Northwestern University, Evanston, IL
"Accelerated Scalar Self-Force on a Schwarzschild Background."

18th Capra Meeting on Radiation Reaction in General Relativity, June 2015
Kyoto University, Kyoto, JP
"Using an Analytical Regularization Scheme to Find the Self-Force on an Accelerated Scalar Charge."

American Physical Society April Meeting, April 2012
Atlanta, GA
"Oppenheimer-Snyder Collapse in AdS Spacetime."

PUBLICATIONS

Ke Qiao, Jie Kong, **Eric Van Oeveren**, Lorin S. Matthews, and Truell W. Hyde. "Mode couplings and resonance instabilities in dust clusters." Physical Review E **88**, 043103 (2013)

Eric D. Van Oeveren and John L. Friedman. "Upper limit set by causality on the tidal deformability of a neutron star." Physical Review D **95**, 083014 (2017).